1993

Polynuclear Mixed-Valence Complexes

David A. Rockcliffe
Loyola University Chicago

POLYNUCLEAR MIXED-VALENCE COMPLEXES

by

David A. Rockcliffe

A Dissertation Submitted to the Faculty of the Graduate School

of Loyola University of Chicago in Partial Fulfillment

of the Requirements for the Degree of

Doctor of Philosophy

May, 1993

ABSTRACT

Iron(II) and cobalt(II) Schiff base complexes of bis(1-ferrocenyl-1,3-butanedione)-ethylenediimine were prepared and examined electrochemically and spectroscopically for intervalence transfer phenomena. Electrochemical experiments showed that the M^{II}/M^{III} couple for the iron and cobalt complexes occurred at -563 mV and -688 mV respectively while the Fc/Fc^{+} couple occurred at 777 mV and 838 mV respectively. Titration of these complexes with a solution of bromine in acetonitrile did not reveal intervalence transfer bands. Ruthenium(III) and iron(III) complexes of 1,1,1-trifluoro-4-ferrocenyl-2,4-butanedionato (FcTFBD), 1-phenyl-3-ferrocenyl-1,3-propanedionato (FcPPD) and 1-ferrocenyl-1,3-butanedionato (FcBD) were prepared and examined electrochemically and spectroscopically. The ruthenium complexes showed M^{III}/M^{II} reduction potentials at -80 mV, -576 mV and -801 mV and Fc/Fc^{+} couples at 868 mV, 734 mV and 601 mV respectively whereas those of iron displayed M^{III}/M^{II} reduction potentials at -339 mV, -882 mV and -878 mV and Fc/Fc^{+} couples at 791 mV, 646 mV and 623 mV respectively. The near infrared-visible spectra of the ruthenium(III) complexes exhibited bands at 900 nm, 710 nm and 575 nm. The delocalization parameter α^2 was calculated as 5×10^{-3}, 2×10^{-3} and 3×10^{-3} for the respective FcTFBD, FcPBD and FcBD complexes. The range of values for the delocalization parameters indicates that these mixed-valence complexes are weakly

delocalization parameters indicates that these mixed-valence complexes are weakly coupled, valence isolated class II compounds of the Robin and Day classification scheme. None of the related iron(III) complexes displayed intervalence transfer bands in the near infrared-visible region.

ACKNOWLEDGEMENTS

The author is grateful to Dr. Patrick M. Hnery for the opportunity to work in his research group and for his continued guidance, patience and encouragement throughout this research project. Helpful discussions on the electrochemical aspects of this project were held with Dr. Alanah Fitch and advice on organic synthesis was obtained from Dr. David Crumrine and Dr. Charles Thompson and thanks are extended to them. Thanks are extended to all the members of the author's progress committee for ensuring a well balanced project. The author would also like to thank Dr. Dwayne La Brake and Dr. Scott Hurst for their assistance in glass-blowing and equipment preparation. Thanks are also due to laboratory partners Dr. K. Zaw, Dr. John Francis and Dr. Glenn Noronha for their helpful suggestions and friendship. The author would like to thank all his friends and contemporaries who provided moral support and contributed much to the overall experience in graduate school.

Special thanks to Hazel Olsen whose assistance way beyond the call of duty has, on many occasions, facilitated various aspects of the work presented in this dissertation.

TABLE OF CONTENTS

LIST OF TABLES

LIST OF FIGURES

LIST OF ABBREVIATIONS

β-Polyketones

[FcBD]	1-ferrocenyl-1,3-butanedione
[FcTFBD]	1,1,1-trifluoro-4-ferrocenylbutanedione
[FcPPD]	1-phenyl-3-ferrocenyl-1,3-propanedione
[FcHT]	1-ferrocenyl-1,3,5-hexanetrione
[PHT]	1-phenyl-1,3,5-hexanetrione

Schiff Bases

[(BPBD)en]	bis(1-phenyl-1,3-butanedione)ethylenediimine
[(BTFPD)en]	bis(1,1,1-trifluoro-2,4-pentanedione)ethylenediimine
[(BFcBD)en]	bis(1-ferrocenyl-1,3-butanedione)ethylenediimine
[(BPHT)en]	bis(1-phenyl-1,3,5-hexanetrione)ethylenediimine
[(BFcHT)en]	bis(1-ferrocenyl-1,3,5-hexanetrione)ethylenediimine

Schiff Base Complexes of Iron Cobalt and Ruthenium

[Fe(BPBD)enPy]	ethylenediiminebis(1-phenyl-1-3-butanedionato)-pyridineiron(II)
[Fe(BFcBD)enPy]	ethylenediiminebis(1-ferrocenyl-1,3-butanedionato)-

	pyridine-iron(II)
$[Fe_2(BPHT)en(Py)_2]$	ethylenediiminebis(1-phenyl-1,3,5-hexanetrione)-dipyridinediiron(II)
$[Fe_2(BFcHT)en(Py)_2]$	ethylenediiminebis(1-ferrocenyl-1,3,5-hexanetrionato)-dipyridinediiron(II)
[Fe(BPBD)enCl]	ethylenediiminebis(1-phenyl-1,3-butanedionato)chloro-iron(III)
[Fe(BFcBD)en Cl]	ethlyenediiminebis(1-ferrocenyl-1,3-butanedionato)-chloroiron(III)
$[Fe_2(BPHT)enCl_2]$	ethylenediiminebis(1-phenyl-1,3,5-hexanetrionato)-dichlorodiiron(III)
$[Ru(BPBD)en(PPh_3)_2]$	ethylenediiminebis(1-phenyl-1,3-butanedionato)bis-(triphenylphosphine)ruthenium(II)
$[Ru(BTFPD)en(PPh_3)_2]$	ethylenediiminebis(1,1,1-trifluoro-2,4-pentanedionato)-bis(triphenylphosphine)ruthenium(II)
$[Ru(BTFFcBD)en(PPh_3)_2]$	eythylenediiminebis(1,1,1-trifluoro-4-ferrocenyl-2,4-butanedionato)bis(triphenylphosphine)ruthenium(II)
$[Ru(BFcBD)en(PPh_3)_2]$	ethylenediiminebis(1-ferrocenyl-1,3-butanedionato)-bis(triphenylphosphine)ruthenium(II)
$K[Ru(BFcBD)enCl_2]$	potassium ethylenediiminebis(1-ferrocenyl-1,3-butane-dionato)-dichlororuthenate(III)

$K[Ru(BPBD)enCl_2]$	ethylenediiminebis(1-phenyl-1,3-butane-dionato)dichlororuthenate(III)-
[Co(BPBD)en]	ethylenediiminebis(1-phenyl-1,3-butanedionato)-cobalt(II)
[Co(BTFPD)en]	ethylenediiminebis(1,1,1-trifluoro-2,4-pentanedionato)-cobalt(II)
[Co(BFcBD)en]	ethylenediiminebis(1-ferrocenyl-1,3-butanedionato)-cobalt(II)

Tris(β-diketonato) Complexes of Iron(III) and Ruthenium(III)

$[Fe(TFPD)_3]$	tris(1,1,1-trifluoro-2,4-pentanedionato)iron(III)
$[Fe(PBD)_3]$	tris(1-phenyl-1,3-butanedionato)iron(III)
$[Fe(PD)_3]$	tris(2,4-pentanedionato)iron(III)
$[Fe(FcTFBD)_3]$	tris(1,1,1-trifluoro-4-ferrocenyl-2,4-butanedionato)iron(III)
$[Fe(FcPPD)_3]$	tris(1-phenyl-3-ferrocenyl-1,3-propanedionato)iron(III)
$[Fe(FcBD)_3]$	tris(1-ferrocenyl-1,3-butanedionato)iron(III)
$[Ru(TFPD)_3]$	tris(1,1,1-trifluoro-2,4-pentanedionato)ruthenium(III)
$[Ru(PBD)_3]$	tris(1-phenyl-1,3-butanedionato)ruthenium(III)
$[Ru(PD)_3]$	tris(2,4-pentanedionato)ruthenium(III)
$[Ru(FcTFBD)_3]$	tris (1,1,1-trifluoro-4-ferrocenyl-1,3-butanedionato)-

	ruthenium(III)
$[Ru(FcPPD)_3]$	tris(1-phenyl-3-ferrocenyl-1,3-propanedionato)ruthenium(III)
$[Ru(FcBD)_3]$	tris(1-ferrocenyl-1,3-butanedionato)ruthenium(III)

CHAPTER 1

INTRODUCTION

1.1 Background

Mixed-valence compounds contain two or more homonuclear or heteronuclear elements in two different formal oxidation states. Numerous examples are found in naturally occurring minerals of which magnetite (Fe_3O_4) hausmannite (Mn_3O_4) and vivianite ($Fe_3(PO_4)_{2.8}).H_2O$ are examples. The origin of preparative mixed-valence chemistry is considered to be the nineteenth century synthesis of Prussian blue, a compound that was not originally examined for its physical properties but was used as an ink and a dye. Many researchers examined mixed-valence systems during the early part of this century,[1] the salient feature noted then was the presence of a strong absorption in the visible region resulting in a color that is unrelated to the properties of the individual ions. Several rationales were put forward in order to explain this observation.[2,3,4]

A resurgence in the interest in mixed-valence compounds was signalled by the publication of papers by Allen and Hush,[5] Hush[6] and the classification scheme by Robin and Day,[7] all of which appeared in 1967. At that point in time only solid and solution phase lattice systems were treated.

The first discrete mixed-valence complex ion was prepared by Creutz and Taube[8] in 1969. Following the Creutz-Taube ion was the preparation of the biferrocene cation by Cowan and Kaufmann.[9] Subsequently, several mixed-valence systems were prepared, making use of a variety of metal ions and bridging ligands.[10] The interest in mixed-valence systems had then turned to discrete entities since the compositions of these compounds are amenable to systematic variations.

The Robin and Day formulation describes class II compounds as those in which metal-metal interaction is weak. The focus of attention has been mainly on these weakly coupled systems since they are able to provide information towards the understanding of the intervalence transfer process.

Theoretical development accompanying the Robin and Day classification scheme was pioneered by Hush who proposed a single frequency theoretical model for class II compounds in which two harmonic oscillators of the same frequency are assumed to be coupled by an electron. Schatz[11] later accounted for nuclear vibration and, in doing so, provided a more rigorous and unified treatment for mixed-valence systems in general. The Schatz treatment offers a wider application of theory and a more refined Robin and Day classification. Other theoretical work was accomplished through the application of molecular orbital theory,[12,13] superexchange theory[14] and molecular charge transfer theory.[15]

Symmetrical mixed-valence complexes were studied initially but the quest for a greater understanding of intervalence transfer phenomena necessitated the preparation of unsymmetrical, heterobinuclear and polynuclear compounds. It is

hoped that, with the improved understanding of the intervalence transfer process, the unique properties of mixed-valence systems could be taken advantage of in the design of electrical conductors and catalysts. Our interest in this work lies in the possible use of the prepared mixed-valence complexes in the design of polyelectron transfer catalysts.

1.2 Description of Mixed-Valence Compounds

An important characteristic of a mixed-valence system is the degree of electron delocalization between the metal centers of differing oxidation states. According to Robin and Day treatment,[7] a consequence of electron delocalization is metal-metal interaction which makes possible the thermal electron exchange process

$$[M_A^{2+}\text{-L-}M_B^{3+}] \rightarrow [M_A^{3+}\text{-L-}M_B^{2+}] \qquad 1.1$$

and an intervalence transfer of the type

$$[M_A^{2+}\text{-L-}M_B^{3+}] \rightarrow [M_A^{3+}\text{-L-}M_B^{2+}]^* \qquad 1.2$$

where M_A and M_B are two metal ions which are bridged by a ligand L. The light induced transition is a unique feature of mixed-valence compounds which is not observed in the isolated ions, the fully oxidized or fully reduced systems. The energy of this transition is such that the absorption band occurs in the near infra-red or

visible region of the electromagnetic spectrum.

1.2.1 The Robin and Day Classification

The Robin and Day scheme[7] classifies mixed valence compounds on the basis of the extent of ground state electron delocalization between metal ions and surrounding ligands in an ionic lattice structure. For a simple system where two ions A and B with isolated valences n and n+1 are linked by a bridging entity, the first approximation of the zero order state is

$$\psi_0 = \psi_a^{\,n}\psi_b^{\,n+1} \qquad 1.3$$

Also contributing to the ground state will be the configuration

$$\psi_\ell = \psi_a^{\,n+1}\psi_b^{\,n} \qquad 1.4$$

which is slightly higher in energy than ψ_0. A suitable purturbation matrix, mixing ψ_0 and ψ_ℓ will give the following expression for the ground state wave function.

$$\Psi_g = (1-\alpha^2)\psi_0 + \alpha\psi_\ell \qquad 1.5$$

When the wave function is normalized, α is expressed as follows

$$\alpha = N^2[1 - \{1 + (2E_\ell^2 - 2E_\ell(E_\ell^2 + 4V^2)^{1/2})/4V^2\}^{-1}] \qquad 1.6$$

where N is the normalization constant. The coefficient α may be regarded as a valence delocalization parameter whose value depends on the mixing matrix element V, which mixes ψ_ℓ and ψ_0, and the energy E_ℓ of ψ_ℓ above ψ_0. The classification scheme is based on the relationship between α and E_ℓ. Representation of class I compounds is appropriate when E_ℓ is large resulting in a small value for α. A lattice system with ions in very different environments may be represented in this way. The result is infinitely small or no metal-metal interaction, the sites bearing particular valencies state being distinguishable, and a charge transfer of the type A→B becomes a high energy process. The ions in this case are referred to as being completely valence trapped. On the other hand class III formulation is applicable when E_ℓ is very small and α is large giving rise to extensive ground state electron delocalization between the metal ions of differing oxidation states. Electron movement is now best described as charge transfer between molecular orbitals. Two situations may exist here. Firstly, the electron delocalization may exist to the extent where oxidation states are indistinguishable, both ions having non-integral values. The second situation is one where valence trapping occurs to the extent that two different oxidation states are discernible although the metal ions are strongly coupled.

When α is small but finite, the result is an intermediate class II case in which the sites of the ions are regarded as being similar yet distinguishable. Metal-metal interaction is small but significant enough to promote electron movement between

metal centers by both a thermally and an optically induced pathway.

The classification of borderline class II/class III compounds may be a contentious matter. The particular category into which a compound is placed depends on the experimental technique used for investigation. An example may be found in the Creutz-Taube ion where Mossbauer[16] and ultraviolet-visible[8] spectroscopy have determined the system to be localized, whereas, near infra-red[8] and ^{1}H NMR[17] studies suggest a significant degree of delocalization. The discrepancy may be understood in terms of the range of timescales of the experiments (10^{-20} to 10^{-7} s).

1.2.2 The Hush Model

Intervalence transfer theory for class II compounds, as developed by Hush,[6] is based on two basic assumptions. (a) The metal centers are considered to be harmonic oscillators, of identical frequency, which are coupled by an electron. (b) The electron transfer process is treated in the limit of high temperature *i.e.* $kT \gg h\nu$. Hush derived the following relation between the energy of an optical and a thermal process

$$E_{th} = E_{op}^2/4(E_{op} - \Delta E) \qquad 1.7$$

where ΔE is the internal energy difference between the system at vibrational equilibrium before and after electron transfer, E_{th} is the activation barrier to the thermal electron transfer pathway and E_{op} is the energy associated with the Franck-

Condon optical transition (equation 1.2). This expression obtains for an unsymmetrical system. For a symmetrical system the expression reduces to

$$E_{th} = E_{op}/4 \qquad 1.8$$

since ΔE is zero. The optical transfer is then predicted to have four times the energy requirement of the thermal transfer.

Other relations based on the Hush model have been derived in order to quantify the energy associated with electron transfer. When measurements are taken in the solution phase, the total energy associated with the electron transfer is accounted for in terms of the energy of reorganization of the inner coordination sphere (E_{in}) and the outer sphere energy change resulting from the solvent polarization adjustment from equilibrium as a consequence of the charge transfer (E_{out}). The energy relation is simply expressed as follows for an unsymmetrical system

$$E_{op} = E_{in} + E_{out} + \Delta E \qquad 1.9$$

where ΔE is defined as in equation 1.7. The dielectric continuum model, developed by Marcus,[18] was invoked in order to obtain an expression for the solvent reorganization term in equation 1.9. The assumption made was that the medium between the two interacting ions functions similarly to a continuous dielectric with the ions themselves occupying cavities in the medium. The expression deduced is as

follows:

$$E_{out} = (\Delta e)^2(1/2a_i + 1/2a_j - 1/r)(1/D_{op} - 1/D_s) \quad 1.10$$

where a_i and a_j are the radii of the inner coordinating spheres of the metal ions, r is the metal-metal distance, D_{op} and D_s are respectively the refractive index and the static dielectric constant of the solvent. Equation 1.10 demonstrates solvent dependence of the position of the band maximum for the intervalence absorption profile.

The expression used for calculating the energy adjustment of the inner coordination sphere is based on a vibration model.[19] The following equation may be used for calculating the inner sphere energy contribution,

$$E_{in} = n[2f_2f_3/(f_2 + f_3)](d_2 - d_3)^2 \quad 1.11$$

where n is the number of metal-ligand bonds, f_2 and f_3 are the Hooke's law force constants for the metal-ligand bonds with the metal in the oxidation states n and n+1, and $d_2 - d_3$ is the difference in the equilibrium bond lengths for the two metal centers.

Other relations based on the Hush model enable the calculation of band width at half height and the valence delocalization parameter α. The expression for the latter is as follows:

$$\alpha^2 = [(4.2 \times 10^{-4})\epsilon_{max}\Delta\nu_{1/2}]/(\nu_{max} r^2) \qquad 1.12$$

where ϵ_{max} is the extinction coefficient of the intervalence band, ν_{max} is the frequency maximum of the band, $\Delta\nu_{1/2}$ is the band width at half height and r is the distance between the two metal centers. The relation given is based on the assumption that the intervalence transfer band is Gaussian in shape. This is not necessarily true for all complexes.

In the high temperature limit, the relation between the half width and the band maximum is expressed in the following equation

$$\Delta\nu_{1/2} = [16(\ln 2)k_B T(E_{op} - \Delta E)]^{1/2} \qquad 1.13$$

where k_B is the Boltzman constant and T is the absolute temperature. This equation is applicable to both the symmetrical and unsymmetrical mixed-valence systems.

Application of the equations based on the Hush model (equations 1.7 through 1.13) has been successful only in mixed-valence systems where metal-metal interactions are weak. Although other models have been proposed with a view to providing a more general application of the equations describing the behaviour of mixed-valence compounds, the Hush relations continue to be very widely used. The classification of mixed-valence compounds as class II is usually judged by how well they conform to the Hush relations.

1.2.3 Other Models

Several models have been proposed in an effort to provide a more complete description of mixed-valence complexes. A three-site method was developed by Ondrechen.[20] Other contributions were made independently by Lauher[11] and Chiu.[15] A rather noteworthy effort is the two-site Piepho, Krausz and Shatz (PKS) model in which the derived equations account for electronic as well as vibronic coupling of the metal centers. Inclusion of vibronic coupling in the mathematical description of mixed-valence complexes produced a better description of class III complexes. The model has been successful at deriving several previous results, providing a refinement to the Robin and Day classification scheme and predicting band contours. It has been applied to and has provided reasonable success in predicting the properties of bridged mixed-valence dimers.[11,21,22,23]

The relations of the PKS model were obtained by an iterative fit of the properties of the intervalence transfer band to a parameter representing vibronic coupling λ, an electronic coupling parameter ε and the energy υ (in wavenumbers) of the totally symmetric metal-ligand stretching mode. The energy of the intervalence transfer absorption according to the PKS model is given below:

$$E_{op} = 2\lambda^2\upsilon \quad cm^{-1} \qquad 1.14$$

Other PKS relations are as follows,

$$\upsilon = 1/c\ [f/(4\pi^2\mu)]^{1/2}\ \ cm^{-1} \qquad 1.15$$

$$\alpha^2 = 1/2[1 - \{(\lambda^2 + W)^2/(\varepsilon^2 + (\lambda^2 + W^2)^2)\}^{1/2}] \qquad 1.16$$

where W is a parameter which is related to the energy difference E_ℓ-E_0, μ is the reduced mass, f is the metal-ligand force constant (which is assumed to be independent of the oxidation state of the metal). All other symbols have their usual significance. In the expression for the delocalization parameter α, the Robin and Day classification is obtained by considering the relation between ε and $(\lambda^2 + W)$. Classes I, II and III correspond to cases where $\varepsilon \ll (\lambda^2 + W)$, $\varepsilon \leq (\lambda^2 + W)$ and $\varepsilon > (\lambda^2 + W)$ respectively.

One shortcoming of the PKS model is the exclusion of solvent reorganization in calculations of energetics.

1.2.4 Uses for the Hush Model

The applicability of the Hush model is manifested in how well the system under examination conforms to the relations stated in section 1.2.2. According to equation 1.9 there is a linear relation between E_{op} and ΔE provided that E_{in} and E_{out} remain constant. Goldsby and Meyer[24] demonstrated the validity of this relation using ruthenium dimers in which variations in E_{out} and E_{in} were minimized by using metal-ligand systems with similar bond lengths, bond energies and ionic radii. On examining the intervalence transfer bands for a number of complexes the results were

found to be consistent with the relation

$$E_{op} = \Delta E + K \qquad 1.17$$

where K is a constant.

A further test for the Hush model is provided by substituting equation 1.10 in equation 1.9 to give

$$E_{op} = E_{in} + (\Delta e)^2(1/2a_i + 1/2a_j - 1/r)(1/D_{op} - 1/D_s) + \Delta E \qquad 1.18$$

Solvent dependency is demonstrated by a plot of E_{op} against $(1/D_{op} - 1/D_s)$ for different media. This plot yields a straight line[25,26,27] from which E_{in} may be determined for a symmetrical mixed-valence system ($\Delta E = 0$) or an unsymmetrical system if ΔE is determinable. In practice, the observed scatter in points is considered to be manifestations of the assumptions of the dielectric continuum model. Equation 1.18 above is expected to give a good fit in cases where the internuclear distance is much greater than the sum of the ionic radii since a dielectric continuum is assumed to exist between two non-interpenetrating spheres. In actual fact, the equation is used for instances where the value of r is in the vicinity of $a_i + a_j$. Application of this two sphere model is not entirely appropriate when there are significant counter ion effects,[28] specific ion-dipole interactions are large,[29] dielectric saturation occurs[30] or the bridging ligand results in a small value for r, invalidating the solvent

continuum assumption.[31] There is generally reasonably good agreement between theoretical predictions and experimental results. The solvent dependence expression of equation 1.18 above is one of the more widely used of the Hush relations which provides information for class II systems.

Interionic distance dependance is similarly illustrated by combining equations 1.10 and 1.9 and performing the appropriate rearrangement to give the following expression for a symmetrical complex.

$$E_{op} = [E_{in} + (\Delta e)^2(1/2r_1 + 1/2r_2)(1/D_{op} - 1/D_s)] - (\Delta e)^2/r(1/D_{op} - 1/D_s) \quad 1.19$$

A plot of E_{op} versus $1/r$ is linear with the intercept giving a value for E_{in}. The interionic distance r is varied by changing the bridging ligand. Validity of the distance dependence relation through the use of equation 1.19 has been established using a series of ruthenium dimers.[32]

The temperature dependence on band width (equation 1.13) is normally employed in determining the band width at half height. The change in internal energy, ΔE, may be estimated from the difference in redox potentials between the two metal centers or the reduction potentials of model complexes.[30] The band width at half height is usually determined at T=300 K using the following expression.[6]

$$\nu_{max} - \Delta E = [(\Delta\nu_{1/2})^2]/2.31 \quad 1.20$$

It is generally observed that the experimentally determined value is greater than the theoretical prediction for class II complexes.[33]

The inner sphere reorganization energy E_{in} is conveniently calculated with the aid of equations 1.18 and 1.19 rather than equation 1.11. When applying equation 1.11 the force constants are estimated using infrared absorption data and the difference d_2 -d_3 is estimated using crystallographic data. The intercept determination of E_{in} using equation 1.18 or 1.19 generally produces values which are larger than those obtained by equation 1.11. The discrepancy is attributed largely to electronic splitting of spectroscopic states[30] of the metal ions.

The applicability of the Hush relations depends, in general, on the rate of electron transfer in relation to the time scale for solvent reorientation ($\sim 10^{-11}$ s). If valence trapping by the solvent is effective because of the relatively slow movement of the electron, then the intervalence transfer parameters are sensitive to solvent characteristics and the Hush formulas suitably describe the mixed-valence systems. Any discrepancy observed when using the Hush relations is usually construed as non-conformity to class II behavior.

1.2.5 Potential Energy Surfaces

The energetics of thermal and optical electron transfer in mixed-valence compounds may be profiled using potential energy diagrams in which the Born-Oppenheimer potential energy of the system is plotted as a function of the nuclear coordinates. The nuclear coordinates are composite representations of all the

nuclear positions of the system in space and are a function of the vibrational, translational and rotational motions of all reactants and products. Complete representation is possible only in $3N$-dimensional space (where N is the total number of species in the system), therefore the two dimensional representation in Figure 1.1 is really a section through the N-dimentional picture. Figure 1.1 represents the important features of potential energy diagrams for symmetrical and unsymmetrical binuclear mixed-valence systems undergoing the reaction

$$M_1^{2+}\text{-}M_2^{3+} \rightarrow M_1^{3+}\text{-}M_2^{2+} \qquad 1.21$$

Equation 1.21 represents a reaction which essentially produces an oxidation isomer of the reactant. The difference in internal energy between the two systems is ΔE, its magnitude being a reflection of the difference in thermodynamic stability between the reactant and product oxidation isomers. The interaction energy between the two metal ions is represented by $-2H_{ab}$. Its magnitude is dependent on the extent of electron coupling which is a function of interionic distance and electron shielding experienced by the interacting ions. The thermal energy barrier, E_{th}, is the activation energy for electron transfer. A large value for the energy gap $-2H_{ab}$ results in a small value for E_{th}, giving rise to extensive ground state electron delocalization since the barrier to electron motion is now easy to surmount. The transition energy E_{op} is the energy of the photoinduced charge transfer, the nature of which will be dealt with presently.

Several changes may occur on moving along a potential energy surface (Figure 1.1). If the interaction energy H_{ab} is large, then the system is unable to cross the energy gap between the upper and lower surfaces and it will move smoothly from the R surface to the P surface provided that the thermal barrier to motion is overcome. Since P represents a potential surface corresponding to the mobile electron being located on M_2, then the movement described results in an electron transfer from M_1 to M_2. This process is referred to as an adiabatic electron transfer since the system moves along a continuous surface. The energy changes involved here are those associated with intramolecular bond adjustment and solvent reorganization in response to non-equilibrium conditions established as a consequence of electron transfer.

The mechanism of electron transfer requires prior adjustment of bond lengths and solvent molecules in such a way as to give matching energy to the overlapping orbitals through which electron movement occurs. Such adjustments to the system are necessary if electron transfer takes place in accordance with Franck-Condon restrictions.

In contrast to cases with large interaction energies, if H_{ab} is small then the probability of the system moving to surface P will be very small and the course along R will be maintained. The small interaction energy reduces the likelihood of formation of the product oxidation isomer.

Electron transfer may also occur through a radiation induced process (E_{op}) or by tunneling. For a light induced transition, the system moves from the minimum of the

Figure 1.1 Potential Energy Diagrams for (a) Symmetrical and (b) Unsymmetrical - Mixed-Valence Systems

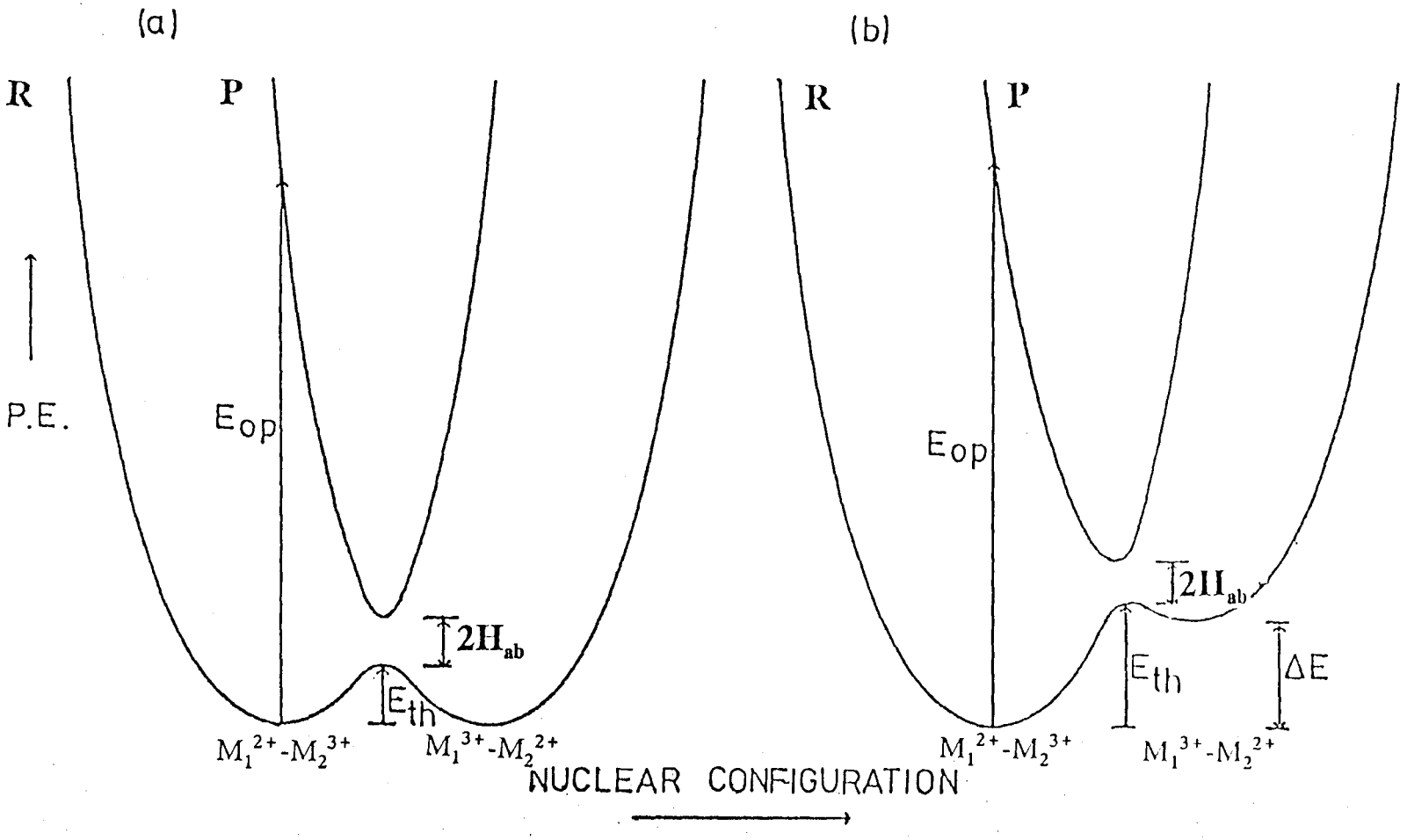
(a)
(b)
R
P
P.E.
E_{op}
$2H_{ab}$
E_{th}
M_1^{2+}-M_2^{3+}
M_1^{3+}-M_2^{2+}
$2H_{ab}$
E_{th}
ΔE
NUCLEAR CONFIGURATION

R surface to an upper level of the P surface before relaxing to the minimum of the latter surface. Electron movement of this nature must be a vertical process on the potential energy diagram since, according to the Franck-Condon principle, nuclear motion is invariant on the timescale of electronic motion. The initial product formed after electron transfer contains M_1 in an M^{3+} environment and M_2 in an M^{2+} environment. This product is in a vibrationally excited state, the excitation energy being associated with bond length adjustment and solvent reorganization.

The greater the coupling between the metal centers, the greater is the probability of the intervalence transfer and the smaller is the barrier to thermal electron transfer. When coupling is very strong, the thermal barrier disappears and there is complete electron delocalization. For weak coupling, the energy of the intervalence transfer band is related to the thermal barrier by equation 1.7.

The interaction energy H_{ab} is very small or equal to zero for class I compounds. On the basis of transition probability as a function of the magnitude of H_{ab}, no intervalence transfer is expected for class I compounds. An infinitely small value for H_{ab} means that for an adiabatic process along R, the system will remain on this surface and there will be very little likelyhood of movement to the P surface. Class III compounds experience a large value for the energy gap $-2H_{ab}$ which now has the same magnitude as the energy of the radiation induced electron transfer process. The barrier to the thermal process is removed completely. For class II compounds, H_{ab} is small but significant enough to give a finite probability to the E_{op} transition.

The tunneling phenomenon as applied to mixed-valence systems, has been

theoretically predicted[34] and invoked in explaining long range electron transfer which is pertinent to biological systems. The phenomenon is usually observed when the classical barrier to electron transfer is very large. Tunneling over distances of 15 Å[35,36,37] and greater[38,39] has been reported.

1.2.6 The Nature of the Inner and Outer Sphere Barrier to Electron Transfer

As mentioned before, electron transfer across a thermal barrier occurs in accordance with Franck-Condon restrictions. Equation 1.9 indicates the two major contributing factors to the barrier for an adiabatic process. The inner sphere energy, $E_{in,}$ originates in the vibrational energy of the metal-ligand bonds since these undergo adjustment prior to electron transfer. The restraining bond energy is regarded as a type of "vibrational trap." The outer sphere energy associated with solvent reorganization, E_{out}, must also undergo redistribution in preparation for electron transfer since each ion site changes oxidation state resulting in newly defined ion-dipole interactions. The solvent reorganization energy constitutes what is commonly referred to as the "solvent trap." Solvent polarization reorganization and vibrational readjustment also occur in non-adiabatic processes in which case they are referred to as the Franck-Condon parameters.

Several attempts at modelling the solvent barrier process, with the objective of providing more generally applicable equations have been reasonably successful although the literature has demonstrated the importance of specific ion-dipole interactions[29,31] which reduce the likelihood of success at a unified theory. Ellipsoid

cavity[40] models have received considerable attention in this regard.

The strengths and limitations of the dielectric continuum model have been revealed in the literature. In spite of acknowledged weaknesses, the model is used extensively in demonstrating class II behaviour in mixed-valence complexes. Breakdown occurs in instances where vibrational trapping is moderate and the electron transfer rate is greater than the rate of solvent dipole reorientations (~10^{-11} s). Solvent dependency of E_{op} is no longer observed and electron delocalization becomes pronounced.

1.3 Discrete Binuclear Mixed-Valence Compounds

The initial binuclear mixed-valence complexes prepared were those based on ruthenium or iron metal centers and incorporated organic molecules as bridging ligands. The specific metals were chosen for their relative stability in both the 2+ and 3+ oxidation states. For ruthenium complexes, ammine groups were preferred as non-bridging ligands while the bridging ligands contained π-acceptor cyano or π-donor N-heterocyclic functionalities. These units were chosen because researchers were familiar with their metal-ligand interactions which are evident from spectroscopic studies.

1.3.1 Symmetrical Mixed-Valence Compounds

The earliest mixed-valence compounds prepared and investigated were symmetrical in nature. The high-symmetry nature of these complexes made them

amenable to investigating bridge effects in electron transfer reactions. A diversity of bridging ligands were used in an effort to study specific aspects of the mixed-valence systems. Compounds containing ruthenium ions usually employed bridging ligands related to bipyridyl, dinitrogen and nitriles. Involved studies on these complexes showed that stronger coupling of the metal centers results when the bridges are unsaturated.[41] If the bridge saturation is interrupted by methylene linkages then interaction markedly decreases. Strong delocalization is usually encountered with short π-acid type dicyano bridges in which the π^* orbitals provide a pathway for movement of the unpaired electron, or with strong π-donor bridges. Recently, coupling of two ruthenium centers has been accomplished with the assistance of dipyridyl polyene bridges,[42] over a distance of 16-20 Å. Diphenyl phosphine groups linked by a methylene unit have also been employed in bridging osmium dimers,[43] probably allowing simultaneous operation of through-bond and through-space effects. The intervalence transfer properties revealed that most of these complexes belong to class II or III.

Symmetrical mixed-valence complexes are particularly suited to the study of bridge effects of the intervalence transfer process, since the terminal units may be held constant while systematically varying the nature of the bridge. The type of useful information emerging from these studies is mainly related to distance effects in the intervalence transfer process and the impact of π-acceptor and π-donor units as bridging and terminal ligands. A general observation is that the interaction energy decreases with increasing interionic distance for similar bridges and that π-donor

bridges enhance metal-metal interaction to a greater extent than π-acceptor groups.

Biferrocene complexes which are linked at the cyclopentadienyl unit were also prepared and examined for their mixed-valence properties. One important observation is that the metal-metal interaction increases as the cyclopentadienyl units are constrained in a coplanar fashion.[44] Ferrocene complexes with bridges between the cyclopentadienyl units have been prepared and it has been reported[45,46]that the Hush relations are generally obeyed by these systems.

1.3.2 Unsymmetrical Mixed-Valence Compounds

Complexes may be regarded as being unsymmetrical owing to the presence of different types of ligands on each homonuclear metal center or the presence of different metal ions. Interest in these complexes arose through the desire to examine the effects of redox asymmetry and the importance of matching bridge orbitals with those on the metal. The approach to the design of unsymmetrical systems was to induce valence trapping by incorporating non-bridging ligands such as bipyridine, through which the unpaired electron could be delocalized. Class II character was expected to be produced since terminal delocalization would reduce the electron involvement in strong coupling through pi-interaction of the bridge. Later, strategies involving solvent trapping were employed successfully.[47,48] The importance of the terminal ligands in valence trapping is showed by the class II classification of the compound $[(bpy)_2ClRu(pyz)Ru(NH_3)_5]^{4+}$ as opposed to the class III description of the Creutz-Taube ion $[(NH_3)_5Ru(pyz)Ru(NH_3)_5]^{5+}$.

1.3.3 Unsymmetrical Homonuclear Mixed-Valence Complexes

Homonuclear complexes with different types of ligands were prepared and examined in relation to effects of redox potentials relative to electron delocalization. Meyer[41] examined solvent dependence on the intervalence transfer process and found that complexes of composition $[(bpy)_2ClRuLRu(NH_3)_5]^{4+}$ conform to class II behaviour when L is pyrazine,4,4′-bipyridine and trans 1,2-bis(4-pyridyl)ethylene. The extent of delocalization of the complexes mentioned above was estimated from values for the delocalization parameter and solvent dependence of the energy of the intervalence transfer band. When 1,2-bis(4-pyridyl)ethane was employed as the bridging ligand, the ruthenium centers were found to be uncoupled. This result is understandable since the pyridine groups of the bridge are linked by methylene groups so there is no continuous orbital pathway for electron movement between the ruthenium centers. The studies also show a high-energy shift in the peak of the intervalence band for L=pyz when substituting Cl with NO_2 then CH_3CN. The observed trend is accounted for in terms of the nature of each substituent. The CH_3CN group is a π-acceptor and, of the three ligands, it is expected to make the greatest contribution towards stabilization of the $[(bpy)_2L'Ru^{II}$-] end of the complex through electron delocalizaion. Back donation of electron density to the $[-Ru^{III}(NH_3)_5]$ end of the dimer, through the bridging group, is expected to effect further stabilization. The enhanced stability of the mixed-valence state results in a greater value for the intervalence transition energy.

A class II description is appropriate for several unsymmetrical homobinuclear

complexes based on ferrocene. Compounds of particular interest were those containing ring substituents, which force the biferrocene moiety to adopt a skewed conformation[49,50] and in doing so reducing the extent of π-overlap between the cyclopentadienyl rings on adjacent ferrocene units. The finding was reduced metal-metal interaction relative to cases where a trans configuration and consequently improved π-overlap is possible. In other studies,[51] asymmetry was introduced by linking the upper and lower cyclopentadienyl rings on one ferrocene unit, with methylene groups. The latter studies featured ferrocene units which were substituted in such a manner that formation of the trans conformation was not inhibited. A cursory investigation reveals that metal coupling appears to be affected by the nature of the methylene linkages but not in a straightforward relation. Further work needs to be done on there systems in order to determine the precise nature of the effect of bridges on Fe-Fe interactions.

1.3.4 Heterobinuclear Mixed-Valence Compounds

Taube's group originally investigated cobalt-ruthenium complexes using the cobalt(III) center as an oxidizing species for the ruthenium(II) center,[57,58] with the objective of studying the rate parameters for adiabatic electron transfer. These compounds were compared with ruthenium dimers in assessing the metal- metal interactions and were classified as valence trapped species. The observed lack of rate dependence of the thermal electron transfer on the metal-metal interaction is difficult to explain in light of what is known about class II complexes.

Table 1.1 Data for Selected Heterobinuclear Compounds Prepared Prior to 1981

Compound	IT Bands(kK)	Ref
$[(NH_3)_5CoNCM(CN)_5]^{6-}$		52
M=Fe	25.95	
M=Ru	32.05	
$[(CN)_5CoNCM(CN)_5]^{-}$		53
M=Fe	26.0	
M=Ru	32.1	
$[(NH_3)_5RuNCM(CN)_5]^{-}$		54
M=Fe	10.4	
M=Os	12.6	
$[(CN)_5FeNCM(CN)_5]^{6-}$		54
M=Ru	12.5	
M=Os	9.4	
$[(NH_3)_5CoNCRu(CN)_5]^{-}$	26.6	52
$[(NH_3)_5RuNNOs(NH_3)_5]^{5+}$	4.3, 7.7	55
$[(His)_2CoNCFe(CN)_5]^{3-}$ [a]	~20.0	56

a) His is histidine

Contributions from non-adiabatic factors were invoked in order to explain the rate of electron transfer in these complexes.

Given in Table 1.1 are data related to selected heterobinuclear complexes which were prepared and investigated spectroscopically prior to the year 1981. Characterization of intervalence transfer properties in accordance with the Robin and Day scheme was not accomplished.

The first heterobinuclear discrete class II complexes prepared and characterized in accordance with the Hush criteria were reported in 1981.[59] The cyano and acrylonitrile bridges of these ferrocene-ruthenium ammine complexes afford an effective orbital pathway for electron transfer. The class II behavior of the mixed-valence species $[FcCNRu^{III}(NH_3)_5]^{3+}$ may be attributed to extensive delocalization of the electron in the ferrocene end resulting in only a weak interaction through the bridge.

The mixed-valence properties of four representative heteronuclear dimers are summarized in Table 1.2. The intervalence transfer properties of the complexes presented point to a weakly coupled formulation and the linear solvent dependence of the absorption energy on E_{op} corroborates this class II description.

Investigations on the compound $[(bpy)_2ClOs(pyz)Ru(NH_3)_5]^{4+}$ have revealed, in a cursory fashion, that the extent of valence trapping is medium dependent.[47] The initial site of oxidation in electrochemical studies was shown to be dependent on the solvent in which measurements were taken. Similar manipulation of the extent of delocalization has been demonstrated with biruthenium complexes in mixed solvent systems.[48,60]

Other features of heterobinuclaer complexes which are represented in Table 1.2 deserve comment. It is generally observed that the measured band width at half height for the intervalence band is greater than the theoretically predicted value for class II compounds. Apart from the shortcomings introduced by the assumptions made in deriving equation 1.13, discrepancies could be introduced through lack of

accounting for certain vibrational modes in the theoretical equation which was derived for $h\nu \ll kT$. The presence of active low energy metal-ligand vibrations in the mixed-valence system may result in a broader absorption profile than theoretically predicted. Other observations made in relation to peak width are concerned mainly with osmium-ruthenium dimers. Spin-orbit coupling causes splitting, in the vicinity of 4000 cm^{-1}, in the $d\pi$ orbitals which are localized on the osmium ion.[43] The result is the appearance of more than one transition in the near infrared region, depending on the magnitude of the spin-orbital splitting energy. The recognition of transitions due to spin-orbit coupling was first made for the complex $[(bpy)_2ClOs(PPh_2CH_2Ph_2P)ClOs(bpy)_2]^{3+}$ [43] in which case the intervalence transfer band was determined as the broad band whose energy is a function of the solvent. Analogous splitting of the $d\pi$ orbital in ruthenium complexes is proposed but the energy separation is calculated to be too small to appear as structure on the intervalence transfer band. The result is a broad absorption band.

Another feature of Table 1.2 worth mentioning is the agreement between the measured and calculated values of $\Delta\nu_{1/2}$ for $[(bpy)_2ClRu(4,4'\text{-bpy})OsCl(bpy)_2]^{3+}$. The bridging ligand is relatively large in size and may be responsible for contributions to energetic adjustments subsequent to electron transfer. Since the value of E_{op} and hence $\Delta\nu_{1/2}$, is influenced by the nature of the bridging ligand, then, in light of current knowledge, the result should be considered as fortuitous rather than interpreted as giving greater credence to the theoretical equation.

The effect of changing the bridging ligand, on the extent of delocalization, is

Table 1.2 Data for Selected Heterobinuclear Mixed-Valence Complexes

Compound	L	$\Delta\nu_{1/2}$ (calc) cm^{-1}	$\Delta\nu_{1/2}$ (obs) cm^{-1}	α^2	ϵ $M^{-1}cm^{-1}$	Ref
$[FcLRu(NH_3)_5]^{3+}$	CN	$3.7x10^3$	$4.9x10^{3a}$	$2.3x10^{-3}$	412	59
$[(bpy)_2ClOsLRu(NH_3)_5]^{3+}$	pyz	-	$1.3x10^{3b}$	$2x10^{-3c}$	1200	47
$[(CN)_5FeLRu(NH_3)_5]$	pyz	$3.7x10^3$	$4.3x10^3$	$9.8x10^{-3}$	1550	61
$[(bpy)_2ClRuLOsCl(bpy)_2]^{3+}$	pyz	$4.1x10^3$	$4.3x10^3$	$4.6x10^{-3}$	1120	62
$[(bpy)_2ClRuLOsCl(bpy)_2]^{3+}$	4,4'-bpy	$4.9x10^3$	$4.9x10^3$	$5.4x10^{-3}$	370	62

a Dowling, N.I. PhD Thesis, University of Guelph, 1983.

b value calculated from estimate of the extinction coefficient

c estimated value

observed in the values for the delocalization parameters for $[(bpy)_2ClRu(pyz)OsCl(bpy)_2]^{3+}$ and $[(bpy)_2ClRu(4,4'\text{-}bpy)OsCl(bpy)_2]^{3+}$. The requirement for constant E_{in} and E_{out} is achieved by careful choice of metal-ligand systems. A greater value of α^2 for L=pyz, implies an enhancement in delocalization relative to 4,4′-bpy, a result which is expected on the basis of the distance dependence of metal-metal interactions.

Mention should be made of the data for the complex $[(CN)_5Fe(pyz)Ru(NH_3)_5]$ which was first reported in 1977,[63] but its intervalence transfer properties were never unequivocally characterized. A later report by Haim[64] favoured a class I valence isolated formulation. Such classification seemed to be at variance with information acquired from similar systems. The iron end of the complex, $[(CN)_5Fe^{II}\text{-}]$, is isoelectronic with $[^{II}Ru(NH_3)_5]$ and the two units are reportedly very similar in chemistry when iron(II) is in the t_{2g}^6 configuration,[65,66] therefore the stabilization effects of back bonding through the bridging ligand ought to be operative in the iron-ruthenium mixed-valence complex as in the case of the Creutz-Taube ion, $[(NH_3)_5Ru(pyz)Ru(NH_3)_5]^{5+}$. A further argument in favour of weak coupling of the iron-ruthenium centers is the weakly coupled formulation applied to the complex $[(CN)_5Fe(pyz)Fe(CN)_5]^{5-}$. Class II behaviour implies that the valence trapping effects of the $[(CN)_5Fe^{II}\text{-}]$ unit, owing to electron delocalization by back-bonding through the cyano ligands, are not difficult to overcome. A recent preparation and reinvestigation of the complex $[(CN)_5Fe(pyz)Ru(NH_3)_5]$ showed definite class II characteristics.[60] The extent of delocalization in the complex was

determined as being less than 1% and the interaction energy was calculated as 600 cm^{-1}.

The foregoing points toward general similarities in the intervalence transfer characteristics between homonuclear and heteronuclear mixed-valence complexes. Heteronuclear complexes are more versatile for investigative work in that they allow simultaneous examination of valence trapping and bridge-metal energy match effects.

1.4 Bridges in Binuclear Mixed-Valence Complexes

Early studies on electron transfer phenomena have acknowledged the importance of the role of the intervening species between the two interacting metal ions. A substantial number of studies have been dedicated to elucidating the role of the bridge in electron transfer reactions. To date, mixed-valence complexes with a wide variety of bridging systems have been prepared and studied. The important feature of discrete complexes is the sharing of a bridging entity which has electron mediating properties.

The mechanism of coupling which is propagated through bridges is intimately related to the π-acceptor ability of ligands with low-lying unfilled π^* orbitals and the π-donor ability of ligands with filled π-orbitals. In general, orbital overlap is postulated[13,67] as essential to the propagation of inner sphere metal-metal interaction. Figure 1.2 is a schematic representation of the type of orbital overlap which leads to through-bridge coupling of the metal ions.

The work of Richardson and Taube[68] represents one of the more recent efforts

to provide a theoretical description of bridge assisted intervalence transfer processes. The provisions of their work form a reasonably good basis for predicting the intervalence transfer properties for biruthenium ammine complexes with cyano derived organic bridging ligands. Since the validity of the treatment has been established, it is reasonable to expect future extrapolation of the expressed ideas behind the theory to more complicated systems.

The essential ideas of the theoretical treatment of Richardson and Taube combine the principles of superexchange theory with Mulliken[69] expressions on spectroscopic parameters. One of the more important equations emerging from the treatment is the expression for the delocalization parameter.

$$\alpha = \frac{\beta_1\beta_2}{h\nu_{IT}} \left(\sum_{i=1}^{m} \frac{a_{iN}^{*} a_{iN'}^{*}}{E_i^{*} - E_o} - \sum_{i=1}^{n} \frac{a_{iN} a_{iN'}}{E_i - E_o} \right) \qquad 1.22$$

β is a constant which depends on the orbital overlap, $E_i^*-E_0$ and E_i-E_0 are taken as the energies of the MLCT and LMCT states respectively and a_{in} and a_{in}^* are coefficients of the 2p orbital on the bridging ligand. Equation 1.22 demonstrates a few points about the functioning of the bridging system. When α is large, $E_i^*-E_0$ is small, indicating that there should be a reasonably good energy match between the metal π and the ligand π^* orbitals. A point in corroboration of this result is the increase in metal-metal interaction found for good π-acceptors. When the charge

Figure 1.2 Schematic Representation Of π-Overlap Between Ligand Bridge and Metal Orbitals.

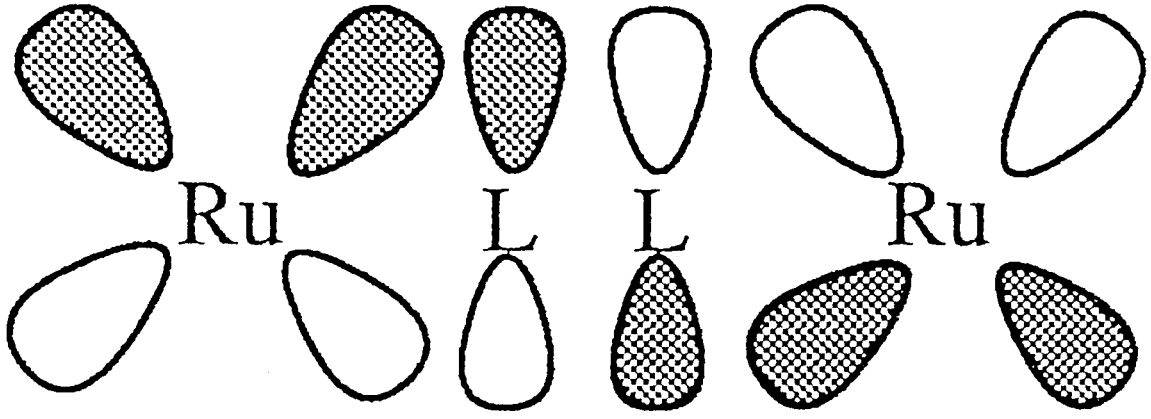
Ru
L
L
Ru

transfer energies are large $E_i^*-E_0$ and E_i-E_0 will be very large and the coupling will be small. The coupling dependence on both the HOMO and the LUMO is expressed in the inverse relationship between the energy differences $E_i^*-E_0$ and E_i-E_0 and the valence delocalization parameter.

1.5 Mixed-Valence Schiff Base Complexes

Although the majority of work on the spectroscopic properties of mixed-valence systems has focussed on dimeric and trimeric types of systems, there is an emerging interest in molecular units based on Schiff bases. The schematic structure for one of the more frequently studied macrocyclic systems is shown below:

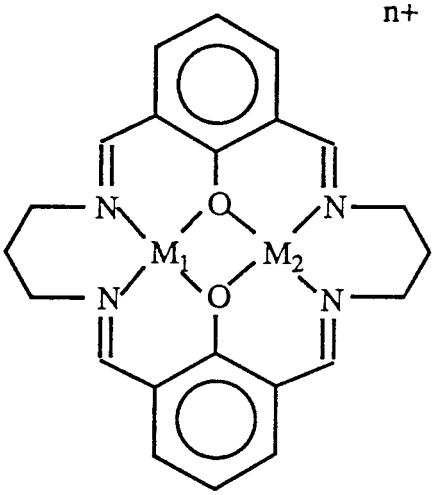

I

Structure I contains two metal ions in very close range of each other (~3.15 Å).[70] Lintvedt[71] argues in favour of antiferromagnetic coupling in a related system on the basis of EPR and magnetic susceptibility data hence the expectation that other types of through-bond interactions may be possible. Close examination of structure I

reveals that a through-bond interaction is possible via oxygen atoms.

Oxo-bridged ruthenium dimers of composition $[(AA)_2XRuORuX(AA)_2]^{n+}$ where AA is 1,10-phenanthroline or 2,2′-bipyridine and X is Cl^-, NO^- or H_2O, have been prepared and investigated by Meyer.[72] The mixed-valence species were determined as delocalized from ESCA measurements. Gagne[70] proposes extensive delocalization as being responsible for the largely separated peak potentials in the complexes $[(NH_3)_5RuORu(NH_3)_5]^{5+}$ [73] and $[(bpy)_2ClRuORu\text{-}Cl(bpy)_2]^{3+}$ [72] on the basis of the conproportionation constant ($K_c = 10^{34}$ and 10^{38} respectively). The same argument has been extrapolated to a number of iron, cobalt and copper complexes of I which have been designated as delocalized. The above results suggest that interactions through oxygen bridges of Schiff base complexes may lead to class III systems.

Mixed-valence copper complexes derived from I furnished data which could not be interpreted unequivocally.[74] One indication in favor of a class III description is the high value obtained for the conproportionation constant ($K_c = 4.83 \times 10^6$) for the reaction given below

$$[1,1] + [2,2] \rightarrow 2[2,1] \qquad 1.23$$

where the oxidation state for each copper ion is represented in parentheses. The value of the conproportionation constant is in the region of that obtained for the Creutz-Taube ion and is much larger than those for class II compounds. Spectroscopic measurements produced data for an intervalence transfer transition in

the near infrared region, however, the complex was not classified according to the Robin and Day scheme. The reason for this exclusion is tied to the complex nature of the intervalence transfer band when measured in various solvents. In contrast to the near infra-red data, EPR measurements provided data consistent with a valence trapped description, at least on the timescale of that experiment (10^{-8} to 10^{-4} s).

Although the mixed-valence properties of related Schiff base complexes of iron[75] and ruthenium[76] have been studied, there is a dearth of information on how well these complexes conform to the Hush model.

1.6 Polynuclear Mixed-Valence Systems

In the interest of providing a greater understanding of the nature of electron transfer processes in extended systems, linear mixed-valence complexes were prepared and investigated. Of key importance was the detection of interactions between the remote metal sites, giving rise to long range electron transfer. Taube[77] provided evidence of end-to-end metal interaction in the system $[(NH_3)_5Ru(pyz)Ru(NH_3)_4(pyz)Ru(NH_3)_5]^{7+}$. A composite band in the near infra-red region was interpreted as comprising of the following two transitions

$$[3,2,2] \rightarrow [2,3,2]$$

and

$$[3,2,2] \rightarrow [2,2,3]$$

Polymeric systems of composition $[(NH_3)_5RuLRu(bpy)_2LRu(NH_3)_5]^{6+}$,[78] $[Fc(Fc)_nFc]^{m+}]$[78] (n = 1 to 3) and $[Ru(NH_3)_5RuNCFcCNRu(NH_3)_5]^{5+}$ [79] were prepared, however, spectroscopic examination revealed only isolated adjacent site interactions.

1.7 Scope of the Study

The objective of this project is to examine the mixed-valence properties of a number of Schiff base complexes of iron, ruthenium and cobalt with a view to gathering information towards assessing their utility as polyelectron transfer catalysts, particularly for dioxygen reduction. Two important requirements are the reversible uptake of oxygen and a polyelectron transfer capability. Choice of the Schiff base unit is based on literature evidence of these complexes for oxygen sensitivity and the electroactive ferrocene unit was incorporated into the assembly to provide the polyelectron capability. The relatively good facility with which ferrocene is functionalized permits the synthesis of polyketones from which Schiff bases are prepared. Complexes of cobalt, iron and ruthenium are readily prepared resulting in systems each with two ferrocene units. Schematic structures of prepared complexes are shown below. These structures are interesting from several points of view. Structure II is a non-linear polynuclear mixed-valence system whose structure is such that any interaction between the ferrocene units must occur through the central metal ion of the Schiff base, providing an example of yet another remote site through-metal interaction. System III permits the simultaneous study of remote and

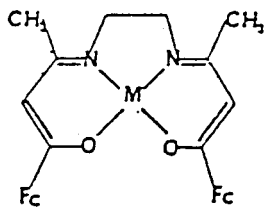

II

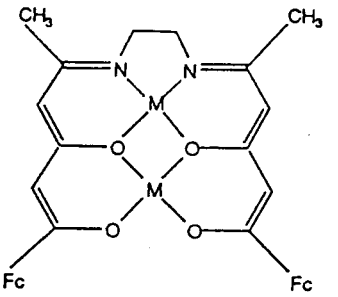

III

adjacent site interactions.

The Schiff base complexes described above may be extended to polymeric systems in which case several metal ions will be available as reaction sites and electron sources. The project was envisioned as developing in such manner.

In view of the proposed seven coordinate species[80] ruthenium tris(β-diketonato) complexes were prepared and examined with regard to their intervalence properties. These types of complexes are proposed to be delocalized in nature. They were compared with similar iron complexes. A Schematic representation of tris(β-diketonato) complexes is shown below.

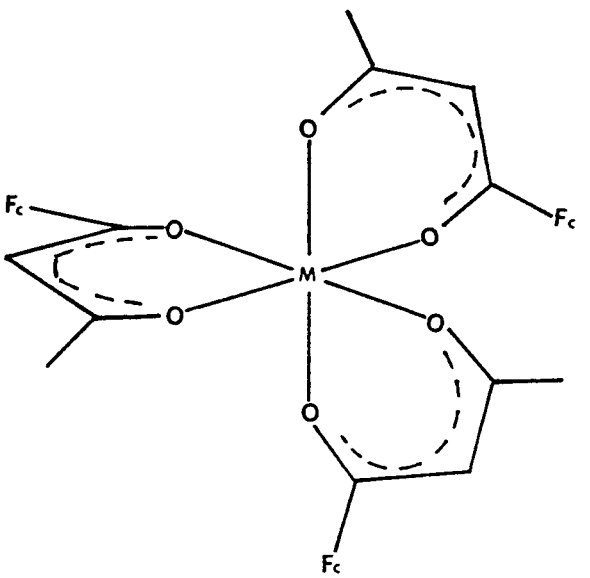

CHAPTER 2

EXPERIMENTAL

2.1 Reagents and Materials

Most of the starting materials and reagent grade solvents were purchased from Aldrich Chemical Company and were used as supplied except in cases when otherwise is stated. Anhydrous solvents were dispensed from Sure Seal™[81] bottles for storage of air-sensitive reagents. Dry ethyl ether was prepared by distillation of the wet solvent from calcium hydride under nitrogen. The dry solvent was stored over molecular sieve (Davison Chemical 4 Å) and under argon. Spectroscopic grade solvents supplied by Aldrich Chemical Company were used for recording ultraviolet-visible spectra.

2.2 Techniques

The preparation of polyketones required moisture exclusion techniques. All reaction glassware were dried overnight at 110 °C before use. The apparatus was assembled and lightly flamed while passing argon through the system. Moisture sensitive solvents and solutions were transferred via cannulas and/or syringes. Reflux reactions under nitrogen or argon were normally performed in a three-neck round

bottom flask fitted with a condenser, an inert gas adapter and a suba seal septum. Reagents were introduced through the neck with the septum. The reactions were accomplished under a slight positive pressure of the inert gas.

Several of the prepared Schiff base complexes were found to be air-sensitive. Their syntheses were accomplished in Schlenk glassware with ground glass tapered joints which facilitates rapid assembly and dismantling procedures. Preparations were performed with the apparatus attached to a manifold with a two-way valve which permits alternate argon purge and evacuation procedures. Prior to use, the apparatus was subjected to five evacuation/purge cycles. Solids were introduced under argon. Solvents were deoxygenated by purging with argon for a period of 20 min. Refluxing was accomplished in a Schlenk reaction flask fitted with a condenser and having a slight positive pressure of argon. The air-sensitive products were stored under argon in vials with caps containing Teflon™ mininert valves.

Product identification methods include ^{1}H, ^{13}C, ^{31}P or ^{19}F NMR spectroscopy, infra-red spectroscopy and cyclic voltammetry. Microanalyses and spectroscopic characterizations are presented in Chapter 3.

2.3 Instrumentation

Ultraviolet and visible spectra were recorded in the solution phase on a Perkin Elmer PE 330 grating spectrophotometer. Infrared spectra were recorded as nujol or fluorolube mulls on a Perkin Elmer Model 1310 infrared spectrophotometer. NMR spectral measurements were made on a 300 MHz Varian VXR 300

spectrometer operating in the Fourier transform mode.

2.4 Preparation of β-Polyketones

1-Ferrocenyl-1,3-Butanedione (FcBD): The solvent 1,2-dimethoxyethane (120 mL) was transferred to a round bottom flask under nitrogen and cooled to -70 °C with a dry ice/methanol mixture. Methyllithium (45 mL of a 1.4 M solution in diethyl ether) was added under nitrogen then diisopropylamine (9.0 mL) was introduced into the mixture. The solution was stirred for 30 min and the temperature of the system was allowed to rise to room temperature. Acetylferrocene (12.3 g) was added and the solution was stirred for 1 hr before introducing methylacetate (7.5 mL). The reaction system was stirred for 6 hr under nitrogen at room temperature then the solid precipitate which formed was quickly filtered and washed with dry ethyl ether. The solid residue was added to 200 mL of M hydrochloric acid and slightly heated. The hydrolyzed product was then extracted with three 100 mL portions of ethyl ether. The combined ethereal phases was dried over magnesium sulfate and evaporated to recover a red black solid. The crude product was chromatographed on silica gel (grade 12) using dichloromethane as eluant. The first 40 mL off the column was discarded. The dichloromethane was evaporated to recover a dark red solid which was recrystallized from heptane. The yield was 27%.

1,1,1-Trifluoro-4-Ferrocenyl-2,4-Butanedione (FcTFBD): The synthesis of this red compound was accomplished using the procedure for preparing FcBD but with acetyl

ferrocene and trifluoroacetate as starting materials. Identical mole ratios were required. The crude product was chromatographed on silica gel (grade 12) and recrystallized from hexane, giving a yield of 26%.

1-Phenyl-3-Ferrocenyl-1,3-Propanedione (FcPPD): The preparation of this red compound was accomplished using the procedure for FcBD, with acetyl ferrocene and methyl benzoate as starting materials. The solid was purified according to the procedure for FcTFBD. The yield was 40%.

Methyl Ferrocenate: This ester was prepared by a Fisher esterification of ferrocene carboxylic acid in methanol. A saturated alcoholic solution of hydrochloric acid was prepared by passing dry gaseous hydrochloric acid through anhydrous methanol (80 mL) in a round bottom flask, until vapor could be seen rising from the surface of the solvent. Ferrocene carboxylic acid (2.34 g) was then added to the methanol and the solution was refluxed for 16 hr. Water was slowly added to the cooled solution in order to precipitate the yellow ester. The product was dried and recrystallized from an ethanol/water mixture. The recrystallized product was dried in vacuo over phosphorus pentoxide. The yield was 66%.

1,Ferrocenyl-1,3,5-Hexanetrione (FcHT): The yellow ester from the synthesis reported above was used in a Claisen type condensation with 2,4-pentanedione to form the triketone. The synthesis is based on the procedure for triketone

preparation developed by Miles *et al.*[82]

The solvent 1,2-dimethoxyethane (150 mL) was transferred to a dry degassed flask fitted with a condenser. Sodium hydride (1.47 g of a 60% dispersion in mineral oil) was added under nitrogen, the suspension was brought to reflux under nitrogen then 2,4-pentanedione (1.25 mL) was syringed into the flask very slowly. Refluxing was continued for one hour during which time 3 g of 18-crown-6 was introduced into the flask. Methyl ferrocenate (2.98 g) was added to the reaction system and refluxing was continued for 14 hr. The solvent was then removed on a rotary evaporator, the flask was placed in an ice/water mixture and 75 mL of diethyl ether was added at 0°C (slowly at first). The aqueous phase was separated and the ethereal phase was extracted with 90 mL of water then 90 mL of 1% sodium hydroxide solution. The aqueous phases were combined and the product was poured into a mixture of 100 g of crushed ice and 50 mL of concentrated hydrochloric acid. The pink precipitate formed was filtered and air dried to give the crude product which was then recrystallized from heptane and a brick red solid was obtained. The yield of the recrystallized product was 50%.

2.5 Preparation of Schiff Bases

The general procedure for preparing ferrocene-containing Schiff bases involved dissolving the β-diketone and ethylenediamine in benzene or ethanol in a 2:1 mole ratio. Either the product precipitated after stirring with slight heating for about 15 min or the solution was gently refluxed for 30 min after which the solvent was

evaporated under vacuum. In the latter case, the compound formed as an oil and was used in the preparation of the Schiff base complexes without purification.

The system of nomenclature places the polyketone from which the Schiff base is derived, in parenthesis.

Bis(1-Phenyl-1,3-Butadione)ethylenediimine (BPBD)en: White crystals of this compound were prepared according to the procedure of M^{c}Carthy *et al.*[83] and recrystallized from toluene.

Bis(1,1,1-Trifluoro-2,4-Pentanedione)ethylenediimine (BTFPD)en: White crystals of this compound were obtained using the procedure of Martell *et al.*[84] and recrystallized form 50% ethanol.

Bis(1-Ferrocenyl-1,3-Butanedione)ethylenediimine (BFBD)en: A brown yellow solid was obtained by the general procedure and recrystallized from heptane.

Bis(1-Phenyl-1,3,5-Hexanetrione)ethylenediimine (BPHT)en: A green crystalline compound was obtained using the procedure developed by Lintvedt *et al.*[85] The crude product was recrystallized from acetone.

Bis(1-Ferrocenyl-1,3,5-Hexanetrione)ethylenediimine (BFHT)en: This brown orange compound was prepared by the general procedure outlined at the beginning of this

section. The product separated as an oil.

2.6 Preparation of Schiff Base Complexes of Dipositive Ions

The following are preparative procedures for Schiff base complexes of iron, ruthenium and cobalt. All M^{2+} complexes showed at least a small degree of sensitivity to air.

In preparing Schiff base complexes incorporating ferrocene, the ligands were usually prepared in ethanol, which was evaporated under vacuum at the end of the reaction in order to recover the product. The ferrocene-containing ligand was found to separate as an oil which was difficult to obtain in the solid form after dissolution in most common solvents. The oil was then dissolved in the degassed solvent for the preparation of the complex.

The system of nomenclature used here first gives the Schiff base ligand from which the complex is derived, then the axial ligands followed by the metal ion.

2.6.1 Schiff Base Complexes of Iron(II)

Schiff base complexes containing iron(II) as the central metal ion were prepared in Schlenk apparatus using the procedure developed by Niswander and Martell[86] in which a deoxygenated aqueous solution of ferrous sulfate heptahydrate was added to a solution of the appropriate ligand in an argon purged 1:1.7 mixture of 1-propanol and pyridine. The reactants were added in a 1:1 mole ratio of ferrous sulfate to Schiff base for mononuclear complexes and a 2:1 ratio for binuclear

complexes. The reaction mixture was refluxed for 12 hr under argon then the solvent was evaporated to half volume under vacuum in order to precipitate the product. The air-sensitive products which resulted were filtered, dried in vacuo and stored under argon.

Ethylenediiminebis(1-Phenyl-1,3-Butanedionato)pyridineiron(II) [Fe(BPBD)enPy]: This Schiff base complex was prepared from (BPBD)en and ferrous sulfate heptahydrate. The purple solid was recrystallized from a 1:1 pyridine/1-propanol mixture. The solid product was found to be stable, when in the solid form, for several weeks when stored under argon. In solution the color becomes orange after prolonged exposure to air and a yellow precipitate forms.

Ethylenediimenebis(1-Ferrocenyl-1,3-Butanedionato)pyridineiron(II) [Fe(BFcBD)enPy]: The ligand (BFcBD)en was prepared in ethanol and the complex was prepared according to the general procedure outlined above. The crude product was recryltallized from a mixture of acetonitrile and water to give a red brown solid. The product was stable in the solid form but decomposed verly rapidly when in solution in which case a brown orange precipitate forms.

Ethylenediiminebis(1-Phenyl-1,3,5-Hexanetrionato)dipyridinediiron(II) [Fe_2(BPHTen$(Py)_2$]: A brown purple crystalline solid was obtained. The product was air stable when in the solid form.

Ethylenediiminebis(1-Ferrocenyl-1,3,5-Hexanetrionato)dipyridinediiron(II) [Fe_2(BFcHT)en$(Py)_2$]: A red crystalline solid was obtained. The product was extremely air-sensitive and consequently was difficult to handle.

2.6.2 Schiff Base Complexes of Ruthenium(II)

Mononuclear ruthenium(II) Schiff base complexes were prepared in Schlenk apparatus by a modification to the procedure reported by Thornback and Wilkinson.[87] The ferrocene-containing ligands were prepared in ethanol. The general procedure involved dissolving the ligand in deoxygenated tetrahydrofuran followed by the addition of sodium hydride in a 2:1 mole ratio to the Schiff base. A stoichiometric quantity of solid tris(triphenylphosphine)ruthenium(II) chloride (Strem) was added and the mixture was refluxed under argon for at least 24 hr. The solvent was evaporated under vacuum to approximately one-third the original volume and petroleum ether was added in order to precipitate the product. The solid was filtered and washed with petroleum ether and dried on a vacuum line and stored under argon.

Ethylenediiminebis(1-Phenyl-1,3-Butanedionato)bis(triphenylphosphine)-ruthenium(II): [Ru(BPBD)en$(PPh_3)_2$]: This compound was obtained by the general procedure outlined above, as a brown solid which was stable under argon for about one month.

Ethylenediiminebis(1,1,1-Trifluoro-2,4-Pentanedionato)bis(triphenylphosphine)-ruthenium(II) [Ru(BTFPD)en(PPh_3)$_2$]: This compound was obtained as a light brown solid which was found to be stable for a minimum period of one month in the solid form when stored under argon.

Ethylenediiminebis(1,1,1-Trifluoro-4-Ferrocenyl-2,4-Butanedionato)bis(triphenyl-phosphine)ruthenium(II) [Ru(BTFFcBD)en(PPh_3)$_2$]: The crude product was dissolved in acetone, the solution was filtered, then the solvent was evaporated. The oil which formed was dissolved in THF then recovered by the addition of petroleum ether. The dark brown solid obtained was found to be stable under argon for several weeks.

Ethylenediiminebis(1-Ferrocenyl-1,3-Butanedionato)bis(triphenylphosphine)-ruthenium(II) [Ru(BFcBD)en(PPh_3)$_2$]: The product was obtained as a brown solid which was stable for several weeks under argon.

2.6.3 Schiff Base Complexes of Cobalt(II)

Mononuclear Schiff base complexes containing cobalt(II) were prepared in Schlenk apparatus by refluxing the appropriate ligand with a stoichiometric quantity of cobalt(II) acetate tetrahydrate in deoxygenated ethanol, under argon, for at least 6 hr. In the case of ferrocene-containing Schiff bases, the ligand was generated in situ using degassed ethanol. The product precipitated out of solution and was

filtered and stored under argon.

Ethylenediiminebis(1-Phenyl-1,3-Butanedionato)cobalt(II) [Co(BPBD)en]: The complex which precipitated was a red orange crystalline solid which was recrystallized from acetone. It was found to be stable indefinitely in the solid form.

Ethylenediiminebis(1,1,1-Trifluoro-2,4-Pentanedionato)cobalt(II) [Co(BTFPD)en]: An orange finely divided crystalline solid was obtained for this preparation which was accomplished by the method of Van Den Bergen *et al.*[88] The product was found to be air stable for more than two months when in the solid state.

Ethylenediiminebis(1-Ferrocenyl-1,3-Butanedionato)cobalt(II) [Co(BFcBD)en]: This compound was obtained as an orange solid which was recrystallized from acetone. The product was found to be stable for about two months, when stored under argon, after which time it decomposed to a brown solid.

Ethylenediiminebis(1,1,1-trifluoro-6-phenyl-1,3,5-Hexanetrionato)dicobalt(II) [Co_2(BTFPHT)en]: The preparation of this binuclear complex by the method of Kreh *et al.*[89] resulted in red crystals which were found to be air stable in the solid form for a period of more than two months.

2.7 Preparation of Schiff Base Complexes of Tripositive Ions

The following procedures were useful for the preparation of Schiff base complexes of iron(III) and ruthenium(III). They were all found to be air stable complexes.

2.7.1 Schiff Base Complexes of Iron(III)

Ethylenediiminebis(1-phenyl-1,3-butanedionato)chloroiron(III) [Fe(BPBD)enCl]: Anhydrous iron(III) chloride (0.41 g) was dissolved in approximately 10 mL of ethanol and added to a refluxing solution of the ligand (BPBD)en in approximately 30 mL of ethanol. Refluxing was continued for 10 hr then the volume of solution was reduced to approximately 10 mL. The purple black crystals which formed were filtered, washed with petroleum ether and air dried. The crystals were dissolved in hot benzene and reprecipitated by the addition of petroleum ether. They were then filtered, washed with petroleum ether and dried in vacuo.

Ethylenediiminebis(1-Ferrocenyl-1,3-Butanedionato)chloroiron(III) [Fe(BFcBD)enCl]: This compound was prepared according to the procedure for [Fe(BPBD)enCl] and a brown solid was obtained. The product was recrystallized from absolute ethanol.

Ethylenediiminebis(1-Phenyl-1,3,5-Hexanetrionato)dichlolodiiron(III) [Fe_2(BPHT)enCl$_2$]: This compound was obtained as a green black solid by the procedure for [Fe(BPBD)enCl].

2.7.2 Schiff Base Complexes of Ruthenium(III)

Potassium Ethylenediiminebis(1-Ferrocenyl-1,3-Butanedionato)dichlororuthenate(III) K[Ru(BFcBD)enCl$_2$]: The ligand (BFcBD)en (0.17 g) was dissolved in approximately 30 mL of hot absolute ethanol and the complex $K_2[RuCl_5.H_2O]$ (0.11 g) (Strem) was added in small portions. The solution was gently refluxed for 19 hr and a purple brown precipitate formed. The solid was filtered, washed with ethyl ether and recrystallized from absolute ethanol.

Potassium Ethylenediiminebis(1-Phenyl-1,3-Butanedionato)dichlororuthenate(III) K[Ru(BPBD)enCl$_2$]: This compound was obtained as a brown solid according to the procedure for K[Ru(BFcBD)enCl$_2$].

2.8 Preparation of Tris(β-diketonato) Complexes of Ruthenium(III) and Iron(III)

Preparation procedures for tris(β-diketonato) complexes of ruthenium and iron followed examples from the literature.

2.8.1 Iron Tris(2,4-diketonato) Complexes

Iron complexes were prepared[90] by dissolving anhydrous iron(III) chloride in water and adding a solution of the ligand in ethanol. The reaction was almost immediate, however, the reaction mixture was refluxed for fifteen minutes in order the ensure complete formation of the complex. The reagents were added in a 1:3 mole ratio of iron chloride to 2,4-diketone. The crude product, which precipitated

from the reaction solution, was filtered, dried, recrystallized from ethanol and dried in vacuo. The following complexes were all made by the procedure stated above.

Tris(1,1,1-Trifluoro-2,4-Pentanedionato)iron(III) [Fe(TFPD)$_3$]: (red solid).

Tris(1-Phenyl-1,3-Butanedionato)iron(III) [Fe(PBD)$_3$]: (red solid).

Tris(2,4-Pentanedionato)iron(III) [Fe(PD)$_3$]: (red solid).

Tris(1,1,1-Trifluoro-4-Ferrocenyl-2,4-Butanedionato)iron(III) [Fe(FcTFBD)$_3$]: (purple black solid).

Tris(1-Phenyl-3-Ferrocenyl-1,3-Propanedionato)iron(III) [Fe(FcPPD)]: (red brown solid).

Tris(1-Ferrocenyl-1,3-Butanedionato)iron(III) [Fe(FcBD)$_3$]: (red brown solid).

2.8.2 Ruthenium Tris(β-diketonato) Complexes

Ruthenium complexes were prepared according to the method of Endo *et al.*[91] in which a "ruthenium blue" solution is first prepared by refluxing, under argon, ruthenium chloride hydrate (40% Ru) in a mixture of 25 cm^3 of water and 50 cm^3 of ethanol in a water bath. Refluxing was continued until the color of the solution

turned blue. The appropriate ligand was added and refluxing was continued for about three hours. The solution was cooled and one portion of a stoichiometric amount of sodium hydrogencarbonate was added and refluxing was again continued for 2-3 hours under argon. This procedure was continued until the solution developed a red-purple color. The initial product was air oxidized to the Ru(III) species and the solution was concentrated to half the original volume. The precipitate which formed was collected by filtration and washed with cold ethanol. The crude material was dissolved in benzene and chromatographed on a column of alumina (Brockmann II neutral). The first fraction was collected while the second fraction remained at the top of the column. The solvent was evaporated to recover the solid which was recrystallized from ethanol. The following complexes were prepared in the manner stated above.

Tris(1,1,1-Trifluoro-2,4-Pentanedionato)ruthenium(III) [$Ru(TFPB)_3$]:(redcrystalline solid).

Tris(1-Phenyl-1,3-Butanedionato)ruthenium(III) [$Ru(PBD)_3$]: (dark red crystalline solid).

Tris(2,4-Pentanedionato)ruthenium(III) [$Ru(PB)_3$]: (dark red crystalline solid).

Tris(1,1,1-Trifluoro-4-Ferrocenyl-1,3-Butanedionato)ruthenium(III[$Ru(FcTFBD)_3$]:

(red solid).

Tris(1-Phenyl-3-Ferrocenyl-1,3-Propanedionato)ruthenium(III) [Ru(FcPPD)$_3$]: (red brown solid).

Tris(1-Ferrocenyl-1,3-Butanedionato)ruthenium(III) [Ru(FcBD)$_3$]: (red brown solid).

2.9 Equipment for Electrochemistry

Cyclic voltammetry and differential pulse polarography were performed on an IBM EC 225 voltammetric analyser equipped with a current feedback *i*R compensating *i*/E converter. Voltammograms were displayed on a Nicolet Model 206 oscilloscope equipped with a two channel unit. Permanent traces of the voltammograms were recorded on an IBM 7424 MT X-Y-T recorder. Potentials were read with an accuracy of approximately ± 2 mV.

Electrochemical measurements were made in a two compartment cell using a platinum flag working electrode, a platinum foil counter electrode and a saturated calomel reference electrode. The cell arrangement is shown in Figure 2.1.

2.10 Techniques For Electrochemical and Intervalence Transfer Studies

Sample measurements were recorded in mM concentrations in a suitable non-aqueous solvent which was 0.1 M in tetrabutyl-ammonium hexafloro-phosphate (TBAH). Cyclic voltammetric measurements were accomplished within the range -

2.0 to 2.0 V relative to a suitable internal standard and at a scan rate of 0.200 V s^{-1}. Voltammograms were used to determine the peak current ratio i_{pa}/i_{pc}, peak potentials, separations and formal potentials. It was observed that reproducibility was limited to approximately six scans after which adsorption on the working electrode caused immense variations in subsequent runs. Controlled potential coulometry was performed in the same cell that was used for cyclic voltammetry but with a platinum gauze electrode.

The electrolytic solution was deoxygenated by bubbling it with argon for at least 5 min. The argon gas (99.998%, Airco) was prescrubbed with two acidic chromous chloride solutions and dried by passage through sulfuric acid and drierite prior to application.

The electrochemical cell was routinely cleaned by rinsing it several times with distilled acetone then finally with reagent grade acetone followed by 2-propanol. Extensive cleaning was accomplished by soaking the cell in concentrated nitric acid, rinsing with copious amounts of water and finally following the procedure outlined above.

Solutions of cerium(IV) in acetonitrile were prepared by dissolving 2.74 g of cerium(IV) ammonium nitrate in 100 ml of acetonitrile to give an approximately 0.05 M solution in Ce(IV). The solution was appropriately diluted and standardized by measurement of the absorbance at 326 nm (ϵ = (6.98 ± 0.07) x 10^3 M^{-1} cm^{-1}).[92] Only freshly prepared cerium(IV) solutions were used.

Iodine solutions in acetonitrile were prepared by dissolving an appropriate amount

Figure 2.1 Schematic Representation of Electrolytic Cell

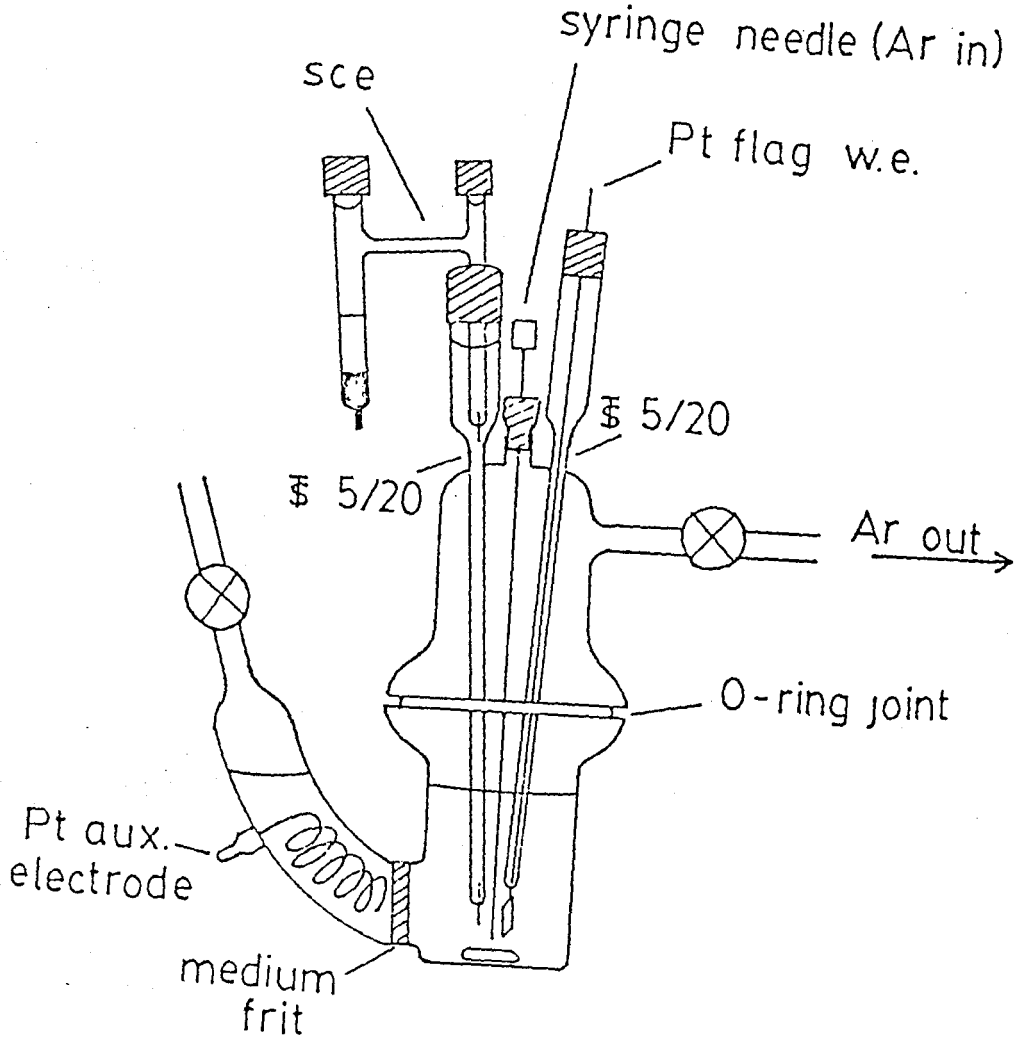
syringe needle (Ar in)
sce
Pt flag w.e.
$ 5/20
$ 5/20
Ar out
O-ring joint
Pt aux. electrode
medium frit

of the solid to give an approximately 0.1 M solution. The solution was standardized[93] against standard sodium thiosulfate.

Bromine solutions in acetonitrile were prepared by dissolving an appropriate volume of liquid bromine in acetonitrile to give a solution that was approximately 0.1 M. The solution was standardized against standard sodium thiosulfate in a similar manner to the case of iodine solutions.

2.11 Electrochemical Solvents and Electrolyte

The supporting electrolyte, TBAH was prepared according to the method of Lange and Muller[94] and recrystallized from 95% ethanol to give white needle-like crystals. The product was dried at 100°C for 24 hr and stored in a desiccator.

Acetonitrile, butyronitrile, propionitrile, benzonitrile, propylenecarbonate and dichloromethane were purchased as anhydrous or spectroscopic grade solvents. When spectroscopic grade solvents were used, solutions 0.1 M in TBAH were prepared by passing the solvent through an alumina column and directly into a volumetric flask containing a stopper with a mininert valve. The column contained a valve with a Luer lock for holding a stainless steel needle which fitted directly into the mininert valve. Anhydrous solvents were used directly.

Pyridine and dimethylsulfoxide (DMSO) were distilled from sodium hydroxide and stored under argon.

2.12 General Methods for Spectroscopy

Near infra-red spectra were recorded on a Perkin Elmer PE 330 grating spectrophotometer in the region 2100 to 800 nm. Intervalence transfer band maxima were read with and accuracy of approximately ± 5 nm. Samples were recorded in quartz cuvettes suitable for work in the near infra-red region, with a concentration of approximately 5.0×10^{-4} M in analyte. The mixed-valence species were generated by electrolyzing the solution containing the sample at a potential between the two peaks of interest, or by adding enough oxidant to oxidize one metal center. A sample of known concentration of complex in the appropriate solvent was prepared by syringing a specific volume of electrochemical solvent into the cell then introducing a weighed sample of the complex. The voltammogram was recorded in order to establish the potential at which electrolysis must be accomplished. After electrolysis, a portion of the solution was transferred, using a syringe, to an argon flushed cuvette and placed in an argon flushed sample chamber of the spectrophotometer. The cuvette was thermostatted at 25 ±2 °C for spectral measurements.

The electrochemical cell, syringes and needles were dried at 100 °C before use.

Infrared spectra were recorded on a Perkin Elmer PE 1310 spectrophotometer. Peaks were recorded with an accuracy of ± 2 cm^{-1}.

CHAPTER 3

RESULTS

3.1 Synthesis and Characterization of Ligands

One objective of the synthesis procedures was to produce ferrocene-containing Schiff base mononuclear and binuclear complexes of ruthenium, cobalt and iron. This was achieved in three steps.

(a) Preparation of the polyketone

(b) Preparation of the Schiff base ligand

(c) Preparation of the metal complex.

Schiff base condensations occurred with great facility therefore steps (a) and (c) proved to be the most challenging aspect of the preparative work. Preparations were usually based on reported procedures for similar compounds except for tris(2,4-diketonato) complexes of ruthenium(III) and iron(III) in which cases new preparative procedures were developed.

Diketones were prepared by a Claisen-type condensation between acetylferrocene and methyl acetate. The previously reported[95] procedure involved use of sodium amide as base, however, it was found that a safer method involving use of lithium diisopropyl amide could be used effectively although the yields were smaller.

Lithium diisopropylamide was generated by adding diisoproplyamine to a solution of methyllithium in diethyl ether.

Triketones were prepared by a literature procedure[82] which recommended the use of sodium hydride as base. An outline of the synthetic pathway is shown in Figure 3.1.

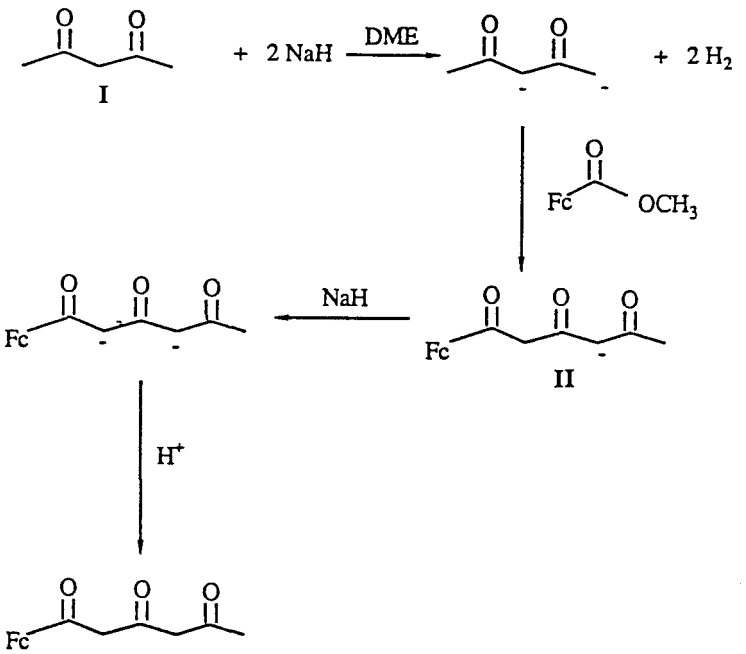

Figure 3.1 Synthesis Sequence for Triketones

The use of three equivalents of base is important since the monoanion II, initially produced, has an acidic proton which is capable of neutralizing the reactive position of the dianion of 2,4-pentanedione I. Initially, yields were less than 10% but improvement was achieved by the addition of 18-crown-6. Yields were improved to 50% in this manner.

Diketones containing trifluoromethyl groups were prepared in a similar manner.

The attempted preparation of the trifluorotriketone by a similar procedure resulted in the production of a diketone. This lack of success may be caused by the probable hydrolysis of the sodium salt of the initial triketone product to produce a diketone and trifluoroacetic acid.

Table 3.1 ^{1}H NMR Shifts for Prepared Polyketones

Compound	$-CH_3$	$-CH_2-$	$=CH-$
[FcBD]	2.08	2.30	5.70
[FcHT]	1.95	2.14-2.30	5.17-5.85
[FcTFBD]	-	-	6.08
[FcPPD]	-	-	6.37
[PHT]	2.01	2.30	5.31,5.81

3.1.1 NMR Characterization of Polyketones

^{1}H NMR data for the polyketones prepared are summarised in Table 3.1. Omitted from Table 3.1 are the signals arising from a monosubstituted ferrocene unit and the phenyl system in 1-phenyl-1,3,5-hexanetrione. These signals occur between 4.20 and 4.90 ppm in all polyketone compounds prepared. One prominent feature of Table 3.1 is the deshielding of the methyne proton of 1,1,1-trifluoro-4-ferrocenyl-2,4-butanedione relative to cases with terminal methyl groups.

There is strong evidence (from ^{1}H NMR studies) for the existence of more than one isomeric form of β-diketones in chloroform solvent. The possible structures for

the enol forms of β-diketones are shown below.

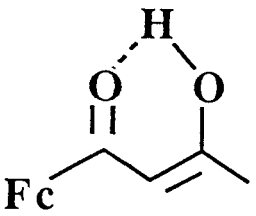

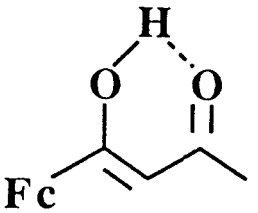

The precise location of the double bonds between the carbonyl carbons has not been elucidated, however, ^{1}H NMR signals corresponding to the methylene protons of the keto form are evident at ~5.70 ppm. Resonances corresponding to the keto forms are evident in the region 2.10-2.30 ppm (-CH_2-).

The ^{1}H NMR spectra for 1-ferrocenyl-1,3-butanedione shows largely the enol form whereas 1,1,1-trifluoro-4-ferrocenyl-butanedione and 1-phenyl-4-ferrocenyl-pentanedione were found to exist almost completely in the enol form. The known ^{1}H NMR spectrum of 2,4-pentanedione shows the same pattern of signals as for the β-diketones mentioned above. Enolization is known to occur to ~60% in this case.

The ^{1}H NMR spectrum for 1-ferrocenyl-1,3,5-hexanetrione (Figure 3.2) shows the existence of several isomeric forms. The signals occurring between 3.40 and 3.70 ppm are assigned to methylene protons which arise from the presence of the keto form. The signals within the range 5.1 to 5.7 ppm are ascribed to enolic protons from various enol forms. The terminal methyl protons have signals in the range 1.9 to 2.3 ppm. The spectrum for 1-phenyl-1,3,5-hexanetrione showed a similar pattern

but a lesser extent of enolization was observed.

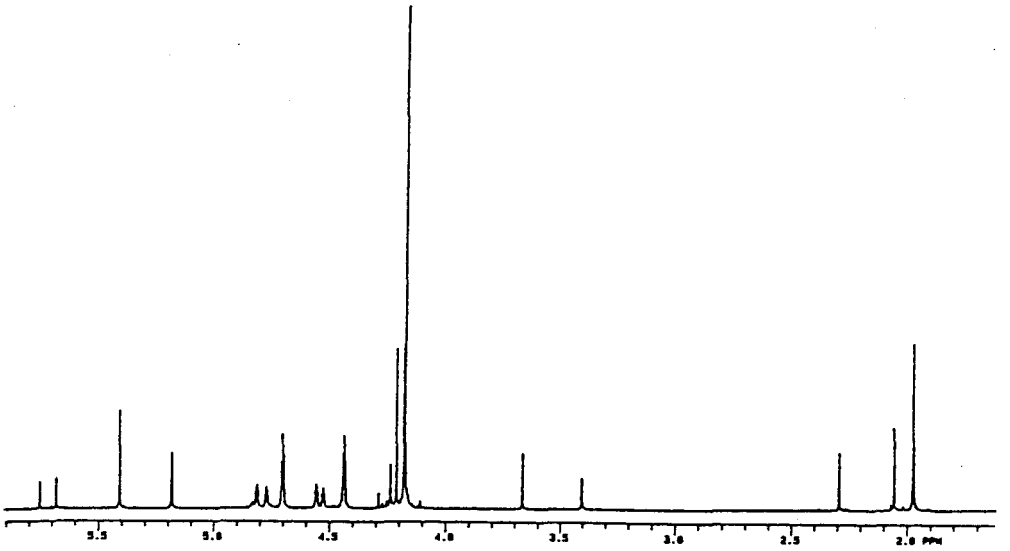

Figure 3.2 ^{1}H NMR Spectrum for 1-Ferrocenyl-1,3,5-hexanetrione

The compound 1-ferrocenyl-1,3,5-hexanetrione was purified by preparing the brown binuclear copper(II) complex, which is considered to be similar in structure to the polyketonate complexes prepared by Lintvedt and Fenton,[96] and regenerating the polyketone with phosphoric acid according to the method of Hauser and Lindsay.[95] The diamagnetic nature of the copper complexes prepared by Lintvedt was explained by antiferromagnetic coupling of the copper centers which are in close proximity.[97] Based on Lintvedt's structure, a schematic representation of the copper(II) complex is shown below. Characterization of the ferrocene complex by ^{1}H NMR showed a broad signal at 2.00 ppm (methyl protons), the monosubstituted ferrocene pattern was observed between 4.10 and 4.60 ppm and a broad signal at 6.15 ppm was indicative of methine protons. The line widths indicate that

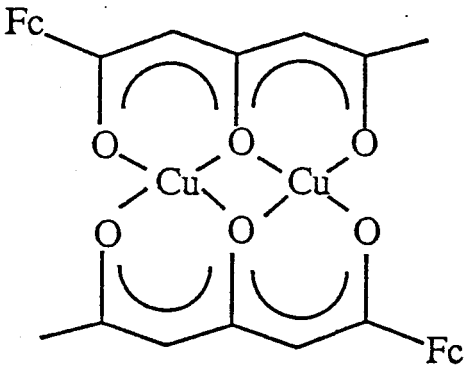

paramagnetism in the sample is not completely quenched. The ^{1}H NMR spectrum of the binuclear copper(II) complex provided a convenient means of characterizing the ferrocene triketone.

Data from ^{13}C spectra were also acquired for the polyketones. Such data, presented in Table 3.2, assist in corroborating the proposed solution structure of the compounds prepared.

Table 3.2 ^{13}C Chemical Shifts for Polyketones

Compound	$-CH_2-$	$-CH_3/-CF_3$	$=CH-$	$C=O$
[FcBD]	56.00	30.61,24.13	96.99	186.30,192.47
[FcHT]	51.13,53.44	21.88-30.00	94.56-100.83	-
[FcTFBD]	-	112.21-123.40*	93.31	-
[FcPPD]	-	-	93.72	179.50,194.14
[PHT]	49.94,54.87	21.92,30.05	95.84-100.82	173.63-193.90

*quartet

The general pattern for 1-phenyl-1,3,5-hexanetrione is upheld for the ferrocene-containing polyketones, with the ferrocene peak occurring between 67.00-73.00 ppm.

The ^{19}F spectrum was recorded for 1,1,1-trifluoro-4-ferrocenyl-1,3-butanedione and the fluorene shift was obtained at 78.39 ppm relative to trifluoroacetic acid at 78.50 ppm. This compares favorably with the signal at 79.31 ppm for 1,1,1-trifluoro-2,4-pentanedione. The ^{19}F signal was usually used as a means of identifying the product.

3.1.2 NMR Characterization of Schiff Base Ligands

The Schiff base of 1-ferrocenyl-1,3-butanedione was the only imine ligand which was consistently isolated in a tractable state. All other ferrocene-containing Schiff bases were obtained as oils. Table 3.3 presents a comparison of chemical shifts for the ^{1}H and ^{13}C NMR spectra of Schiff bases of 1-ferrocenyl-1,3-butanedione and 2,4-pentanedione. Assignments for the ferrocene-containing Schiff bases were based on those for existing model compounds. Table 3.3 shows that signals from the methyl and enolic protons shift upfield in the Schiff bases relative to the free polyketone. The same observation is made in relation to the formation of the Schiff base derivative of the ferrocene triketone. In all cases, and N-H signal was observed downfield at ~11.10 ppm, indicating that there may be tautomeric equilibrium between at least two forms. Possible isomeric structures are shown below.

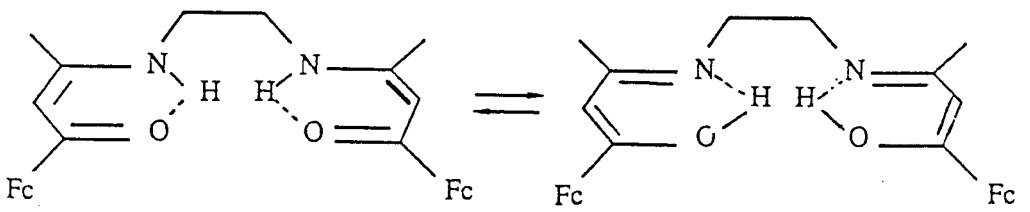

Table 3.3 Chemical Shifts for Schiff Base Ligands

Compound		$-CH_3$	$=CH-$	$-CH_2-$	C=O	C=N
[(BFcBD)en]	^1H	1.90	5.28	3.48	-	-
	^{13}C	19.6	93.8	44.0	192.5	162.4
[(BPD)en]	^1H	1.88,1.97	4.97	3.39	-	-
	^{13}C	18.5,29.0	96.5	42.7	195.6	162.5
[(BPBD)en]	^1H	2.07	5.72	-	-	-
	^{13}C	19.23	92.96	43.81	188.34	164.76
[(BFcTFBD)en]	^1H	-	6.08	3.41	-	-
[(BFcHT)en]	^1H	1.85-1.96	5.09-5.39	3.40	-	-
[(BPHT)en]	^1H	2.06	5.68	3.56	-	-
	^{13}C	19.23	92.93	43.77	188.26	164.78

Uninterpretable ^{13}C spectra were obtained for [(BFcTFBD)en] and [(BFcHT)en].

Further evidence for the presence of the amine isomer is provided in Figure 3.3.

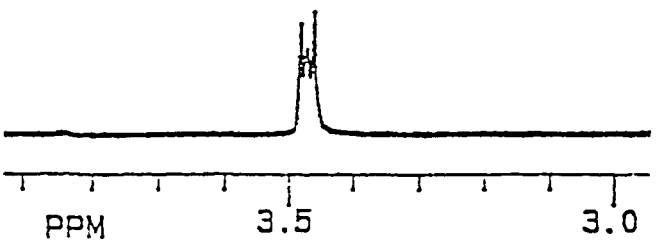

Figure 3.3 Multiplet at 3.48 ppm for [(BFcBD)en]

The intensity relation shows that the arrangement of signals is not one of a triplet.

The center peak is explained[98] as the signal due to the presence of the methylene bridge protons of the imine isomer, whereas, the outer peaks form a doublet arising from the splitting of the methylene protons by an adjacent N-H proton in the amine isomer.

3.1.3 Microanalyses

Table 3.4 summarises the results of microanalyses for the newly-prepared ferrocene diketones and the Schiff base derived from the ferrocene diketone.

Table 3.4 Microanalyses for [(BFcBD)en] and Ferrocene Diketones

Compound		%H	%C	%N	%F	%O
[FcHT]	calc.	5.17	61.57	-	-	15.37
	found	5.12	61.80	-	-	15.71
[FcTFBD]	calc.	3.42	51.89	-	17.59	-
	found	3.47	51.92	-	17.35	-
[(BFcBD)en]	calc.	5.72	63.86	4.96	-	5.67
	found	5.77	63.64	5.08	-	5.43

Oxygen determination was not possible for TFFcBD since the presence of fluorine interferes with the method of determination. The analyses for C, H, N and O are within acceptable ranges.

3.2 Mononuclear Schiff Base Complexes

Mononuclear complexes are considered to be those which contain one central metal ion such as iron, cobalt or ruthenium. The synthesis procedure for such Schiff base complexes involved refluxing the ligand with the metal ion of interest in a suitable solvent. Preparations of ruthenium(II) Schiff base complexes were accomplished in THF solvent and were precipitated from solution by the addition of petroleum ether. The source of ruthenium was the labile complex $Ru(PPh_3)Cl_2$, consequently, the product was expected to have axial triphenylphosphine groups coordinated to the central metal ion. The ^{31}P NMR spectrum of the product $[Ru(BFcBD)en(PPh_3)_2]$ revealed singlets at 19.2 ppm upfield relative to the starting material. This observation was also made for other ruthenium Schiff bases. The ^1H NMR spectrum displayed multiplets between 6.80 and 7.90 ppm indicating the presence of the triphenyl phosphine groups and singlets at 5.68 and 2.05 ppm associated with the Schiff base ligands. The signals belonging to the latter were significantly shifted relative to the free ligand and this is good evidence that complexation had occurred. Cyclic voltammetric scans, however, showed the definite presence of the ferrocene unit but no Ru^{II}/Ru^{III} couple was detected. Although there is evidence for the formation of the expected complex, the results of elemental analyses were not encouraging. The preparation of both $[Ru(BFcBD)en(PPh_3)_2]$ and $[Ru(BTFFcBD)en(PPh_3)_2]$ were considered to be unsuccessful.

Cobalt Schiff base complexes were prepared from cobalt acetate in ethanolic solution without the addition of base. The orange product is insoluble in ethanol and

was collected by filtration. The product was considered to be formed as a dimer.[99] Evidence of the dimeric structure is provided by cyclic voltammetry in acetonitrile and dichloromethane. The dimeric nature of such complexes is discussed in Chapter Four.

The ferrocene-containing cobalt Schiff base complexes were found to be air-sensitive, changing from pale yellow to brown on exposure to air. The elemental analysis in Table 3.5 shows that the oxygen adduct may have been formed during the process of analysis.

Table 3.5 Microanalysis for Mononuclear Schiff Base Complexes

Compound	%H	%C
[Co(BFcBD)enO_2]	calc. 5.04	56.16
	found 4.84	55.85
[Fe(BFcBD)en]	calc. 4.89	58.29
	found 4.75	57.98

The analysis for carbon for the complex [Co(BFcBD)] was acceptable only when the Schiff base unit was considered to be dimeric in nature. Characterization by cyclic voltammetry shows the presence of cobalt(II) in an N_2O_2 environment and a wave with current intensity corresponding to two ferrocene centers (Table 3.7).

Iron Schiff bases [Fe(BFcBD)enPy] and [Fe(BPBD)enPy] were obtained from a water/1-propanol/pyridine mixture as dark purple solids. Pyridine was considered

to be axially coordinated, giving a five-coordinate complex.[86] The complexes containing axial pyridine are sensitive to oxygen uptake, producing a brown-yellow oxygenated product. These compounds lose pyridine readily, the smell of pyridine in the sample vial becoming very pungent with time. Other evidence of the loss of pyridine is provided by the disappearance of the Fe^{II}/Fe^{III} wave in the cyclic voltammogram (Table 3.7) and the reduction in intensity of the aromatic peaks in the infrared spectrum of the compound.

Schiff base complexes of iron(III) and ruthenium(III) were also prepared. Their characterization by cyclic voltammetry is described in section 3.5.

3.3 Binuclear Schiff Base Complexes

The preparation of binuclear complexes of ruthenium(II), iron(II) and cobalt(II) was attempted. Cyclic voltammetry and elemental analysis revealed that the cobalt and ruthenium complexes were not successfully prepared. Complexes of iron(II) were prepared and characterized by cyclic voltammetry. Two redox centers were observed, neither of which gave a reversible wave. The complexes derived from the ligand [(BFcHT)en] was extremely air sensitive, decomposing within minutes when allowed to stand in air. The instability of this complex precluded elemental analysis.

3.4 Tris(β-diketonato) Complexes

Complexes of iron(III) and ruthenium(III) with ferrocene-containing derivatives of 2,4-pentanedione as ligands were prepared using literature procedures. Complexes

of ruthenium were prepared making use of the "ruthenium blue method"[91] in which ruthenium(III) chloride is reduced with ethanol prior to the addition of the ligand. At the end of the reaction the complex is air-oxidized to the 3+ state.

Iron(III) complexes were prepared by adding an ethanolic solution of the diketone to an aqueous solution of ferric chloride.

Cyclic voltammetric characterization of both iron and ruthenium complexes show two reversible redox waves. The M^{III}/M^{II} couple was assigned to the wave at the more cathodic potential on comparison with model tris(β-diketonato) complexes.

The microanalysis for the tris(β-diketonato) complexes are given in Table 3.6. Analysis for carbon in the iron complex [$Fe(FcBD)_3$] was not reliable. This compound was found to be difficult to handle since it readily acquired electrostatic charge causing it to adhere to the sides of the sample vial. The carbon data for $Fe(FcPPD)_3$ and $Fe(FcBD)_3$ were not obtained in an acceptable range on repeated analyses. In spite of these results, their electrochemical and spectroscopic data (sections 3.5, 3.6 and 3.7) indicate strong structural similarities to the model FeL_3 complexes. For this reason the possibility that the results of the elemental analyses may be a function of the characteristics of the solid sample is considered.

3.5 Electrochemistry of Schiff Base Complexes and Tris(β-diketonato) Complexes

Table 3.7 presents voltammetric data on Schiff base complexes of cobalt, iron and ruthenium. Ruthenium(III) and iron(III) complexes were prepared and characterized by cyclic voltammetry. The results are also presented in Table 3.7.

Table 3.6 Microanalysis for Tris(diketonato) Complexes

Compound	%H	%C
$Ru(TFFcBD)_3$	calc. 2.83	47.13
	found 2.81	46.99
$Ru(FcPPD)_3$	calc. 4.14	62.55
	found 4.08	62.28
$Ru(FcBD)_3$	calc. 4.33	55.53
	found 4.35	55.15
$Fe(TFFcBD)_3$	calc. 2.95	49.21
	found 2.98	48.92
$Fe(FcPPD)_3$	calc. 4.32	65.24
	found 4.38	65.74
$Fe(FcBD)_3$	calc. 4.55	58.44
	found 4.15	51.29

The Co^{II}/Co^{III} couple is not usually reversible unless the metal ion is six-coordinated. The wave ascribable to this couple in the compound [Co(BFcBD)en] is observed in pyridine and not in acetonitrile or dichloromethane solvent. In pyridine, where the complex is likely to be six-coordinated through the axial coordination of solvent molecules, the observed wave possesses a very large peak to peak separation between the scan rates 25 - 300 mV s^{-1} (ΔE_p = 150 mV on average) therefore the currents recorded are not diffusion limited.

The iron Schiff base complex [Fe(BFcBD)enPy] showed a reversible Fe^{II}/Fe^{III}

Table 3.7 Voltammetric Data for Schiff Base Complexes

Compound	$E_{1/2}$(mV)	
	M^{2+}/M^{3+}	Fc/Fc^{+}
[Co(BFcBD)en][a]	-688	838
[Co(BPBD)en][a]	-597	-
[Fe(BFcBD)enPy]	-563	777
[Fe(BPBD)enPy]	-504	-
	M^{3+}/M^{2+}	Fc/Fc^{+}
[Fe(BFcBD)enCl]	-642[b]	550
[Fe(BPBD)enCl]	-607[b]	-
$K[Ru(BFcBD)enCl_2]$	-50	505
$K[Ru(BPBD)enCl_2]$	(c)	

a) in pyridine 0.1 M in TBAH at a scan rate of 25 mV s^{-1}. All other measurements were taken in acetonitrile, 0.1 M in TBAH at a scan rate of 200 mV s^{-1}
b) only a cathodic wave was observed.
c) the voltammogram did not contain well-defined waves.

couple associated with the presence of five-coordinate iron(II) with axially coordinated pyridine when investigated in acetonitrile solvent. The iron couple is reversible within the scan rate range 25 - 300 mV s^{-1}. The Fe(III) complex [Fe(BFcBD)enCl] showed an irreversible wave associated with the Fe^{III}/Fe^{II} couple. The identical observation is made for the complex [Ru(BFcBD)enCl], the cathodic peak occurring at -50 mV. A voltammogram for the model Ru(III) complex was not

successfully obtained since it showed large cathodic currents with no peaks.

Voltammetric data for the prepared tris(β-diketonato) complexes are presented in Table 3.8. Potentials are quoted relative to the saturated calomel electrode utilizing potassium chloride. Voltammograms were recorded within the range -2.00 to +2.00 volts.

Table 3.8 Voltammetric Data for Tris(diketonato) Complexes[a]

Ligand	Redox Couple in mV			
	Fe^{3+}/Fe^{2+}	Fc/Fc^{+}	Ru^{3+}/Ru^{2+}	Fc/Fc^{+}
[FcTFBD]	-339	791	-80.0	868
[TFPD]	-158	-	-6.00	-
[FcPBD]	-882	646	-576	734
[PBD]	-744	-	-467	-
[FcBD]	-878	623	-801	601
[PB]	-810	-	-641	-

a) half wave potential for ruthenium complexes were recorded in acetonitrile, 0.1 M in TBAH. Iron complexes were recorded in dichloromethane, 0.1 M in TBAH.

Assignments of the M^{III}/M^{II} couples in Table 3.7 were based on comparisons with model complexes and the current intensities of the Fc/Fc^{+} couple relative to that of the central metal ion. The potentials given for the Schiff base complexes are formally oxidation potentials whereas those for the tris(β-diketonato) complexes are

reduction potentials.

The half wave potentials for the reversible couples were obtained by applying the equation

$$E_{1/2} = E_f - (0.059)/n[\log(D_{red}/D_{ox})] \qquad 3.1$$

The assumption that $D_{red} = D_{ox}$ is made therefore $E_{1/2} = E_f$. The half wave potential is taken as the average of the potentials of the anodic and cathodic peaks of the wave.

Figure 3.4 shows typical voltammograms for Schiff base and tris(diketonate) complexes. Both categories show two voltammetric waves corresponding to the redox process at the central metal ion($E_{1/2}(1)$) and the more anodic Fc/Fc^+ couple($E_{1/2}(2)$), the intensity relation between the peak currents for $E_{1/2}(1)$ and $E_{1/2}(2)$ is consistent with the latter couple being closely spaced one-electron processes.

Table 3.9 presents electrochemical data on ligands used in complex formation. All the waves for the free ligands were found to be quasi reversible. Although $i_{pc}/i_{pa} = 1$ the peak to peak separation was in excess of 150 mV indicating that the process is not diffusion controlled. The processes approached the criterion for reversibility as the scan rate was decreased.

Complexes of the type RuL_3 (where L is a diketonate ligand) show two redox waves corresponding to the reversible Ru^{III}/Ru^{II} and the Ru^{III}/Ru^{IV} couples. The latter couple occurs at the more anodic potential and has been previously

Table 3.9 Voltammetric Data for Ligands[a]

Ligand	$E_{1/2}(Fc/Fc^+)$/mV	
	Acetonitrile	Dichloromethane
[(BFcBD)en]	567	-
[FcTFBD]	781	729
[FcPBD]	668	653
[FcBD]	647	641

a) 200 mV s^{-1} in acetonitrile 0.1 M in TBAH

reported.[100] In addition to the reversible couples, an irreversible wave was observed at -1.23 V. A corresponding wave was also obtained when recording voltammograms of $Ru(FcL)_3$ (where FcL is the diketone containing a ferrocene unit) complexes. This wave is considered to be associated with adsorption at the electrode since its intensity increased with time. A reduction of Ru(II) to Ru(I) was discounted since such a couple would have been observed initially.

3.6 Ultraviolet - Visible Spectra

The salient features of the electronic absorption spectra in the visible and near ultraviolet regions of the electromagnetic spectrum are shown in Table 3.10.The electronic spectrum for the cobalt Schiff base shows a series of shoulders and one dominant absorption band at 322 nm in addition to a very characteristic shoulder at

Figure 3.4 Cyclic Voltammograms for [Fe(BFcBD)enPy] (A) and [Ru(FcPPD)$_3$] (B)

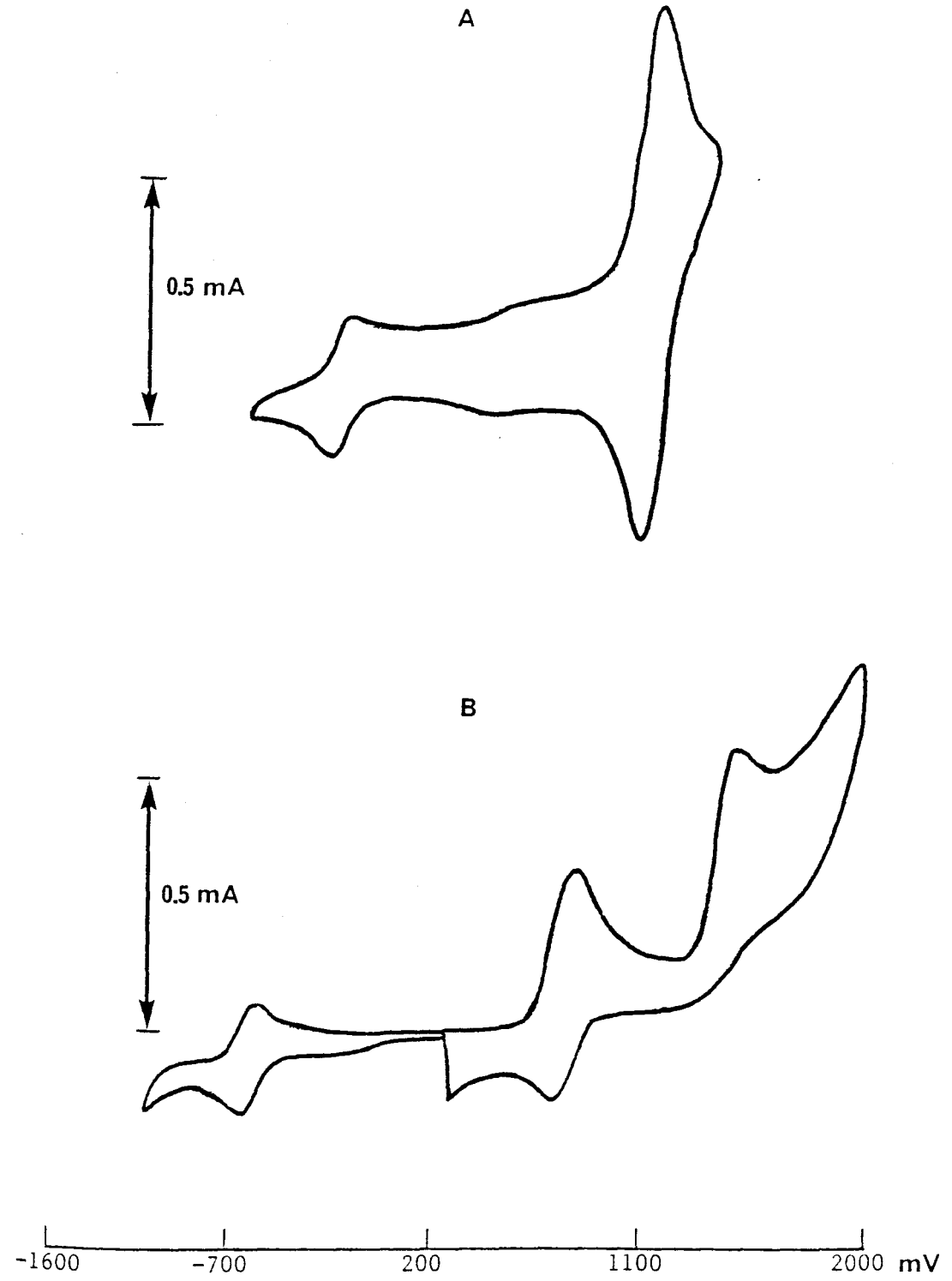
A
0.5 mA
B
0.5 mA
-1600
-700
200
1100
2000
mV

Table 3.10 Ultraviolet-Visible Spectral Data For Complexes

Compound	λ_{max}/nm(ϵ x10^{-3}/$M^{-1}cm^{-1}$)				
[Co(BFcBD)en]	~220(sh)	322(10.5)	~220(sh)	465(sh)	~420(sh)
[Fe(BFcBD)en]	230(19.7)	305(16.0)	360(sh)	430(3.09)	
[Ru(FcTFBD)$_3$]	309(33.4)	395(14.9)	520(10.1)		
[Ru(FcPPD)$_3$]	251(44.2)	323(42.3)	412(14.6)	480(sh)	
[Ru(FcBD)$_3$]	303(28.8)	388(12.9)	445(sh)		
[Fe(FcTFBD)$_3$]	310(26.1)	360(13.0)	445(6.5)	545(sh)	
[Fe(FcPPD)$_3$]	248(38.1)	320(34.2)			
[Fe(FcBD)$_3$][a]	308(28.8)	435(5.56)	~530(sh)		

a) spectrum recorded in dichloromethane. All other spectra recorded in acetonitrile.

~220nm. These are probably transitions associated with the pseudoaromatic nature of the Schiff base ligand.[101]

The iron Schiff base complex in acetonitrile exhibits an electronic spectrum that is dominated by an absorption at 305 nm. The infra-red spectrum showed that pyridine is lost with time resulting in a complex that was not sensitive to oxygen uptake. The spectrum recorded was considered to be that of the free complex without axially co-ordinated pyridine since there was no change in absorption bands with time even when the sample was oxygenated in the cuvette.

The Ru(FcL)$_3$ complexes showed well defined absorption peaks. These spectra are very similar to those of RuL_3 complexes and almost all the bands are observed to be blue-shifted relative to RuL_3. The three absorption bands of the RuL_3 spectra have been ascribed transitions to excited states which are configuration-interactive

and mixtures of the ligand-to-metal charge transfer excited states and the ligand (π,π^*) excited triplets and singlets.[102] The spectra of the ferrocene-containing complexes are very similar to those for the RuL_3 complexes therefore it could be speculated that the electronic and structural characteristics of the two sets of complexes are similar. Although ferrocene has absorptions in both the visible and uv regions, they appear to be masked by the dominant complex transitions. Complexes with phenyl substituted ligands show an additional band in the uv region which may be assigned a $\pi \rightarrow \pi^*$ transition associated with the phenyl ring since no corresponding band was observed for the non-phenyl systems. The observed shift in this absorption wavelength on comparing the RuL_3 and $Ru(FcL)_3$ cases was very small relative to the shifts in other bands. The implication is that the band may be ascribed to an isolated unit. Absorption maxima may also vary owing to the presence of facial and meridional isomers. The result of the presence of the isomeric forms is a slight broadening of the absorption profile.

The similarities, stated above, among the spectra of RuL_3 complexes were observed for FeL_3 complexes. The bands of the $Fe(FcL)_3$ complexes were also red shifted relative to those for FeL_3 complexes. This observation was also made for the complex with trifluoro substituents, [$Fe(FcTFBD)_3$], although it should be appreciated that a proper comparison is inappropriate since its spectrum was recorded in dichloromethane. Spectral assignments for FeL_3 complexes have been made by Singh and Sahai.[103] Bands in the uv region have been assigned to $\pi \rightarrow \pi^*$ transitions whereas those in the region 350 - 400 nm were assigned $d \rightarrow \pi$ transitions.

Transitions of the type n → d* occur between 400 and 700 nm and d → d transitions were located below 700 nm.

There is also a close resemblance in the spectra of all β-diketonato complexes which were recorded. This observation should not be very surprising since iron and ruthenium belong to the same group in the periodic table of the elements and the ligands are similar in structure. For this reason the interactions between the metal ions and the ligand systems are expected to be similar throughout the iron and ruthenium series of complexes prepared for this study. The striking similarities among the uv spectra of the complexes suggest that the bands arise from ligand based transitions.

Table 3.11 presents spectral data for the ferrocene-containing ligands. Each

Table 3.11 Ultraviolet-Visible Spectral Data for Ligands[a]

Ligand	λ_{max}/nm(ϵ x 10^{-3} M^{-1} cm^{-1})		
[(BFcBD)en]	270(14.6)	338(32.2)	450(1.68)
[FcTFBD]	310(9.02)	464(1.5)	
[FcPBD]	335(11.3)	488(1.38)	
[FcBD]	240(10.3)	446(1.07)	

a) in acetonitrile.

ligand contains an absorption band, in the uv region, which is associated with the conjugated system (probably a $\pi \rightarrow \pi^*$ transition). Bands above 350 nm arise from d→d transitions within the ferrocene unit.[104] The ligand spectra do not show ferrocene-based transitions in the uv region.

3.7 Infra-red Spectra

The tris(diketonato) complexes of iron and ruthenium show very strong characteristic absorption bands in the 1520 - 1620 cm^{-1} region for C = O and 1430 - 1580 cm^{-1} for C = C stretches.[105] The C = O stretch is also very distinct in Schiff base complexes and is found to be shifted to longer wavelengths with reference to the free ligand. Table 3.12 gives the frequencies of the C = O absorption for some of the prepared ligands and complexes.

The infrared spectra for the complex [Co(BFcBD)en] and the ferrocene-containing diketones were featureless, showing only broad absorption over the entire region being scanned therefore bands could not have been unequivocally assigned. In both cases the spectra were uninterpretable between 1400 - 1650 cm^{-1}. Repeating mull preparation did not improve the nature of the spectrum obtained.

The carbonyl absorption frequency in tris(diketonato) complexes increases from the case of the unsubstituted through the phenyl-substituted to the trifluoro-substituted. The absorption of the trifluoro substituted is greatest since the electron-withdrawing power of the trifluoro group strengthens the C = O bond by allowing more electron density between the carbon and oxygen atoms. For both iron and

Table 3.12 Frequencies for the Carbonyl Stretch in Complexes and [(BFcBD)en]

Complex	ν(C=O)/cm^{-1}	
	Complex	Ligand
[Fe(BFcBD)en]	1563	1600
[Ru(FcTFBD)$_3$]	1564	-
[Ru(FcPPD)$_3$]	1515	-
[Ru(FcBD)$_3$]	1512	-
[Fe(FcTFBD)$_3$]	1584	-
[Fe(FcPPD)$_3$]	1525	-
[Fe(FcBD)$_3$]	1520	-

ruthenium complexes the decreasing frequency of the C = O absorption is in the order of the decreasing electron withdrawing power of the substituent.

3.8 Intervalence Transfer Spectra

Spectra of Ru(FcL)$_3$ complexes in the near infrared and visible regions of the electromagnetic spectrum revealed bands that were broad and low in intensity. These were assigned as intervalence transfer (IT) bands on recognition of their large band widths, low intensities and absence when the complexes were fully oxidized and fully reduced and absence in the model RuL$_3$ complexes which do not contain ferrocene as part of the ligand system. Table 3.13 summarizes band parameters for transitions observed in the Ru(FcL)$_3$ complexes. Figure 3.5 shows the intervalence transfer absorption bands for the complexes listed in Table 3.13.

Table 3.13 Intervalence Transfer Band Parameters for $Ru(FcL)_3$ in Acetonitrile

Complex	λ_{max}/nm	ϵ/M^{-1} cm^{-1}	$\Delta\nu_{1/2}$/nm
$[Ru(FcTFBD)_3]$	900	789	640
$[Ru(FcPPD)_3]$	710	357	312
$[Ru(FcBD)_3]$[a]	575	410	410

a) band parameters for this complex have been estimated since the band occurred as a shoulder on an absorption in the visible region.

The completely reduced species was examined by electrolysing a 0.1 M solution of TBAH in acetonitrile with the complex at a potential ~100 mV more negative then the $E_{1/2}$ for the Ru^{III}/Ru^{II} couple. In each case there was a change in color. The fluorine substituted complex underwent a color change from red orange to purple while the phenyl substituted complex underwent a change from red-orange to green and the unsubstituted complex became deep blue. In each case the original mixed valence complex could be regenerated by electrolysing the solution of each complex at suitable potential. The former color redeveloped and the cyclic voltammogram and ultraviolet-visible spectrum obtained indicated that the original complex was regenerated.

Oxidizing the complexes in order to achieve a 3+ oxidation state for all the ferrocene centers was difficult to perform electrolytically. It was found that the solution reverted to its original color before it could be placed in the sample compartment of the spectrometer. Each complex was titrated with a solution of Ce(IV) ammonium nitrate in acetonitrile and the decrease in the intensity of the IT

band was observed. This procedure was not entirely successful since a strong tail to a band in the visible region rapidly developed in the region of the IT band in each case.

On examining the near-infrared-visible spectra for the $Fe(FcL)_3$ complexes no IT bands were discovered.

Each of the tris(diketonato) complexes was titrated with standard Cerium(IV) solution in search of a Fc-Fc interaction but no bands of the IT type developed in either ruthenium or iron complexes. In contrast to this observation, the ligand [(BFcBD)en] was electrolyzed at a potential beyond the $E_{1/2}$ for the ferrocene wave and a broad absorption reminiscent of an IT band was observed. This band has not been unequivocally assigned as an IT band but it was notably absent in the fully reduced [2,2] ion and its intensity reduced on titration with iodine solution. Band parameters for the speculated mixed valence system are summarized in Table 3.14.

The ruthenium ML_3 complexes were examined in a variety of solvents in order to establish a solvent dependency of the absorption maximum. The results presented in Table 3.15 show that the solvent effect is not very significant. The largest shift is observed, relative to runs in acetonitrile, when the near infra-red spectrum is recorded in benzonitrile, butyronitrile and 2-nitropropane.

The Schiff base complexes of cobalt and iron were titrated with standard Br_2 solution but no M - Fc interaction was observed.

Figure 3.5 Visible-Near Infrared Spectra for $[Ru(FcTFBD)_3]$ (A), $[Ru(FcPPD)_3]$(B) and $[Ru(FcBD)_3]$ (C)

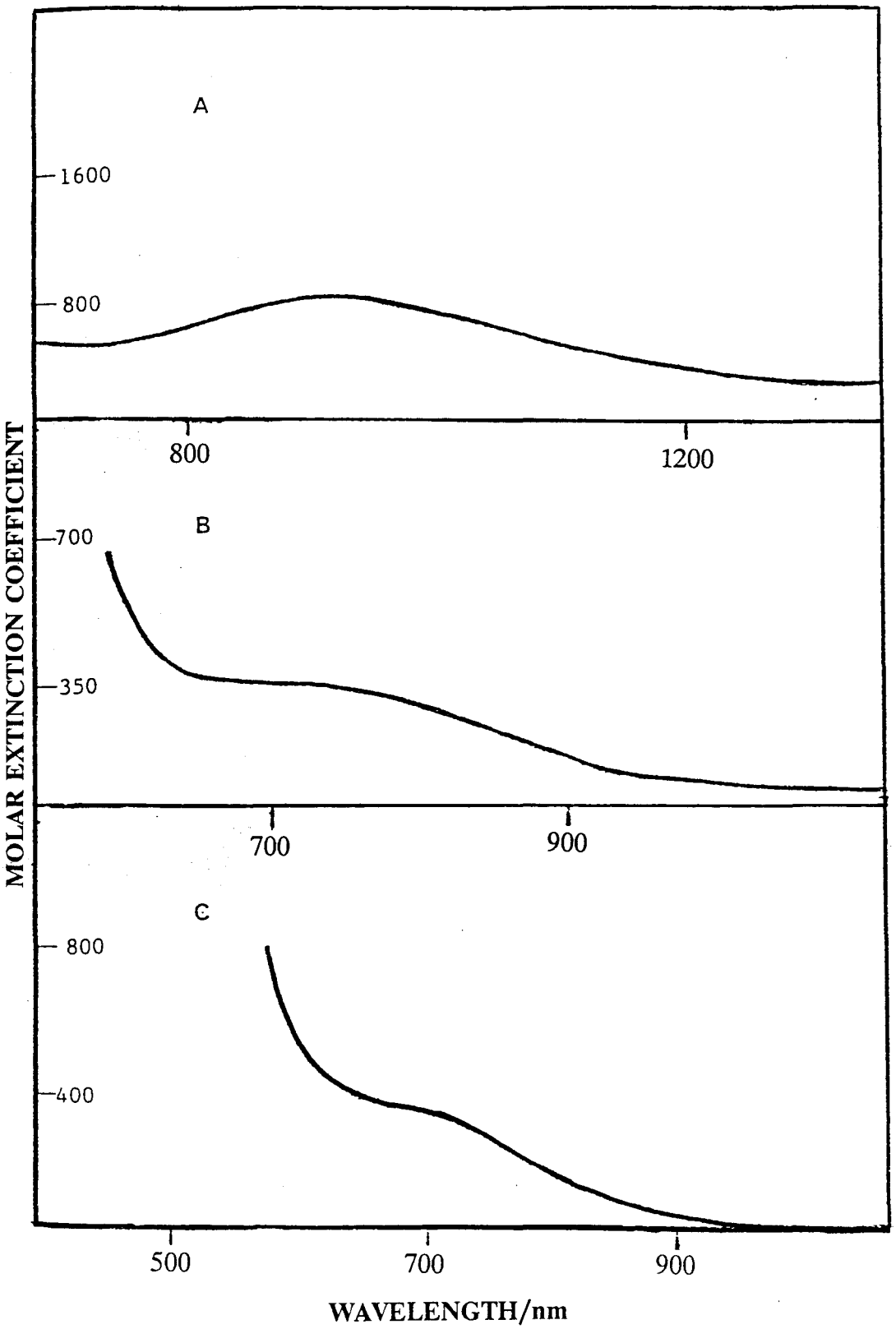
A
1600
800
800
1200
B
700
350
700
900
C
800
400
500
700
900
MOLAR EXTINCTION COEFFICIENT
WAVELENGTH/nm

Table 3.14 Near Infrared Spectrum for Partly Oxidized [(BFcBD)en] in Acetonitrile

Compound	λ_{max}/nm	ϵ/M^{-1} cm^{-1}	$\Delta\nu_{1/2/nm}$
[(BFcBD)en]	805	351	500

Table 3.15 Intervalence Transfer Band Maxima for $[Ru(FcTFBD)_3]$ in Selected Solvents

Solvent	E_{op}/kK
Acetonitrile	11.1
Benzonitrile	11.4
Butyronitrile	11.4
Propionitrile	11.3
Propylene carbonate	11.1
2-Nitropropane	11.4

CHAPTER 4

DISCUSSION

4.1 Choice of Complexes

One of the objectives of this work is to examine effects of the nature of electron delocalization in complexes that are likely to serve as polyelectron transfer catalysts particularly for dioxygen reduction. The essential requirements are the provision of a delocalized system through which the metal centers may communicate and the ability to react with oxygen. Compounds satisfying these requirements were considered to be the tetraaza and Schiff base complexes of iron(II), cobalt(II) and ruthenium(II) and tris(β-diketonato) complexes of iron(III) and ruthenium(III) each having ferrocene as part of their ligand system. The ferrocene unit was used to provide a polyelectron character to the system.

4.2 Tetraaza Complexes

The first choice of polyelectron transfer systems was based on the tetraaza unit. Attempts at preparing the ligand were made by condensing triethylenetetraamine with a ferrocene-containing β-diketone. This reaction was unsuccessful in a variety of solvents. A different synthetic strategy, involving the template effect of nickel(II),

was undertaken. The nickel(II) complex was first prepared then nickel removal was attempted by taking advantage of the complexing ability of cyanide and chloride ligands. In this case the tetraamine was refluxed with the β-diketone in the presence of nickel(II). Success at preparing the nickel complex was obtained for ligand systems which contained a methyl in place of a ferrocene unit. When ferrocene was part of the ligand no reaction occurred. The relatively bulky nature of the ferrocene group coupled with its electron withdrawing character seem to inhibit condensation in both free and template-assisted reactions. Nickel removal was attempted on complexes without a ferrocene unit. Sodium cyanide and hydrochloric acid were used separately as nickel removing agents. ^{1}H NMR analysis of the product showed that the imine function was destroyed in the nickel removal stage.

4.3 Mononuclear Schiff Base Complexes

Schiff bases satisfy both requirements for polyelectron reduction of dioxygen since the diketone system forms a pseudoaromatic unit[101] when bonded to a metal and the oxygen sensitivity of these systems are well documented.[106,86] Ferrocene is placed on the Schiff base system to give the polyelectron transfer character. Mononuclear Schiff bases were prepared with reasonable facility (for iron(II) and cobalt(II)), however, these are merely three-electron systems. The more interesting four-electron system is provided by a binuclear Schiff base complex based on a ferrocene β-triketone.

4.3.1 Preparation of Ligands

The β-diketones containing ferrocene were all prepared by condensing acetylferrocene with the appropriate ester. The literature procedure reports[95] the use of sodium amide as base for generating the anion of acetylferrocene which condenses with the ester. An alternative method was undertaken in which lithium diisopropyl amide (LDA) was used as base. Lithium diispropylamide is a weaker base than sodium amide and is not expected to attack the carbonyl carbon of acetylferrocene. The yield was less than that for the literature preparation of [FcPPD] which was done by a sodium amide method, however, the LDA method proved to be a safer and less tedious procedure.

4.3.2 Preparation of Mononuclear Complexes

Schiff base complex preparations with ligands incorporating ferrocene followed examples from the literature. They were successful in the cases of iron(II) and cobalt(II) but not for ruthenium(II). In the case of ruthenium(II) preparations with [(BFcBD)en] a brown-purple precipitate was obtained from the reaction mixture. Since the ruthenium source was tris(triphenylphoisphine)ruthenium(II) chloride the Schiff base product was expected to contain axially coordinated triphenylphosphine groups. A cis arrangement of the triphenylphosphine groups was discounted since such a configuration would entail either a close approach of the ferrocene groups or a distortion of the methylene groups on the ethylenediamine system. The cyclic voltammogram for the recrystallized product exhibited a composite wave comprising

of two anodic and one cathodic peaks in the region expected for the Fc/Fc^+ couple. There was no wave ascribable to the Ru^{II}/Ru^{III} or the Ru^{III}/Ru^{II} couple. ^1H and ^{31}P NMR analyses indicated the presence of paramagnetism in the product, therefore the complex was thought to be partly in the Ru(III) oxidation state giving rise to the possibility that the irreversible segment of the composite wave is associated with the Ru^{III}/Ru^{IV} couple. The ^{31}P NMR spectrum of the product shows one resonance which is located 19.2 ppm upfield relative to $Ru(PPh)_3Cl_2$. This signal is not within the region of chemical shifts for trans phosphine Schiff base complexes.[87] The elemental analysis is not consistent with the proposed composition of [Ru(BFcBD)en$(PPh_3)_2$]. Identical observations were made on attempting to prepare the Schiff base complex with the ligand [TFFcBD]. Although the complex [Ru(BFcBD)en$(PPh_3)_2$] was not successfully prepared, the related compound [Ru(BPBD)en$(PPh_3)_2$] was prepared according to the method of Thornback and Wilkinson.[87] Electrochemical characterization showed a reversible Ru^{II}/Ru^{III} wave with an $E_{1/2}$ value of 81.2 mV.

Elemental analysis revealed that the preparation of mononuclear ruthenium(II) Schiff base complexes of ferrocene diketones was unsuccessful. A possible explanation for the lack of success in preparing the ruthenium(II) Schiff base complex may be concerned with steric factors. The triphenylphosphine group has a wide cone angle of 145°[107] and may extend outwards to the extent that it is in close proximity to the ferrocene unit therefore producing an unstable system.

Iron Schiff bases were successfully prepared according to the procedure of

Niswander and Martell.[86] The complex, [Fe(BFcBD)enPy], was considered to have axially coordinated pyridine. The cyclic voltammogram of the ferrocene-containing complex displays an Fe^{II}/Fe^{III} wave at -563 mV and an Fc/Fc^{+} wave at 777 mV. Changes in the cyclic voltammogram were observed in which the Fe^{II}/Fe^{III} wave reduced in intensity and an irreversible wave appeared at 1.49 V. This process was considered to signify loss of pyridine from the axial position. Evidence of the loss of pyridine was also provided by the observed reduction in the intensity of aromatic peaks in the infrared spectrum of the complex. It is reasonable to conclude that the absence of pyridine on the complex resulted in the loss of oxygen sensitivity since it was observed that the decomposed complex did not undergo a color change on exposure to air nor was there any spectral change when a solution of the complex (without pyridine) was oxygenated.

The ferrocene-containing Schiff base [Co(BFcBD)en] was successfully prepared in ethanolic solution. The resulting compound was found to be very sensitive to oxygen uptake as demonstrated by the spectral alterations on oxygenating a solution of the complex. Oxygen uptake by the solid compound was accompanied by a color change from orange to dark brown. This observation is in contrast to the prepared Schiff bases with ligands without ferrocene, which were found to be insensitive to oxygen uptake when in the solid phase. The dimeric structure in the latter case (the separation between the two structural units of the dimer was found to be 2.259 Å)[99] restricts the diffusion of oxygen through the crystal lattice to an internal coordination site. The external coordination sites are unavailable for oxygen binding since they

are usually occupied by solvent molecules. A possible deduction is that for the complex [Co(BFcBD)en], the presence of the ferrocene units gives rise to a more open dimeric structure which is pervious to dioxygen. The dimeric structure seems to persist in solution. Evidence of its presence is provided by the differential pulse polarogram which shows three ferrocene/ferrocenium couples when recorded in dichloromethane but only one peak when recorded in acetonitrile. Since acetonitrile is a more polar solvent than dichloromethane, it is more likely to dismantle the dimeric structure. On the other hand dichloromethane allows the dimeric structure to persist therefore there is a possibility for the existence of non-equivalent ferrocene units.

4.4 Electrochemical Techniques

Schiff base complexes of cobalt and iron undergo reversible diffusion controlled electrochemical reactions. Reversibility in the systems investigated was tested in a number of ways. The first indication of reversible electron transfer was the symmetrical nature of the redox wave. Observing a cathodic wave complementary to an anodic wave was the primary indication of reversibility. The peak currents i_{pa} (anodic) and i_{pc} (cathodic) were measured and used in the relation,

$$i_{pa}/i_{pc} = 1 \qquad 4.1$$

to test for reversibility. The redox waves in each case were well separated therefore

measurement of i_{pa} and i_{pc} was accomplished without complications from overlapping diffusion currents. Another means of testing for reversibility was observing the peak to peak separation ΔE_p for the wave in question as a function of the scan rate. The separation ΔE_p should be invariant with scan rate for a reversible diffusion limited electrode reaction.[108] The criterion for peak potential separation

$$\Delta E_p = 59 \text{ mV} \qquad 4.2$$

based on theoretical derivations,[108] was not obeyed by the complexes under investigation. It was observed that ΔE_p values were in the vicinity of 80 mV for the waves associated with the Fe^{III}/Fe^{II}, Ru^{III}/Ru^{II} and Fe^{II}/Fe^{III} couples and within the range 100 to 120 mV for the Fc/Fc^+ couple. The reasons advanced for deviations from the oretical value are associated with the solution resistance of the system.[109] In the present investigation, organic solvents, which are known to have high solution resistances, were used. The estimated *i*R loss for the systems encountered in this investigation is estimated to be less than approximately 3 mV. According to Nicholson,[109] the effect of increased solution resistance is to increase the value of ΔE_p. The voltammetric analyser used is equipped with a current feedback potentiostat which provides compensation for the solution resistance, however, this facility was not used since it was found that there was overcompensation of solution resistance and ΔE_p values of less than 59 mV were obtained.

4.5 Electrochemistry of Mononuclear Schiff Base Complexes

The ferrocene substituted Schiff base complexes contain two redox centers, both of which were investigated. Focusing on the central metal ion, the primary observation for cobalt(II) and iron(II) complexes is that the cobalt couple occurs at a more cathodic potential than the iron couple. This is in keeping with the known better reversible oxygen absorbing properties of cobalt(II) Schiff base complexes. EPR studies have shown that dioxygen absorption in cobalt(II) Schiff base complexes occurs with partial electron transfer to the dioxygen moiety.[110] Investigations have also shown that the basicity of the axial ligand roughly parallels the ease of oxygen uptake for the complex.[110] It is noted that reversible electron transfer in the iron(II) complexes is possible only when there is axially coordinated pyridine which increases the electron density on the iron(II) center and that dioxygen absorption is non-existent in the absence of axial pyridine.

The preparation of complexes of iron(III) and ruthenium(III) was attempted and the products obtained were characterized by cyclic voltammetry. Attempts were made at preparing complexes with and without ferrocene attached to the ligand. The irreversible nature of electron transfer at the central metal ion for all complexes (Table 3.7) may be associated with the presence of axially coordinated chloride ligands whose electron π-donating nature is likely to destabilize the reduced species. Ruthenium-ferrocene complexes exhibited a composite ferrocene wave which consists of two closely spaced anodic peaks and one cathodic peak. The irreversible anodic peak was considered to be associated with the Ru^{III}/Ru^{IV} couple. Electrochemical

analyses show that, for all M(II) Schiff base complexes containing ferrocene, the cyclic voltammogram is characterized by an irreversible wave associated with the central metal ion and a reversible Fc/Fc^+ wave. The Fc/Fc^+ couple occurs at a higher positive potential than that for the free ligand. The expected anodic shift is explained partly by the electron removal from a charged species in the complex as opposed to a neutral species in the free ligand.

4.6 Binuclear Schiff Base Complexes

Mononuclear complexes are capable of transferring a total of only three electrons. Binuclear complexes were considered since they are a potential four-electron transfer system provided that each redox process is reversible. These complexes contain metal ions in two different coordination environments.

4.6.1 Preparation of Ligands

The ligands for binuclear Schiff base complexes were prepared by condensing ethylenediamine with two equivalents of β-triketone. The triketone, [PHT], was successfully prepared by the method of Miles et. al.[82] Preparation of the ferrocene-containing β-triketone, [FcHT], employed sodium hydride as base. Improvement in the yield was accomplished by the addition of 18-crown-6 subsequent to the addition of sodium hydride. It is believed that the crown ether separates the sodium ions, reducing ion-pairing effects and rendering the anion more reactive.

The Schiff base [(BPHT)en] was prepared by the method of Lintvedt et.al.[85] The

corresponding ferrocene-containing Schiff base, [(BFcHT)en], prepared by the same procedure was obtained as an oil which was difficult to purify. The ^{1}H NMR analysis gave the expected resonances and indicated the presence of the amine and imine forms of the compound by coincident singlet and doublet signals centered at 3.40 ppm. When preparing the Schiff base complexes the ligand was generated in situ.

4.6.2 Preparation and Electrochemistry of Binuclear Complexes

Attempts at preparing binuclear cobalt Schiff base complexes, using a published procedure,[89] were unsuccessful. The synthesis procedure for [Co_2(BPHT)en] produced an orange product which was found to be insensitive to oxygen uptake. The absence of air sensitivity and the fact that no Co^{II}/Co^{III} couple was observed in the cyclic voltammogram led to the conclusion that cobalt is coordinated in the O_4 environment of the Schiff base ligand. Bis(β-diketonato) complexes of cobalt(II) were prepared using diketones both with and without the ferrocene unit. On recording the cyclic voltammogram, no waves ascribable to the Co^{II}/Co^{III} couple could be found within the potential range of the solvent (-2.00 - +2.00 V). This finding may be related to the lack of electrochemical data on cobalt bis(β-diketonato) complexes in the literature. These compounds are also found to be insensitive to air.

The red crystalline solid obtained in the attempted preparation of the complex [Fe_2(BFcHT)en($Py)_2$] was extremely air sensitive and was found to be difficult to handle. The attempted preparation of the corresponding binuclear Schiff base

complex $[Fe_2(BPHT)en(Py)_2]$ resulted in a solid which was stable for a period of time that permitted the recording of the cyclic voltammogram. The voltammogram demonstrates a reversible wave in the potential region expected for the Fe^{II}/Fe^{III} couple when iron(II) is in an N_2O_2 environment. The other wave corresponding to iron(II) in an O_4 environment is irreversible, showing only a large anodic current but no corresponding cathodic peak. Similar observations were made for binuclear complexes of iron(III). In this case, a quasi reversible wave was observed for the Fe^{III}/Fe^{II} couple corresponding to iron is in the N_2O_2 environment while the other iron(III) center showed only a large cathodic peak. The quasi reversible nature of the N_2O_2 iron center in the binuclear complexes as opposed to the clearly irreversible electron transfer process for the corresponding center in mononuclear complexes may be accounted for by comparing the extent of delocalization in both systems. The Schiff base β-triketone ligands are able to provide greater delocalization and hence enhanced stabilization of any excess charge on the complex.

Attempts were made at preparing ruthenium(III) binuclear Schiff base complexes using ruthenium(III) chloride as a source of metal ion. Electrochemistry of the recrystallized product shows two small cathodic waves within the potential range 0.00 to -1.50 V, both of which are irreversible. The peak currents are very small and a large capacitive current is observed. The preparation of binuclear complexes based on β-triketone ligands and ruthenium(II) centers was also attempted. The products obtained were found to be extremely air sensitive and were not handled successfully with the available facilities.

4.7 Mixed-Valence Properties of Schiff Base Complexes

The use of M^{III} ions for the preparation of ferrocene Schiff bases means that the direct mixed-valence species would be obtained since ferrocene contains iron(II). The irreversible character of electron transfer in M^{III} ferrocene-containing mononuclear Schiff base complexes (Table 3.7) leads to the expectation that such compounds would not show intervalence transfer properties since irreversible electron transfer generally leads to a change in the solution character of the species. Indeed, such is the observation made on recording their near infra-red spectra.

On electrochemical generation of the mixed-valence compound $[Fe^{III}(BFcBD)enPy]$, rapid decomposition occurred and it was not possible to record the near infra-red spectrum for such a species. The near infra-red spectrum for $[Co^{III}(BFcBD)(Py)_2]$ was also featureless. Electron transfer to the cobalt(III) system is a high energy process since it would have to be preceded by a $t_{2g} \rightarrow e_g$ electron rearrangement within the cobalt(III) system, therefore the absence of an intervalence transfer band was not surprising.

Binuclear complexes were found to be unsuitable for intervalence transfer studies since their redox chemistry is characterized by irreversible electron transfer processes. Schiff base binuclear complexes contain two different environments which house the metal ions. The electrochemistry involving the N_2O_2 environment shows that electron transfer is quasi-reversible. Although nitrogen is a good sigma donor, in the imine function, an unhybridized p-orbital is of accessible energy for excess charge to be delocalized into the ligand system (section 4.4). The electrochemistry of the

mononuclear Schiff base complexes has indicated that axial coordination is also an important factor for the stabilization of the oxidized or reduced species. On the other hand, the O_4 environment does not possess any π-acceptor feature, consequently, accommodation of excess charge may be difficult and the system may have to rely largely on the axially coordinated ligands for stabilization of the reduced species for M^{III} systems. Since stabilization in the O_4 environment is achieved mainly through σ-donation, the oxidized form of the M^{II} complexes ought to be more stabilized than the reduced form of the M^{III} complexes, relative to the neutral compound. The irreversibility shown by iron(II) in the O_4 environment suggests that σ-donation is insufficient for the stabilization of the oxidized species therefore appropriate axial coordination or the incorporation of donor ligand substituents may be needed in order to enhance the stability of the oxidized species.

Binuclear copper(II) complexes based on Schiff bases show reversible electron transfer[85] unlike the iron and ruthenium congeners. The redox process is essentially two one-electron transfers at very closely spaced potentials.[85] When copper(II) is reduced, the additional electron enters a d-orbital of copper forming a d^{10} configuration. Since this system has an intrinsic stability, the demands for stabilization from the ligand system are reduced when compared with iron and ruthenium complexes.0

4.8 Tris(β-diketonato) Complexes of Iron(III) and Ruthenium(III)

In view of the lack of success with studying intervalence transfer properties of

Schiff base complexes, attention was turned to tris(β-diketonato) complexes of iron(III) and ruthenium(III) as candidates for polynuclear electron transfer processes. The possibility of a seven-coordinate ruthenium species[80] suggests that these compounds may be suitable for serving as catalysts in polyelectron transfer reactions.

4.8.1 Preparation of Tris(β-diketonato) Complexes

Complexes of the type ML_3 where L = $FcCOCHCOR^-$ and M = Fe(III) or Ru(III) were prepared by published procedures but using the ferrocene-containing β-diketone in place of the substituted diketone in the specific procedure. These complexes were successfully prepared and were found to be stable in air and acetonitrile and dichloromethane solvents.

4.8.2 Electrochemistry of Tris(β-diketonato) Complexes

The cyclic voltammograms for the ML_3 complexes each exhibits a one-electron reversible wave. Ruthenium complexes show reversibility over a wider range of scan rates than do the iron complexes.

Ruthenium complexes without the ferrocene unit as part of the ligand system show two redox waves, the more anodic wave corresponding to the Ru^{III}/Ru^{IV} couple. The Ru^{III}/Ru^{II} wave is quasi-reversible in the trifluorosubstituted complex over a wide range of scan rates whereas, the reversibility improved with increasing scan rate up to 800 mV for L = $CH_3COCHCOCH_3^-$ and $C_6H_5COCHCOCH_3^-$. The mechanism for electrode reduction was studied by Endo[111] who proposed that the initially

produced species ML_3^- becomes involved in ion association equilibria between the cation of the supporting electrolyte and the anion produced at the electrode. This proposition assists in appreciating why the reduction process becomes more reversible with increase in scan rate. On fast scanning, the ion pairing process is given very little time to become established, consequently, the concentration of the species to be oxidized on the reverse scan will not decrease significantly.

The Ru^{III}/Ru^{IV} couple has been observed when L is $FcCOCHCOR^-$ and R is a methyl or phenyl group but not for R = CF_3. It is manifested as an irreversible wave, the current response showing only an anodic peak at 1.5 V. The wave associated with the trifluorosubstituted complex may occur outside of the potential window for the solvent used. The $E_{1/2}$ value for the $Ru^{III/II}$ couple of $Ru(FcL)_3$ where L has a terminal $-CH_3$ funtion, lies at a more cathodic potential than that for the phenyl substituted complex. This observation is in keeping with the substitution effects discussed below.

Some measure of irreversibility is also proposed for the electrode relaxation process for $Fe(CH_3COCHCOCH_3)_3$.[112,113] The proposed mechanism involves transference of a diketone ligand from the oxidized species to an ion such as Li^+ which is part of the supporting electrolyte. The following scheme represents the relaxation process.

$$FeL_3 + e \rightleftharpoons FeL_3^-$$

$$FeL_3^- + M^+ \rightleftharpoons FeL_2 + ML$$

The extent of irreversibility introduced by the relaxation process is considered to be moderate, however, it is detected as a slight asymmetric appearance of the redox wave. This asymmetry is not evident in this investigation for complexes other than those with terminal methyl groups on the ligands. This implies that, should relaxation be taking place in the same manner, the rate is slower than that for L = 2,4-pentanedionato or that the species initially produced is inert enough to persist in solution. The electron withdrawing effect of the phenyl substituent confers stability on the FeL^- system and ought to inhibit relaxation therefore an asymmetric redox wave is less likely to be observed here. A similar argument may be applied to the trifluoro substituted complex.

Table 4.1 lists the values for the ratios i_{pa}/i_{pc} for various FeL_3/FeL_3^- couples. The

Table 4.1 Current Ratios for FeL_3/FeL_3^- Couples

Ligand	i_{pa}/i_{pc}
$[FcCOCHCOCH_3]^-$	0.89
$[CH_3COCHCOCH_3]^-$	0.96
$[FcCOCHCOC_6H_5]^-$	≈ 1.0[a]
$[CH_3COCHCOC_6H_5]^-$	0.96
$[FcCOCHCOCF_3]^-$	1.1
$[CH_3COCHCF_3]^-$	1.1

a) a rather large capacitive current was obtained.

current ratios show evidence for the occurrence of the described relaxation mechanism for the electrode reduction of FeL_3 complexes. The current ratio is lowest when there are terminal ferrocene and methyl units on the ligand. The electron donating power of ferrocene is expected to destabilize the ML_3^- species and increase the likelihood of relaxation.

The predominant feature concerning the reduction potential of tris(β-diketonato) complexes is the strong inductive effects exercised by the substituent groups. The same effects are observed in the iron(III) and ruthenium(III) series with and without the ferrocene unit as part of the ligand system. The most positive reduction potential is exhibited by complexes containing ligands with trifluoromethyl substituents. The half wave potential of these complexes are separated from others in a particular series by at least 400 mV. Electron withdrawing groups stabilize the negative charge on the reduced complex resulting in a more positive $E_{1/2}$ value. On the other hand an electron releasing group will destabilize the negative charge on the reduced species. This effect is reflected in the gradation in $E_{1/2}$ values presented in Table 3.8. For both ruthenium and iron complexes, $E_{1/2}$ is most positive in complexes with trifluoromethyl substituted ligands and most negative in complexes which have ligands with terminal methyl groups. The trend is identical for both iron and ruthenium complexes, suggesting that the inductive forces may be operating in a similar manner for the two series of compounds. The electron donating quality of the ferrocene unit is also evident on inspection of the data in Table 3.7. On comparing the half wave potentials for the ferrocene substituted and the non-

ferrocene complexes, it is found that the $M(FcL)_3$ cases lie at a more negative potential. This observation is in accordance with the electron donating character of the ferrocene unit since more charge on the central metal ion would lead to destabilization of the reduced form of the complex.

The gradation of the Fc/Fc^+ couple with the nature of the substituents also reflects the electronic influence of the substituents, the trifluoro substituted complex displaying the most positive half wave potential.

Electronic effects of substituents are also evident in the gradation of the half wave potentials for the β-diketonate ligands shown in Table 3.9. If the substituent effect is observed relative to the Fc/Fc^+ couple, then the trend in $E_{1/2}$ values for the ligands is the same as that for the M^{III}/M^{II} couples. Trifluorosubstituted free ligands and complexes show the most positive $E_{1/2}$ values while methyl substituted ligands and complexes show the most negative $E_{1/2}$ values. Although the same trend is observed in both acetonitrile and dichloromethane, the $E_{1/2}$ values for the same ligand are significantly different in the two solvents. The half wave potential for a particular couple is known to be a function of the nature of the solvent.[114] If the redox processes are indeed ligand based, as is proposed in the literature,[115] then it is plausible to expect that the solvent effect on the $E_{1/2}$ values would be emphasized.

The data presented for the Fe^{III}/Fe^{II} couple in this investigation are at variance with those from the literature. The data on the Ru^{III}/Ru^{II} couple is more in concordance with literature results. Table 4.2 gives four examples of $E_{1/2}$ values for

the complex $Fe(CH_3COCHCOCH_3)_3$.

Table 4.2 Half Wave Potentials for Fe(2,4-pentanedione)$_3$

$E_{1/2}$/mV[a]	Solvent	Reference
-0.667	Acetonitrile	114
-0.69,-0.49[b]	Acetonitrile	113
-0.460	Dichloromethane	115
-0.810	Dichloromethane	This work

a) values are corrected for the particular reference electrode and refereneced to the SCE.
b) $E_{1/2}$ value found to be a function of the nature and concentration of the supporting electrolyte.

There is a wide varation in the data recorded for the 2,4-pentanedionato complex of iron(III). Another variation from literature observation is the reduction potential for the iron complexes being consistently lower (more negative) than those for the ruthenium complexes. The same trend was obtained on repeated analyses.

The inductive effects described above may be correlated with the $E_{1/2}$ values for iron and ruthenium complexes. Linear free energy relations between the half wave potential and the sum of the Hammett and Taft constants for the ligand substituents have been presented in the literature for both the iron(III) and ruthenium(III) β-diketonato complexes.[110,116,117,118] Figure 4.1 gives plots of the $E_{1/2}$ values for ruthenium and iron complexes versus the Hammett parameters[119] for the substituents on the ligand. The value of the redox potential is plotted against the sum of the Hammett constants for the substituents on the ligand and a linear correlation is shown. The relatively large positive slope is an indication of the strong

influence of the substituent on the negatively charged transient species ML_3^-. The correlation was found to be good for σ_m values but not for σ_p values. This is understandable in view of the absence of substituents γ to the central metal ion. Correlation among the ruthenium complexes is much better than among the iron complexes. The usually good correlation of $E_{1/2}$ values and Hammett parameters is demonstrated in the literature but there is not much data for iron complexes. The lower correlation among iron complexes, observed in this investigation, indicates the smaller degree of importance of the substituent effect in the stabilization of such complexes relative to the same effects for ruthenium complexes. The orbitals on the ruthenium(III) ion have a greater radial extension than those on the iron(III) ion therefore it is reasonable to expect that there will be greater overlap between ruthenium and ligand orbitals. This improved orbital overlap compared with iron(III) complexes may be responsible for the enhanced inductive effects hence the better correlation for ruthenium(III) complexes.

The σ Hammett parameter[119] constitutes effects which are both inductive and mesomeric in nature. A Taft plot of σ_I values was made in order to assess the contributions from the inductive effects alone. A linear correlation has again been obtained for ruthenium complexes, with the correlation among iron complexes being poorer (Figure 4.2).

4.9 Mixed-Valence Properties of Ruthenium(III) Tris(β-diketonato) Complexes

The tris(β-diketonato) systems under investigation are considered to be

Figure 4.1 Plots of $E_{1/2}$ Versus One Ligand Sum Of Hammett Parameter σ_m for Iron(III) and Ruthenium(III) Complexes.

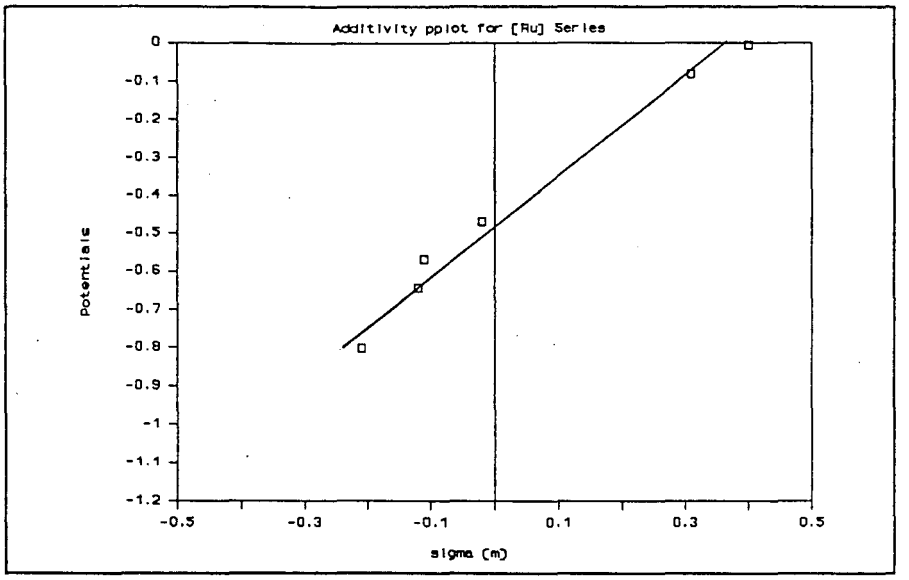
Additivity pplot for [Ru] Series
Potentials
sigma (m)
0
-0.1
-0.2
-0.3
-0.4
-0.5
-0.6
-0.7
-0.8
-0.9
-1
-1.1
-1.2
-0.5
-0.3
-0.1
0.1
0.3
0.5

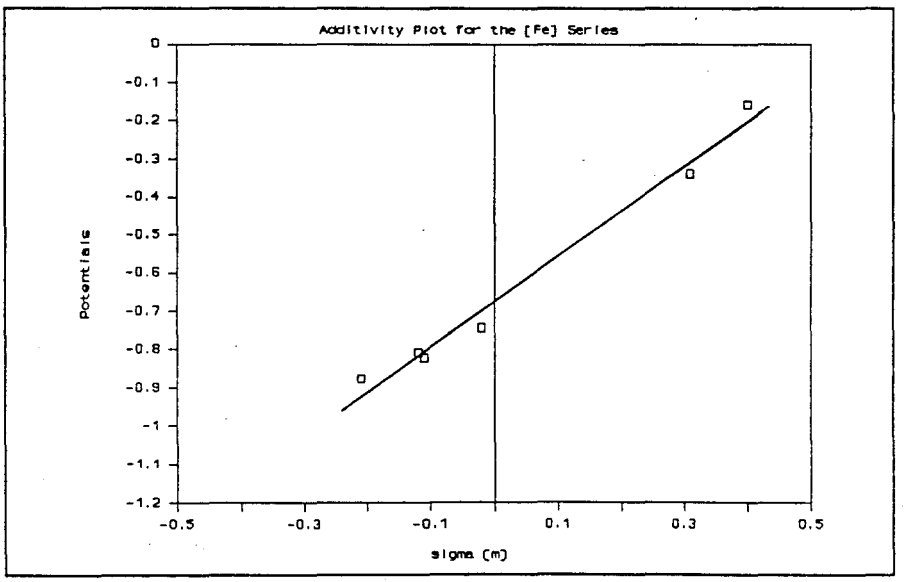
Additivity Plot for the [Fe] Series
Potentials
sigma (m)
0
-0.1
-0.2
-0.3
-0.4
-0.5
-0.6
-0.7
-0.8
-0.9
-1
-1.1
-1.2
-0.5
-0.3
-0.1
0.1
0.3
0.5

Figure 4.2 Plots of $E_{1/2}$ Versus One Ligand Sum of Taft Parameter σ_I for Iron(III) and Ruthenium(III) Complexes.

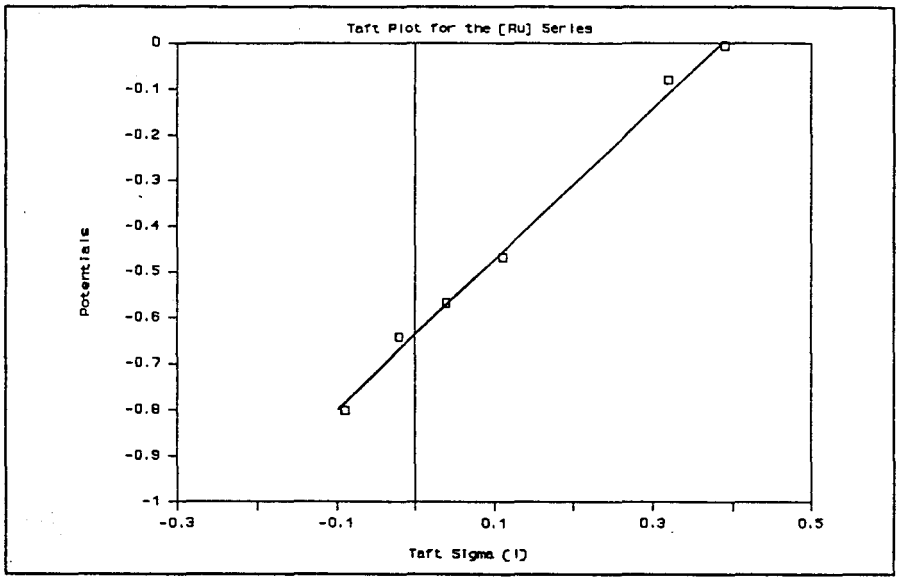
Taft Plot for the [Ru] Series
Potentials
0
-0.1
-0.2
-0.3
-0.4
-0.5
-0.6
-0.7
-0.8
-0.9
-1
-0.3
-0.1
0.1
0.3
0.5
Taft Sigma (I)

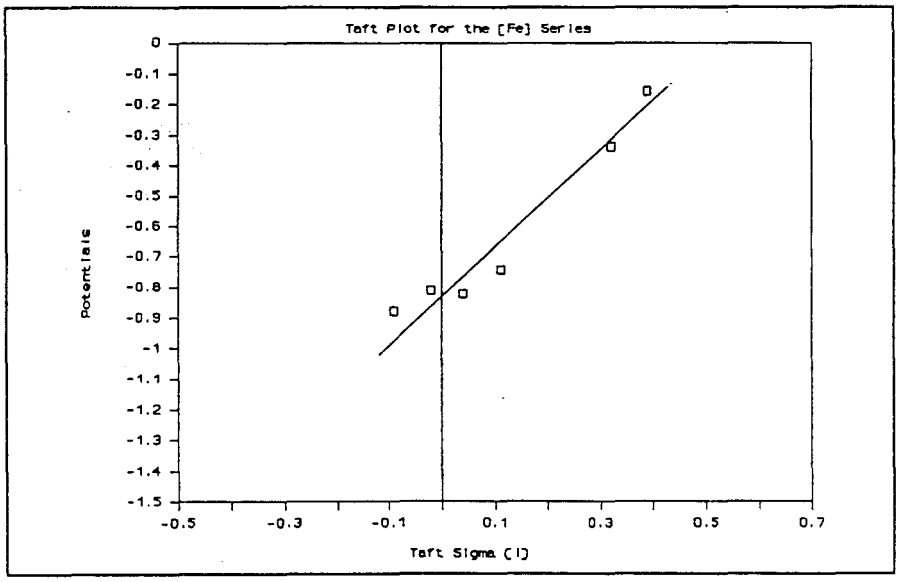
Taft Plot for the [Fe] Series
Potentials
0
-0.1
-0.2
-0.3
-0.4
-0.5
-0.6
-0.7
-0.8
-0.9
-1
-1.1
-1.2
-1.3
-1.4
-1.5
-0.5
-0.3
-0.1
0.1
0.3
0.5
0.7
Taft Sigma (I)

polynuclear in nature since they contain more than two electroactive metal centers. Electrochemical studies have suggested that there is electron delocalization between the central metal ion and the ligand system. Since the complexes are mixed-valence compounds and the ferrocene unit and central metal ion are separated by a delocalized ligand system, then observation of intervalence phenomena may be expected. Absorptions associated with intervalence transfer are usually very broad (showing half widths of 4 - 8 kK),[120] of low intensity and do not exist in the fully reduced and the fully oxidized forms of the complex. The transition process is light induced, the frequency of absorption being observed in the near infrared and visible regions of the electromagnetic spectrum.

For the ruthenium-ferrocene complexes, the bands exhibited at 900, 710 and 575 nm (Figure 3.5) have been assigned IT bands on the basis of their large values for $\Delta\nu_{1/2}$, low intensity and absence in the fully oxidized and fully reduced complexes. The IT transition corresponds to an $Fe^{II} \rightarrow Ru^{III}$ charge transfer, three of which are possible for each complex. If there is extensive delocalization within the complex, then transitions to delocalized exciton states may be possible provided that they are allowed. This possibility is manifested in structure on the IT band. Such structure was not observed in the complexes investigated.

Each complex was examined for remote site interactions between two ferrocene units by titrating the complex with cerium(IV) ammonium nitrate in acetonitrile. The spectral changes which accompany cerium(IV) addition did not show the appearance of other IT bands.

Close examination of the IT spectra for the ruthenium tris(β-diketonato) complexes show that for L = $FcCOCHCOCH_3^-$ the band appears as a shoulder on a relatively intense transition of the visible region, consequently, curve fitting procedures were not very accurate in this case. The IT band for L=$FcCOCHCOC_6H_5^-$ was also partly obscured by a more intense absorption however, E_{op} was estimated by assuming symmetry about λ_{max}. In all cases the half width was calculated using the relation[121]

$$\Delta\nu_{1/2} = [\nu_{max} - \nu_{max/2}(\text{low energy side})] \times 2 \qquad 4.3$$

since only the low energy side of the band is greatly exposed. It is recognized that this treatment may result in the half width being in error since charge transfer bands are usually asymmetric being larger on the high energy side.

A theoretical value for the half width is obtained from the following Hush relation which was given in Chapter 1:

$$E_{op} - \Delta E = \Delta\nu_{1/2}^2/2.31$$

The difference in internal energy between the oxidation isomers, ΔE, may be determined by making use of the relation;

$$\Delta E = \Delta G + T\Delta S \qquad 4.4$$

assuming the absence of PV work and where ΔE may be taken as being equal to ΔH. The electrostatic contribution to the internal energy introduces an additional term to equation 4.4 giving:

$$\Delta E = \Delta G_{redox} + \Delta E_{el} + T\Delta S \qquad 4.5$$

Neglecting electrostatic effects and assuming that $\Delta S \approx 0$ then

$$\Delta E = \Delta G_{redox} \approx nF[E_{1/2}(1) - E_{1/2}(2)] \qquad 4.6$$

where $E_{1/2}(1)$ and $E_{1/2}(2)$ are the half wave potentials for the free donor site and the acceptor site in the complex respectively.

Application of equation 1.20 to the systems under investigation revealed that the observed band widths are ~40% greater than the calculated value. Half width data are presented in Table 4.3.

The extent of ground state delocalization is calculated using the relation:

$$\alpha^2 = (4.2 \times 10^{-4} \epsilon_{max} \Delta\nu_{1/2})/(E_{op} r^2)$$

Table 4.3 lists values for the delocalization parameter α^2 and the electronic coupling parameter H_{ab} which is determined by the relation:

Table 4.3 Intervalence Transfer Properties for Ruthenium Tris(β-diketonato) Complexes

Parameter	Ligand		
	$[FcCOCHCOCF_3]^-$	$[FcCOCHCOC_6H_5]^-$	$[FcCOCHCOCH_3]^{-a}$
E_{op}/kK	11.3	13.4	16.4
$\Delta\nu_{1/2}$ (calc)/kK	3.1	3.1	3.6
$\Delta\nu_{1/2}$ (obs)/kK	5.8	5.2	9.1
$\alpha^2 \times 10^3$	5	2	3
H_{ab}	0.8	0.6	0.9
f [b]	2.1×10^{-2}	8.5×10^{-3}	1.7×10^{-2}

a) parameters for this system are estimates.
b) oscillator strength $f \approx 4.6 \times 10^{-9} \epsilon_{max} \Delta\nu_{1/2}$

$$H_{ab} = \alpha E_{op} \qquad 4.7$$

A value for r is estimated using crystallographic data.[122]

The band half widths are observed to be larger than the theoretically predicted values. This is typical for compounds which are classified as class II according to the Robin and Day formalism. In further support of the class II description is the relatively small values for the delocalization parameter, the oscillator strength and the electronic coupling parameter. A value of 9×10^{-3} was obtained for the Creutz-Taube ion which is known to be a valence delocalized belonging to the class III system and 3×10^{-3} for the complex $[(NH_3)_5Ru^{III}(pyz)Ru^{II}Cl(bipy)_2]^{4+}$ which was classified as class II.

The delocalization parameter may be derived from first order perturbation

theory[123] in which case there is an inverse variation between α^2 and the energy difference between the ground and excited states of the mixed valence system. The energy maximum E_{op} is a good approximation of the energy difference between the ground and excited states.

The band energy maximum E_{op} increases directly with the difference in internal energy ΔE according to the following expression which pertains to nonequivalent sites:

$$E_{op} = \Delta E + \nu_{FC} \qquad 4.8$$

where ν_{FC} is the Franck-Condon energy. Equation 4.8 assumes that variations in the inner sphere reorganization energy (χ_i) and the outer sphere reorganization energy (χ_o) are minimal from one complex to another. A plot of E_{op} versus ΔE (Figure 4.3) gives a straight line with a gradient of 1.2. The deviation from 1 may be accounted for in a possible overestimation of the position of the band maximum for the complex where L = $FcCOCHCOCH_3$. The intercept allows a value for the Franck-Condon parameter to be obtained using the relation

$$\nu_{FC} = \chi_i + \chi_o \qquad 4.9$$

The value of ν_{FC} obtained from the plotted data is 2.2 kK.

Figure 4.3 Plot of E_{op} versus ΔE for Ruthenium-Ferrocene Mixed-Valence Complexes

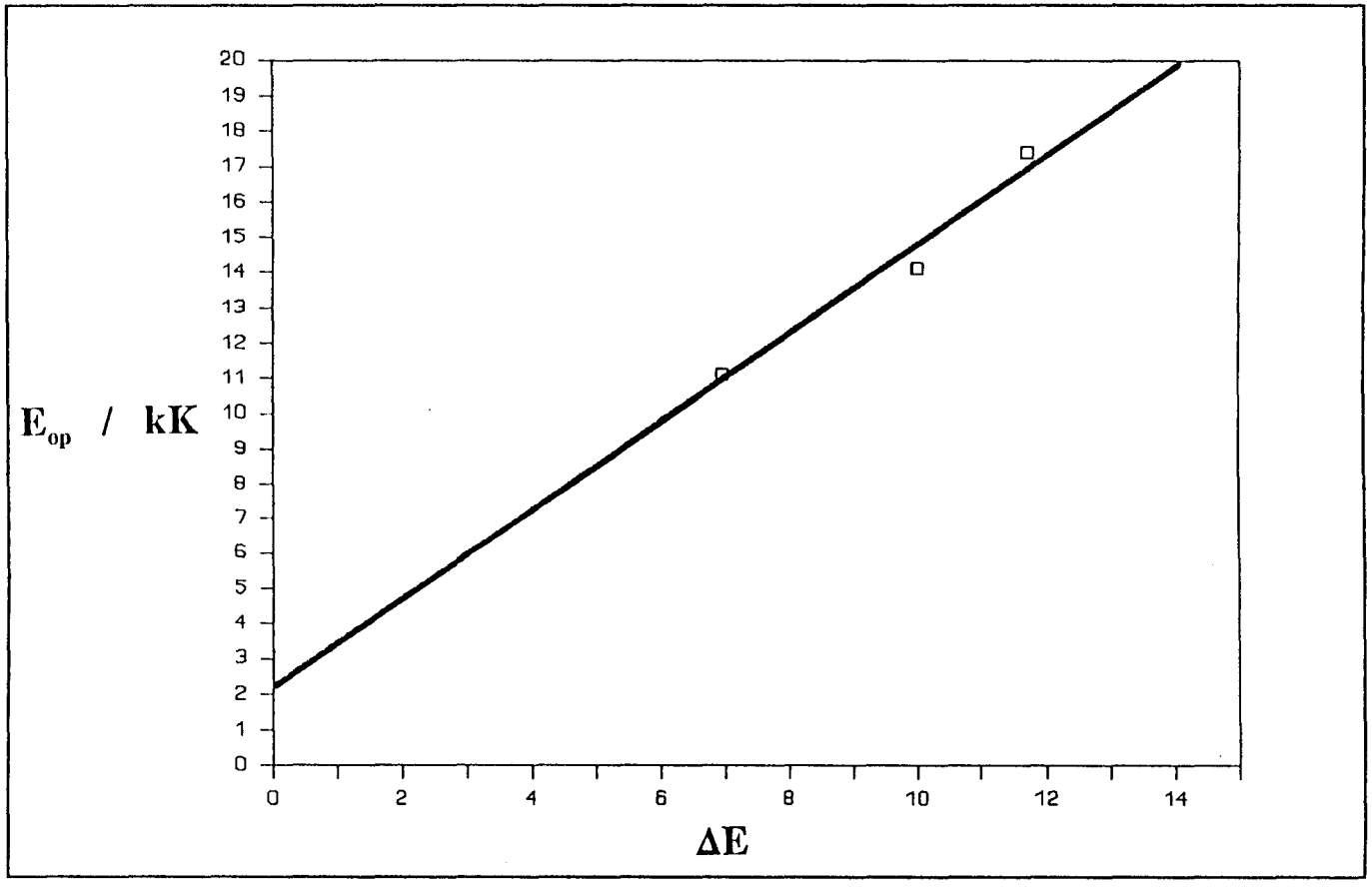
E_{op} / kK
20
19
18
17
16
15
14
13
12
11
10
9
8
7
6
5
4
3
2
1
0
0
2
4
6
8
10
12
14
ΔE

4.10 Solvent Dependence

In the previous section it was shown that the IT energy is comprised of the internal vibrational energy (χ_i), the solvent reorganization energy (χ_o) and the difference in internal energy between the [2,3] and the [3,2] oxidation isomers. The parameter χ_o is determined by applying equations which pertain to particular models. An expression for χ_o was developed by Marcus[124] where the interacting ions are considered to form two non-interpenetrating spheres between which there is a dielectric continuum. The mathematical expression for the outer sphere reorganisation energy is as follows:

$$\chi_o = (\Delta e)^2(1/2a_i + 1/2a_j - 1/r)(1/D_{op} - 1/D_s) \qquad 4.11$$

where the symbols are as defined in equation 1.18. Using equation 1.18, a plot of $E_{op} - \Delta E$ versus $1/D_{op} - 1/D_s$ ought to give a straight line with the intercept giving a value for χ_i. The solvent reorganisation energy may now be determined since it is related to the gradient of the straight line through equation 4.10. The short internuclear distance of the ruthenium-ferrocene diketonato complexes (r is estimated as 5.88 Å) precludes the application of the Marcus expression. The coordination spheres about iron(II) and ruthenium(III) were calculated as 2.47 and 6.93 Å respectively therefore there is a considerable degree of overlap of the two spheres. A more appropriate model for the circumstances of the ruthenium-ferrocene diketonato complexes is that provided by Cannon[125] in which the

molecular system is described by a prolate ellipsoid with a volume and length which are identical to that of the actual system. When the charges on the complexes are considered to be located at the foci of the ellipsoid, the expression the outer sphere reorganisation energy is given by;

$$\chi_o = (L/4\pi\epsilon_o)(1/D_{op} - 1/D_s)[(\Delta p)^2/2ab^2]S(\lambda_o) \qquad 4.12$$

where L is the Avogadro constant, Δp is the difference in dipole moments between the [2,3] and [3,2] isomers (this is equal to *e*r if the valences are localized), a and b are the radii of the semi-major and semi-minor axes of the ellipsoid, and the expression $S(\lambda_o)$ depends only on the eccentricity of the ellipsoid. The parameter λ_o is given by the expression

$$\lambda_o^2 = a^2/(a^2 - b^2) \qquad 4.13$$

where all variables are as previously defined. The parameter a is determined using the expression

$$a = (r + a_{Ru} + a_{Fc})/2 \qquad 4.14$$

where a_{Ru} and a_{Fc} are the radii of the coordination spheres for the ruthenium and ferrocene centers respectively. The volume of the molecule is used to determine b

in the following expressions

$$V = (4/3)\pi ab^2 \qquad 4.15$$

$$V = (4/3)\pi a_{Ru}^3 - (1/3)\pi h^2[3a_{Ru} - h] + (4/3)\pi a_{Fc}^3 - (1/3)\pi h^2[3a_{Fc} - h] \qquad 4.14$$

where h is the measured overlap along the line joining the centers of two spheres centered on iron and ruthenium. When the ellipsoid model is applied to the ruthenium-ferrocene diketonato complexes a value of 429 kJ mol^{-1} is obtained for the external reorganisation energy. This value is unrealistically large especially in view of the fact that E_{op} has a value of 132 kJ mol^{-1}. This large discrepancy indicates that the system under investigation does not fit the ellipsoid model. Although the values for a and b are estimates, the mismatch seems to stem largely from the high value of h (2.12 Å) compared with the radius of the coordination sphere of ferrocene (2.47 Å). It is likely that the ferrocene unit forms part of the coordination sphere of the ruthenium complex and as such it ought not to be treated separately. It should be noted that examples of IT compounds in the literature show internuclear distances which are greater than those of this study (usually 7 to 11 Å) and, in addition, the coordination spheres are smaller. For the ruthenium-ferrocene diketonato complexes a plot of E_{op} - ΔE versus $1/D_{op}$ - $1/D_s$ showed much scatter and only a slight solvent dependence was observed (Table 3.15). This phenomenon has literature

precedence.[126,127] It may be postulated that the molecular system is being solvated as one and not two units consequently there is no discernible response in the external system since the total charge on the molecular unit is unchanged.

4.11 Extent of Delocalization in Tris(β-diketonato) Complexes

Patterson and Holm[116] pioneered the electrochemical investigation of ruthenium tris(β-diketonato) complexes and were able to establish linear correlations between the half wave potential and the Hammett σ_p and σ_m parameters. Investigative research has subsequently shown that for several RuL_3 complexes there are definite substituent electronic effects which influence the value of $E_{1/2}$. Patterson and Holm[116] compared the trend in their ruthenium complexes with that in a series of bis- and tris-dithiolene complexes[128] in which it was observed that the first reduction potential is independent of the nature of the metal ion (nickel, palladium and platinum) and is a function of the type of substituent groups in the ligand system. A qualitative explanation for the observations was provided in which there is proposed overlap of metal t_{2g} and ligand π orbitals forming a molecular orbital into which the hole on the ruthenium(III) ion may be delocalized. The perturbative effect exercised by the substituents on the ligand π system was considered to act in such a manner as to create an improved energy match between the ligand and the metal π orbitals.

Richert *et al.*[114] proposed ligand based redox activity in the reduction and oxidation of FeL_3 complexes. It was observed that the trend in redox potential

parallels that of the free ligand, occurring at a less positive potential. The ML_3/ML_3^- potentials were also determined to be less positive than those for the solvated M^{II} ions.

Lewis and Sishta[129] prepared a ruthenium(III) tris(diketonato) complex with vinylic ferrocene substituents in the position γ to the central metal ion and determined that the complex undergoes an eight-electron change almost completely reversibly. Delocalization has been postulated after observing the decrease in reversibility with the decrease in the number of ferrocene substituents and hence extent of delocalization.

A direct test for delocalization in the tris(β-diketonato) complexes has been provided by this intervalence transfer study since the nature and extent of delocalization in the complexes have been directly assessed. The intervalence transfer characteristics of these complexes demonstrate that there is a delocalized pathway through which two metal centers may communicate. This type of intervalence transfer description is favored over tunneling since in the latter case weaker band intensities which arise from extremely small oscillator strengths, are observed.

This investigation has shown that, although there is some degree of delocalization in the tris(β-diketonato) complexes, the system is largely valence trapped. Such a description necessarily means that the ruthenium center is able to display characteristics of the isolated valences. The marked difference in uv-visible spectrum between the mixed-valence and the totally reduced species (Figure 4.4) provides

further evidence for the existence of isolated valences. Electrochemical studies have suggested that the LUMO into which a reductive electron is placed has ligand character, however, the intervalence transfer studies show that the LUMO ought to have largely metal character.

Richardson and Taube[68] found that, for a series of cyano bridges, there is an exponential decrease in H_{ab} with number of atoms in the conjugated system of the bridging ligand. When applied to this investigation, the implication is that for the ligand system $FcCOCHCOC_6H_5^-$, there should be a reduction in H_{ab} over cases where the terminal group is CF_3, CH_3 or other units which do not extend the delocalization of the ligand. This is borne out by the observed greater interaction energy with the ligands $FcCOCHCOCF_3^-$ and $FcCOCHCOCH_3^-$ (Table 4.3). Structure determination by X-ray crystallography[122] has shown that for mixed ligand complexes containing $CH_3COCHCOC_6H_5^-$ the phenyl ring is in the plane of the remaining ligand system. It is reasonable to assume that the identical situation could be applied here since there are no obvious steric factors which may cause the phenyl ring to be rotated at an angle to the rest of the ligand. Since the phenyl unit is considered to be in the plane of the remaining ligand system then there is opportunity for extension of the delocalized system.

A delocalization description has also been proposed for iron tris(β-diketonato) complexes, however, no intervalence transfer bands were found. There is a possibility that intervalence transfer bands may be obscured completely by more intense transitions in the visible region of the spectrum or else there may be no

Figure 4.4 Ultraviolet-visible Spectra for $[Ru(FcTFBD)_3]$ (A) and $[Ru(FcTFBD)_3]^-$ (B)

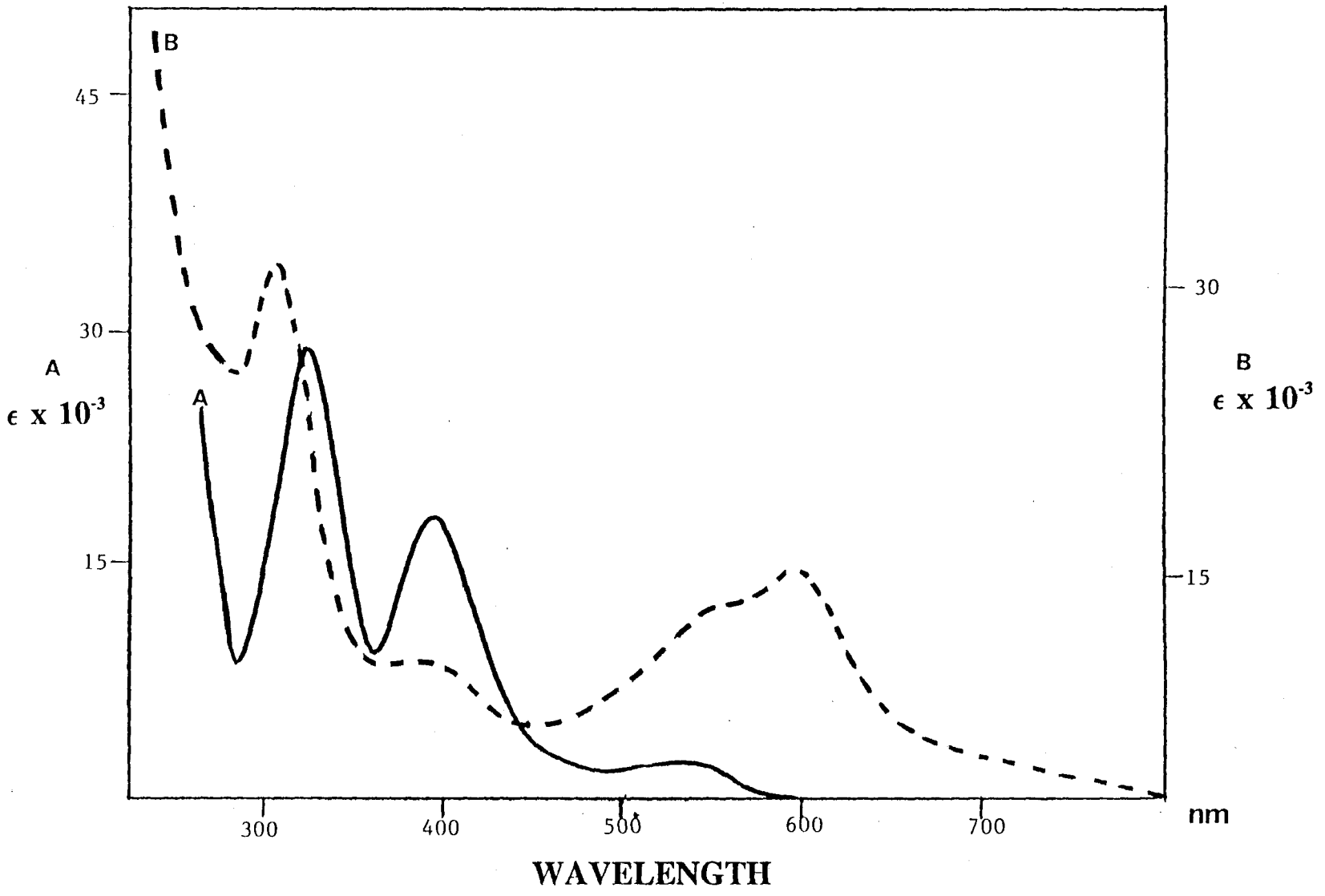
B
45
30
15
A
ε x 10-3
A
30
B
ε x 10-3
15
300
400
500
600
700
nm
WAVELENGTH

transitions of the intervalence type which are possible. If delocalization in iron complexes is explained similarly to that in ruthenium complexes then the effect is largely brought about by the overlap of the t_{2g} orbitals on iron(III) with suitable π ligand orbitals. The perturbative effects of the substituent groups on the ligand are expected to similarly alter the energy match between ligand and metal orbitals. Calculations have shown[68] that not only the LUMO but also both the π and π^* orbitals on the bridging ligand significantly contribute to metal-metal interaction. The radial extension of ruthenium orbitals is greater than that for iron orbitals[68] therefore it is not surprising that seemingly better overlap leading to greater delocalization is achieved with ruthenium systems.

The intervalence transfer study on ruthenium complexes has shown an apparent dependence of E_{op} on the nature of the substituent (Table 4.3). The origin of this dependence is not entirely clear. According to equation 1.12 the extent of delocalization and hence the interaction energy varies inversely with the square root of E_{op}. As the intervalence transfer bands shift into the visible region, the band widths and therefore oscillator strengths become larger in class II complexes. The differences in values for E_{op} appear to be more a reflection of the internal energy differences between the [2,3] and [3,2] isomers for each system. The increased extent of delocalization for the L = $FcCOCHCOCH_3^-$ complex is likely to be a reflection of the large redox inequality of the donor and acceptor sites, an effect which has been acknowledged in the literature.[120]

The above argument may be applied to iron-ferrocene diketonato complexes in

explaining why IT bands are not observed in these mixed-valence systems. The values of ΔE in the iron-ferrocene complexes when the ligands are [FcTFBD], [FcPBD] and [FcBD] are 5.31, 9.23 and 9.76 kK respectively. The values of ΔE for the corresponding ruthenium-ferrocene complexes are 3.28, 7.00 and 8.18 kK respectively. If ΔE contributes largely to E_{op} then the IT bands for the iron-ferrocene complexes when the ligands are [FcPBD] and [FcBD] are expected it be located within the visible region in which case they may be obscured by more intense transitions.

The probability of electron movement from one vibronic level to a set of levels in the product is given by the following expression;

$$W = 4\pi^2/h[H_{ab}{}^2\rho] \qquad 4.15$$

where the parameter ρ contains Franck-Condon factors. If the spectra of iron complexes do contain hidden intervalence transfer bands it is expected that they would arise from a large extent of delocalization (reflected in H_{ab}) or a very significant increase in internal and external reorganization energies (ρ). On comparing the iron and ruthenium complexes it is reasonable to assume that a large value for E_{op} may be caused by a large ΔE since the extent of metal-metal interaction in the iron complexes is not expected to be any greater than that for ruthenium complexes. A large value for E_{op} necessarily means a small value for H_{ab} (equations 1.12 and 4.7) and consequently a small value for W.

This chapter ought not to be closed without mentioning the possible intervalence transfer band displayed by the free Schiff base ligand containing ferrocene (Table 3.14). One handicap in examining this possible mixed-valence species is the lack of knowledge of its structure or composition. A noticeable feature of the totally reduced species is the lack of an orbital pathway for electron movement. This does not necessarily preclude intervalence transfer processes since interaction through saturated bridges have been demonstrated.[130,131] Another possibility is that Fc and Fc^+ units may approach each other very closely forming mixed-valence ion pairs. Intervalence transfer phenomena in mixed-valence ion pairs have been demonstrated in the literature.[127]

4.12 Conclusion

Ferrocene-containing Schiff base complexes of cobalt(II) and iron(II) have been prepared and investigated electrochemically and for intervalence transfer phenomena. The iron(II) Schiff base complexes have been found to be unsuitable for the study of intervalence transfer phenomena lagrgely because of the irreversible nature of the electron transfer associated with the Fe^{2+}/Fe^{3+} couple. Cobalt(II) Schiff base complexes did not exhibit Fe-Co interaction. It is postulated that the energy demands on electron rearrangement in order to facilitate electron transfer, may be too large to be compensated in the system under investigation. The preparation of ferrocene-containing Schiff base complexes of ruthenium(II) was considered to be unsuccessful.

Ferrocene-containing tris(β-diketonato) complexes of iron(III) and ruthenium(III) were prepared and studied electrochemically and spectroscopically. The electrochemical investigation for the tris(β-diketonato) complexes of iron(III) and ruthenium(III) revealed reversible electron transfer for both the M^{III}/M^{II} and the Fc/Fc^{+} couples, with $\Delta E_{1/2}$ values ranging between 200 and 400 mV, and electronic effects which are exercised by both the ferrocene unit and other substituents constituting the ligand system. Linear correlations have been established between the $E_{1/2}$ values and the sum of the one ligand Hammett and Taft constants.

Spectroscopic examination of the tris(β-diketonato) complexes has shown that ruthenium(III) complexes, and not iron(III) complexes, exhibit metal-metal interaction. Intervalence transfer bands were found in the near infrared and visible regions on the spectrum. A study of the intervalence transfer properties of the ruthenium(III) complexes has revealed that the extent of metal-metal coupling is weak. On determining the intervalence transfer parameters it was concluded that these complexes belong to class II of the Robin and Day classification scheme. The lack of solvent dependence on the position of the intervalence transfer band was considered to be associated with the structural nature of the complexes in the solution phase.

The assessment of the delocalized nature of tris(β-diketonato) complexes was previously based on electrochemical data and comparisons with well known systems. The intervalence transfer properties of these systems, in being a probe for the electron delocalization in the complexes, has provided a direct measurement of their

delocalized nature.

REFERENCES

1. P. Day in "*Mixed-Valence Compounds*" D.I. Brown Ed. NATO Advanced Study Instituutes Series No58 D. Reidel Dordrecht, Holland, **1980**

2. Zintl, E. and Rauch, A. *Ber. Deut. Chem. Ges.* **1924,** *57,* 1739.

3. Verwey, E.J.W.; Haayman, P.J.; Romaeijh, F.C.; Van Oosterhout Philips, G.W. *Res. Rep.* **1950,** *5,* 173.

4. Mac Carthy, G.R. *Amer. J. Sci.* **1926,** *12,* 16

5. Allen, G.C. and Hush, N.S. *Prog. Inorg. Chem.* **1967,** *8,* 357.

6. Hush, N.S. *Prog. Inorg. Chem.* **1967,** *8,* 391.

7. Robin, M.B. and Day, P. *Adv. Inorg. Chem. Radiochem.* **1967,** *10,* 247.

8. Creutz, C. and Taube, H. *J. Am. Chem. Soc.* **1969,** *91,* 3988.

9. Cowan, D.O. and Kaufman, F. *J. Am. Chem. Soc.* **1970,** *92,* 219.

10. A presentation of a wide variety of bridges used is given by Creutz, C. *Prog. Inorg. Chem.* **1983,** *30,* 1.

11. Piepho, S.B.; Krausz, E.R. and Schatz, P.N. *J. Am. Chem. Soc.* **1978,** *100,* 2996.

12. Lauher, J.W. *Inorg. Chim. Acta.* **1980,** *39,* 119.

13. Mayoh, B. and Day, P. *Inorg. Chem.* **1974,** *13,* 2273.

14. Mayoh, B. and Day, P. *J. Chem. Soc. Dalton. Trans.* **1974,** 846.

15. Chiu, Yin-Nan. *J. Phys. Chem.* **1976,** *80,* 992.

16. Creutz, C.; Good, M.L. and Chandra, S. *Inorg. Nuc. Chem. Lett.* **1973,** *9,* 171.

17. Elias, J. and Drago, R.S. *Inorg. Chem.* **1972,** *11,* 415.

18. Marcus, R.A. *J. Phys. Chem.* **1963,** *67,* 853.

19. Sutin, N. in "*Inorganic Biochemistry*" *Vol 2,* Eichorn, G.L. Ed, Elsevier, New York, **1973,** 611.

20. Ondrechen, M.J.; Ko, J. and Root, L.J. *J. Phys. Chem.* **1984,** *88,* 5919.

21. Wong, K.Y.; Schatz, P.N. and Piepho, S.B. *J.Am. Chem. Soc.* **1979,** *101,* 2793.

22. Wong, K.Y. and Schatz, P.N. *Prog. Inorg. Chem.* **1981,** *28,* 369.

23. Schatz, P.N. in "*Mixed-Valence Compounds*" D.B. Brown Ed. NATO Advanced Study Institutes Series No58 D. Reidel Dordrecht, Holland, **1980,** 115.

24. Goldsby, K.A. and Meyer, T.J. *Inorg. Chem.* **1984,** *23,* 3002.

25. Powers, M.J.; Callahan, R.W.; Salmon, D.J. and Meyer, T.J. *Inorg.Chem.* **1976,** *15,* 1457.

26. Hupp, J.T. and Meyer, T.J. *Inorg. Chem.* **1987,** *26,* 2332.

27. Lewis, N.A.; Obeng, Y.S. and Purcell W.L. *Inorg. Chem.* **1989,** *28,* 3796.

28. Felix, F. and Ludi, A. *Inorg. Chem.* **1978,** *17,* 1782.

29. Lewis, N.A. and Obeng, Y.S. *J. Am. Chem. Soc.* **1988,** *110,* 2307.

30. Work cited in reference 10.

31. Chang, J.P.; Fuung, E.Y. and Curtis, J.C. *Inorg. Chem.* **1986,** *25,* 4233.

32. Powers, M.J.; Salmon, D.J.; Callahan, R.W. and Meyer, T.J. *J. Am. Chem. Soc.* **1987,** *98,* 6731.

33. Ludi, A. in "*Mixed-Valence Compounds*" D.B. Brown Ed. NAto Advanced Study Institutes Series No58 D. Reidel Dordrecht, Holland, **1980,** 25.

34. Schatz, P.N.; Piepho, S.B. and Krausz, E.R. *Chem. Phys. Lett.* **1978,** *55,* 539.

35. Winkler, J.R.; Nocera, D.G.; Yocom, K.M.; Bordingnon, Z. and Gray, H.B. *J. Am. Chem. Soc.* **1982,** *104,* 5798.

36. Kostic, N.M.; Margalit, R.; Che, C.M. and Gray, H.B. *J. Am. Chem. Soc.* **1983,** *105,* 7765.

37. Isied, S.S.; Worosila, G. and Atherton, S.J. *J. Am. Chem. Soc.* **1982**, *104,* 7659.

38. Mc Gourty, J.L.; Blough, N.V. and Hoffman, B.M. *J. Am. Chem. Soc.* **1983**, *105,* 4470.

39. Mc Gourty, J.L.; Peterson, S. and Hoffman, B.M. *J.Am. Chem. Soc.* **1984**, *106,* 5010.

40. Brunschwig, B.S.; Ehrenson, S. and Sutin, N. *J. Phys. Chem.* **1986**, *90,* 3657.

41. Callahan, R.W.; Brown, G.M. and Meyer, T.J. *Inorg. Chem.* **1975**, *14,* 1443.

42. Woitellier, S.; Launay, J.P. and Spangler, C.W. *Inorg. Chem.* **1989**, *28,* 758

43. Kober, E.M.; Goldsby, K.A.; Narayana, D.N.S. and Meyer, T.J. *J. Am. Chem. Soc.* **1983**, *105,* 4303.

44. Le Vanda, C.; Bechgaad, K.; Cowan, D.O.; Mueller-Westerhoff, U.T.; Eilbracht, P.; Candela, G.A. and Collins, R.L. *J. Am. Chem. Soc.* **1976**, *98,* 3181.

45. Levanda, C.; Bechgaard, K. and Cowan, D.O. *J. Org. Chem.* **1976**, *41,* 2700.

46. Powers, M.J. and Meyer, T.J. *J. Am. Chem. Soc.* **1978**, *100,* 4393.

47. Hupp, J.P.; Neyhart, G.A. and Meyer, T.J. *J. Am. Chem. Soc.* **1986**, *108,* 5349.

48. Ennix, K.S.; McMahon, P.T.; de la Rosa, R. and Curtis, J.C. *Inorg. Chem.* **1987**, *26,* 2660.

49. Le Vanda, C.; Cowan, D.O. and Bechgaad, K. *J. Am. Chem. Soc.* **1975**, *97,* 1980.

50. Le Vanda, C.; Bechgaad, K.; Cowan, D.O. and Rausch, M.D. *J. Am. Chem. Soc.* **1977**, *99,* 2964.

51. Talham, D.R. and Cowan, D.O. *Organometallics.* **1987**, *6*, 932.

52. Volger, A. and Kunkely, H. *Ber.* **1975**, *79,* 83.

53. Volger, A. and Kunkley, H. *Ber.* **1975,** *79,* 301.

54. Ludi, A. *Chimia.* **1972,** *26,* 647.

55. Magnuson, R.H. and Taube, H. *J. Am. Chem. Soc.* **1972,** *94,* 7213.

56. Bagger, S. and Gibson, K. Acta. *Chem. Scand.* **1973,** *27,* 3227.

57. Fisher, H.; Tom, G.M. and Taube, H. *J. Am. Chem. Soc.* **1976,** *98,* 5512.

58. Reider, K. and Taube, H. *J. Am. Chem. Soc.* **1977,** *99,* 7891.

59. Dowling, N.; Henry, P.M.; Lewis, N.A. and Taube, H. *Inorg. Chem.* **1981,** *20,* 2345.

60. Hupp, J.T. and Weydert, J. *Inorg. Chem.* **1987,** *26,* 2657.

61. Yeh, A. and Haim, A. *J. Am. Chem. Soc.* **1985,** *107,* 369.

62. Goldsby, K.A. and Meyer, T.J. *Inorg. Chem.* **1984,** *23,* 3002.

63. Toma, H.E. and Santos, P.S. *Can. J. Chem.* **1977,** *55,* 3549.

64. Yeh, A. and Haim, A. *Inorg. Chem. Acta.* **1979,** *33,* 51.

65. Toma, H.E. and Malin, J.M. *Inorg. Chem.* **1973,** *12,* 1039.

66. Shepherd, R.E. J. Am. Chem. Soc. 1976, 98, 3329.

67. Taube, H. *Ann. N.Y. Acad. Sci.* **1978,** *313,* 481.

68. Richardson, D.E. and Taube, H. *J. Am. Chem. Soc.* **1983,** *105,* 40.

69. Mulliken, R.S. and Person, W.B. "*Molecular Complexes*" Wiley, New York, **1969.**

70. Gagn é , R.R.; Spiro, C.L.; Smith, T.J.; Hamann, C.A.; Thies, W.R. and Skiemke, A. *J Am. Chem. Soc.* **1981,** *103,* 4073.

71. Fenton, D.E. and Lintvedt, R.L. *J. Am. Chem. Soc.* **1978,** *100,* 6367.

72. Weaver, T.R.; Meyer, T.J.; Adeyemi, S.A.; Brown, G.M.; Eckbery, R.P.; Hatfield, W.E.; Johnson, E.C.; Murray, R.W. and Unterecker, D. *J. Am. Chem. Soc.* **1975,** *97,* 3039.

73. Bauman, J.A. and Meyer, T.J. *Inorg. Chem.* **1980**, *19*, 345.

74. Gagne, R.R.; Koval, C.A.; Smith, T.J. and Cimolino, M.C. *J. Am. Chem. Soc.* **1979**, *101*, 4571.

75. OKawa, H.; Horiuchi, K.; Kanda, W.; Sohio, H. and Kida, S. *Bull. Chem. Soc. Jpn.* **1986**, *59*, 2795.

76. Dione, H.; Stephens, F.F. and Cannon, R.D. *Inorg. Chim. Acta.* **1984**, *82*, 149.

77. von Kameke, A.; Tom, G.M. and Taube, H. *Inorg. Chem.* **1978**, *17*, 1790.

78. Brown, G.M.; Meyer, T.J.; Cowan, D.O.; Le Vanda, C.; Kaufman, F.; Roling, P.V. and Rausch, M.D. *Inorg. Chem.* **1975**, *14*, 506.

79. Dowling, N. and Henry, P.M. *Inorg, Chem.* **1982**, *21*, 4088.

80. Matson, B.M. and Pignolet, L.H. *Inorg. Chem.* **1976**, *15*, 564.

81. Sure/Seal is a trademark of the Aldrich Chemical Company. A description of the sealing system is given in any recent catalogue.

82. Miles, M.L.; Harris, T.M. and Hauser, C.R. *J. Org. Chem.* **1965**, *30*, 1007.

83. M^{c}Carthy, P.J.; Hovey, R.J.; Ueno, K. and Martell, A.E. *J. Am. Chem. Soc.* **1955**, *77*, 5820.

84. Martell, A.E.; Belford, R.L. and Calvin, M. *J. Inorg. Nuc. Chem.* **1958**, *5*, 170.

85. Lintvedt, R.L.; Tomlonovic, B.; Fenton, D.E. and Glick, M.D. *Adv. Chem. Ser.* **1976**, *150*, 407.

86. Niswander, R.H. and Martell, A.E. *Inorg. Chem.* **1978**, *17*, 2341.

87. Thornback, J.R. and Wilkinson, G. *J. Chem. Soc. Dalton. Trans.* **1978**, 110.

88. Van Den Bergen, A.; Murray, K.S. and West, B.O. *J. Organomet. Chem.* **1971**, *33*, 89.

89. Kreh, R.P.; Rodriguez, A.E. and Fox, S.P. *J. Chem. Soc. Chem. Commun.* **1984**, 130.

90. Farrar, D.T. and Jones, M.M. *J.Phys. Chem.* **1964,** *68,* 1717.

91. Endo, A.; Kajitani, M.; Mukaida, M.; Shimizu, K. and Sato, G.P. *Inorganica Chimica Acta,* **1988,** *150,* 25.

92. Callahan, R.W.; Brown, G.M. and Meyer, T.J. *Inorg. Chem.* **1975,** *14,* 1443.

93. Vogel, A.I. *"Textbook of Quantitative Inorganic Analysis,"* Fourth Edition, Longman, London, New York, 1981.

94. Lange, W. and Muller, E. *Chem. Ber.* **1930,** *63,* 1058. *Chem. Abs.* **1931,** *25,* 1754.

95. Hauser, C.R. and Lindsay, J.K. *J. Org. Chem.* **1957,** *22,* 482.

96. Fenton, D. and Lintvedt, R.L. *J. Am. Chem. Soc.* **1978,** *100,* 6367.

97. Lintvedt, R.R.; Ranger, G. and Schoenfelner, B.A. *Inorg. Chem.* **1984,** *23,* 688.

98. Dudek, G.O. and Holm, R.H. *J. Am. Chem. Soc.* **1961,** *83,* 2099.

99. De Iasi, R.; Holt, S.L. and Post, B. *Inorg. Chem.* **1971,** *10,* 1498.

100. Tocher, J.H. and Fackler, J.P.(Jr.) *Inorg. Chim. Acta* **1985,** *102,* 211.

101. Taqui Khan, M.M. and Srivastava, S. *Polyhedron,* **1988,** *7,* 1063.

102. Kobayashi, H.; Matsuzawa, H.; Kaizu, Y. and Ichida, A. *Inorg. Chem.* **1987,** *26,* 4318.

103. Singh, P.R. and Sahai, R. *Aust. J. Chem.* **1969,** *22,* 1169.

104. Sohn, Y.S.; Hendrickson, D.N. and Gray, H.B. *J. Am. Chem. Soc.* **1971,** *93,* 3606.

105. See reference 91 and references therein.

106. Jones, R.D.; Summerville, D.A. and Basolo, F. *Chem. Rev.* **1979,** *79,* 139.

107. Tolman, C. *Chem. Rev.* **1977,** *77,* 313.

108. Nicholson, R.S. and Shain, I. *Anal. Chem.* **1965,** *37,* 665.

109. Nicholson, R.S. *Anal. Chem.* **1965,** *37,* 667.

110. Carter, M.J.; Rillema, D.P. and Basolo, F. *J. Am. Chem. Soc.* **1974,** *96,* 392.

111. Endo, A. *Bull. Chem. Soc. Jpn.* **1983,** *56,* 2733.

112. Murray, R.W. and Hiller, L.K. *Anal. Chem.* **1967,** *39,* 1221.

113. Heineman, W.R.; Burnett, J.N. and Murray, R.W. *Anal. Chem.* **1986,** *40,* 1970.

114. Kalinowski, W.K. and Cmiel, A. *Inorg. Chim. Acta* **1981,** *49,* 179.

115. Richert, S.A.; Tsang, P.K.S. and Sawyer, D.T. *Inorg. Chem.* **1989,** *28,* 2471.

115. M^{c}Carthy, H.J. and Tocher, D.A. *Polyhedron,* **1987,** *6,* 1421.

116. Patterson, G.S. and Holm, R.H. *Inorg. Chem.* **1972,** *11,* 2285.

117. Endo, A,; Shimizu, K. and Sato, G.P. *Chem. Lett.* **1985,** 581.

118. Endo, A.; Hoshino, Y.; Hirakata, K.; Takeuchi, Y.; Shimizu, K.; Furushima, Y.; Ikeuchi, H. and Sato, G.P. *Bull. Chem. Soc. Jpn.* **1989,** *62,* 709.

119. Exner, O. "*Correlation Analysis of Chemical Data*" Plenum Press, New York, London, 1988.

120. Callahan, R.W.; Brown, G.M. and Meyer, T.J. *Inorg. Chem.* **1974,** *14,* 1443.

121. Mulliken, R.S. and Person, W.B. "*Molecular Complexes*" Wiley, New York, **1969.**

122. Hoshino, Y.; Yukawa, Y.; Maruyama , T.; Endo, A.; Shimizu, K. and Sato, G.P. *Inorg. Chim. Acta* **1990,** *174,* 41.

123. Mayoh, B. and Day, P. *J. Am. Chem. Soc.* **1972,** *94,* 2885.

124. Marcus, R.A. *J. Phys. Chem.* **1955,** *24,* 966

125. Cannon, R.D. *Chem. Phys. Lett.* **1977,** *49,* 299.

126. Powers, M.J. and Meyer, T.J. *Inorg. Chem.* **1978,** *17,* 1785.

127. Sullivan, B.P.; Curtis, J.C.; Kober, E.M. and Meyer, T.J. *Nouveau Journal De Chimie.* **1980,** *4,* 643.

128. Heath, G.A. and Leslie, J.H. *J. Chem. Soc. Dalton Trans.* **1983,** 1587.

129. Lewis, N.A. and Sishta, B.K.P. *J. Chem. Soc. Chem. Commun.* **1984,** 1428.

130. Stein, C.A.; Lewis, N.A. and Gunther, S. *J. Am. Chem. Soc.* **1982,** *104,* 2596.

131. Lewis, N.A. and Obeng, Y.S. *J. Am. Chem. Soc.* **1989,** *111,* 7624.

VITA

DAVID A. ROCKCLIFFE

The author was born on June 10, 1953 in Georgetown, Guyana. He attended The Queen's College of Guyana from which he graduated in 1972 with three London University Advanced Level subjects. He obtained a B.Sc. degree in chemistry from The University of Guyana in 1977 and a Master of Philosophy degree in Mineral Science from Leeds University (UK) in 1983. He worked as an assistant lecturer at The University of Guyana and at The University of the West Indies (Kingston, Jamaica) before entering Loyola University of Chicago in 1985 in order to pursue studies leading to a Ph.D. degree in chemistry. He is, at present, a post doctoral research associate in the Department of Chemistry at Texas A&M University.

The dissertation submitted by David A. Rockcliffe has been read and approved by the following committee:

Dr. P. M. Henry, Director
Professor, Chemistry
Loyola University of Chicago

Dr. B. Jaselskis
Professor, Chemistry
Loyola University of Chicago

Dr. A. W. Herlinger
Associate Professor, Chemistry
Loyola University of Chicago

Dr. A. Fitch
Associate Prfessor, Chemistry
Loyola University of Chicago

Dr. K. S. Rajan
Scientific Adviser
Illinois Institute of Technology

The final copies have been examined by the director of the Committee and the signature which appears below verifies the fact that any necessary changes have been incorporated and that the dissertation is now given final approval by the Committee with reference to content and form.

The dissertation is, therefore, accepted in partial fulfillment of the requirements for the degree of doctor of philosophy.

Jan. 7, 1993
Date

Patrick M. Henry
Director's Signature